NOTICE: When government or other drawings, specifications or other data are used for any purpose other than in connection with a definitely related government procurement operation, the U. S. Government thereby incurs no responsibility, nor any obligation whatsoever; and the fact that the Government may have formulated, furnished, or in any way supplied the said drawings, specifications, or other data is not to be regarded by implication or otherwise as in any manner licensing the holder or any other person or corporation, or conveying any rights or permission to manufacture, use or sell any patented invention that may in any way be related thereto.

N-63-4-3

410143

AEROSPACE RESEARCH • AERODYNAMICS • PROPULSION • STRUCTURAL DYNAMICS • ELECTRONIC SYSTEMS AND INSTRUMENTS • COMPUTER MODULES

TECHNICAL REPORT NO. 340

DESCRIPTION OF IBM 709/90/94 COMPUTER PROGRAMS AND ANALYSIS FOR FLOW FIELDS ABOUT BODIES OF REVOLUTION IN HYPERSONIC FLIGHT

By
E. Lieberman

RESEARCH
ENGINEERING
PRODUCTION

May, 1963

GENERAL APPLIED SCIENCE LABORATORIES, INC.
MERRICK and STEWART AVENUES, WESTBURY L.I., N.Y. (516) ED 3-6960

FOR ERRATA

AD ________

410 143

THE FOLLOWING PAGES ARE CHANGES

TO BASIC DOCUMENT

GENERAL APPLIED SCIENCE LABORATORIES, INC.
Merrick and Stewart Avenues
Westbury, L.I., New York

AD 410 143

File Copy

MODIFICATIONS TO GASL TECHNICAL REPORT No. 340

A subsequent series of test runs performed on the SUBSONIC program, indicated that the results were not reliable over a large range of flight conditions. Primarily, this was due to a lack of refinement in the original analysis pertaining to the inconsistency incolving γ along the reference line (page 20). In addition, an instability condition affecting the system of pertubation equations when a large number of iteration points were prescribed, was not detected initially.

In the course of solving these and other problems, an exhaustive series of tests were conducted. Both the analysis and the coding were greatly refined; indeed, a reiteration procedure was added which greatly enhances the accuracy of the final solution, at a very small additional cost in machine time. A scaling technique was introduced which not only improved the solution in the elliptic region, but insured that a subsequent execution of the supersonic flow field would have accurate initial conditions, consistent with the subsonic flow properties. The precision of the calculated deviations along the body profile was considerable improved by refining the integration along the reference line.

These, and many other additional features, have yielded a computer program which will generate accurate results with a high degree of reliability at relatively low cost.

GENERAL APPLIED SCIENCE LABORATORIES, INC.
Merrick and Stewart Avenues
Westbury, L.I., New York

ERRATA

TECHNICAL REPORT NO. 340

Page 3:

Last sentence, second paragraph, replace with

" The coefficient, a_4 is then modified parametrically to overcome this situation."

Last sentence, third paragraph, replace with

" The reference line is located; then the "basic polynominal" is scaled so that the body point on the reference line falls on the prescribed profile. See page 19 for details."

Page 4:

Last sentence, third paragraph, add

This "final" polynominal (and reference line) is then scaled.

6. To refine this solution, a second set of sweeps is executed (steps 2-5) using the first "final" polynominal as the second "basic polynominal" and utilizing a new set of "iteration points".

The last paragraph starts as follows:

7. The free stream conditions, ...

Page 18:

Delete last 4 lines

Page 20:

Replace the last 2 sentences with,

"These inconsistencies are minimized by assigning as the γ used in the Subsonic region, the average of the values at the body point and behind the detached shock at the reference line. In addition, the coordinates of the body point are defined by the condition, $\tau = 0$.

Page 22:

Lines 9 and 16, replace y_{DC} with y^2_{DC}

Page 24:

Delete the next-to-last sentence in the first paragraph.

Page 26:

The exponents on lines 4 and 6 should be $-{}^1/2$ (not $+ {}^1/2$).

Page 27:

Replace lines 6, 7, and 8, as follows:

$$c_{in} = \bar{C}_{in} \left[\frac{(\tau_n - \tau_{ns})}{(y_{n+1} - y_{n-1})} \right] k_{u_n}$$

$$d_{in} = \bar{D}_{in} \left[\frac{(\tau_n - \tau_{ns})}{(y_{n+1} - y_{n-1})} \right] k_{v_n}$$

$$e_{in} = -2\,(A_{in} U_{ns} + B_{in} V_{ns}) - \left(A_{in} \left(\frac{dU}{d\tau}\right)_{ns} + B_{in} \left(\frac{dV}{d\tau}\right)_{ns} - E_{in} \right) (\tau_n - \tau_{ns})$$

Page 28:

Delete the first 4 lines and replace equ. (4) with

$$\left.\begin{aligned} \left(\frac{\partial U}{\partial y}\right)_n &= \left[\frac{U_{(n+1)} - U_{(n-1)}}{y_{(n+1)} - y_{(n-1)}}\right] k_{u_n} \\ \left(\frac{\partial V}{\partial y}\right)_n &= \left[\frac{V_{(n+1)} - V_{(n-1)}}{y_{(n+1)} - y_{(n-1)}}\right] k_{v_n} \end{aligned}\right\} \quad 1 \leq n \leq p-1 \tag{4}$$

Page 30:

Add to right of line 5,

; α, β given on page 26.

Add at bottom of page,

Then,

$$k_{u_n} = \left(\frac{\partial U}{\partial y}\right)_n \cdot \left[\frac{U_{n+1} - U_{n-1}}{y_{n+1} - y_{n-1}}\right]^{-1}$$

$$k_{v_n} = \left(\frac{\partial V}{\partial y}\right)_n \cdot \left[\frac{V_{n+1} - V_{n-1}}{y_{n+1} - y_{n-1}}\right]^{-1}$$

Page 31:

Delete the term, $+ a_8 y^8$, in line 2

Replace the symbol, δ, with $\bar{\delta}$, in line 9 and in sketch.

Page 46:

Line 6, add the term, $E_\infty = \dfrac{e^{\theta'/T_\infty}}{e^{\theta'/T_\infty} - 1}$

Page 68:

Line 12, insert, ... pages 37 through 41.

Page 72:

Equ. (16) : $x(2.0) = \frac{3}{4}(x_t - \bar{x}_o) + \bar{x}_o$

Page 75:

Add this sentence at the bottom:

It is necessary to "right-adjust" data words within the indicated field; that is, the word must be shifted to the extreme right of the field.

Page 79:

Delete the last sentence of paragraph 4.

Page 85:

Replace the 2 with a 3 on next to last line.

Page 86:

Add this sentence at the bottom:

Note that the Subsonic Program, coupled with this option of the Supersonic Program, is exactly equivalent to the Flow Field program.

Page 98:

Lines 4, 5, and 6 are to be replaced:

P	Dimensionless pressure = $\frac{p}{\rho_\infty W_\infty^2}$
p	Pressure, lbs/sq. ft.
$R = \widetilde{P} = \delta \frac{\rho}{\rho_\infty}$	Dimensionless density, $\delta = \frac{\gamma - 1}{\gamma + 1}$ where $\gamma = 1/2 \left[\gamma_{shock} + \gamma_{body}\right]_{ref.\ line}$

The range of applicability of these programs is limited only by the numerical fits supplied by ABMA, which express the entropy and density in terms of the known enthalpy and pressure. Those flight conditions of velocity and altitude at which the stagnation temperature is less than 7000°K and stagnation pressure less than 10 atmospheres, lie within the scope of these programs.

Note that the preceding analysis is based upon the assumptions of linear mass flow variation between shock and body at the axis, a parabolic variation across the shock layer, r s, and a cubic variation at the downstream section, c d. These assumptions are consistent with the physics; as one proceeds around the "shoulder", in the downstream direction this variation assumes still higher orders.

After sweeping through the transonic region using this "basic" polynomial, the properties at the point on the body at the reference line, are compared with the prescribed body profile. In general, the calculated values of x, y, and θ at this point (which we will call $\bar{x}$, $\bar{y}$, $\bar{\theta}$) will not be consistent with the prescribed profile. We can compute the coordinates of the point on the prescribed body (x_B, y_B), where $\theta_B = \bar{\theta}$. Then define $K = \dfrac{y_B}{\bar{y}}$. Now this "basic" shock polynomial may be modified so that this calculated point on the body agrees with the prescribed body profile. If we now denote the original coefficients by $\bar{a}_n$, n = 0, 2, 4 instead of a_n, we can define the modified polynomial as $x = F(y) = \sum_{n=0,2,4} a_n y^n$ and relate them as follows:

$$x = F(y) = \left[K\bar{a}_o + \left(x_B - K\bar{x}\right) \right] + \sum_{n=2,4} K^{(1-n)} \bar{a}_n y^n$$

Thus, $a_o = K\bar{a}_o + \left(x_B - K\bar{x}\right)$; $a_n = K^{(1-n)} \bar{a}_n$, n = 2, 4

SUBSONIC ANALYSIS

At the completion of the transonic region, the reference line is defined, and the program then transforms the properties of all points on the reference line, from the physical x-y plane to the τ-y plane. The properties along the reference line required by the Subsonic analysis are U, V, τ and y.

$$U = \frac{W}{W_\infty} \cos\theta \quad , \quad V = \frac{W}{W_\infty} \sin\theta \quad , \quad y = y$$

The values of $\frac{W}{W_\infty}$ at each point are calculated by imposing the condition that the values of pressure along the reference line calculated by the method of characteristics in the transonic region, and by the subsonic analysis in the elliptic region, be consistent. The dimensionless pressure, P, used in the subsonic analysis is defined by the expression, $P = \frac{p}{\rho_\infty W_\infty^2}$; calculate P where p is the value of pressure in psf at points along the reference line, calculated by the method of characteristics. By transposing the expression at the bottom of page 25

$$\sqrt{U^2 + V^2} = \frac{W}{W_\infty} = \left[c - (1+\delta) f \left(\frac{P}{f}\right)^{\left(\frac{2\cdot\delta}{1+\delta}\right)} \right]^{1/2}$$

The above approach is necessary since the value of γ varies from point to point along the reference line as computed by the method of characteristics, while γ (and δ) is held constant in the subsonic analysis.

τ is found by integrating along the reference line from the shock ($\tau = 1$) towards the body according to the following formula. Refer to Fig. II.

$$\tau_n = \frac{\tau_{ns}\,\delta\left[\frac{y_n + y_{ns}}{2} - (y_n - y_{ns})\right] + \left[(R\cdot U)_n + (R\cdot U)_{ns}\right](y_n - y_{ns}) - (x_n - x_{ns})\left[(R\cdot V)_n + (R\cdot V)_{ns}\right]}{\delta\left[\frac{(y_n + y_{ns})}{2} + (y_n - y_{ns})\right]}$$

where $\delta = \frac{\gamma - 1}{\gamma + 1}$, $R_n = \delta \frac{\rho_n}{\rho_\infty}$, $\gamma = 1/2\,(\gamma_b + \gamma_o)$

γ_b is the value at the body on the reference line

γ_o is the value behind shock at intersection with reference line

For the perturbation technique to be valid, the integration of τ along the reference line must be extremely accurate and it is necessary that all parameters used in the integration must be self-consistent. Thus R is set equal to $\left(\frac{P}{f}\right)^{\left(\frac{1-\delta}{\delta+1}\right)}$. The integration is performed using the subsonic mesh points as pivotal points and iterating on τ_n at each step to ensure maximum precision. Since the integrated value of τ at the body will not, in general, be zero, it is necessary to adjust the position (and properties) of the terminal (body) point of the reference line. This last step is iterated until the coordinates of the body point on the reference line is consistent within very close tolerance, with an integrated value of $\tau = 0$.

If a total of J points are prescribed as iteration points (excluding the stagnation point - J = 3 in above sketch), the program executes J additional sweeps through the Transonic-Subsonic regions. For each sweep, one coefficient of the "basic" shock polynominal is perturbed and the resulting deviations calculated. Thus for the jth sweep, j=1, 2, ..., J, the detached shock polynominal is of the form $F(y) = a_o + a_2 y^2 + a_4 y^4 + \Delta a_{2j} y^{2j}$, and the deviations are prescribed as $\bar{\delta}_i^{(j)}$, i = 1, 2, ..., J.

After J sweeps have been completed, a system of simultaneous equations may be written in the unknowns, C_j, as follows: $\delta_i^{(j)} = \bar{\delta}_i^{(j)} - \bar{\delta}_o^{(j)}$ (See sketch)

$$\left\{\begin{array}{l} C_1 \left(\delta_1^{(1)} - \delta_1^{(o)} \right) + C_2 \left(\delta_1^{(2)} - \delta_1^{(o)} \right) + \ldots\ldots + C_J \left(\delta_1^{(J)} - \delta_1^{(o)} \right) = - \delta_1^{(o)} \\ C_1 \left(\delta_2^{(1)} - \delta_2^{(o)} \right) + C_2 \left(\delta_2^{(2)} - \delta_2^{(o)} \right) + \ldots\ldots + C_J \left(\delta_2^{(J)} - \delta_2^{(o)} \right) = - \delta_2^{(o)} \\ \cdot \quad \cdot \quad \cdot \quad \cdot \quad \cdot \qquad\qquad\qquad\qquad \cdot \quad \cdot \quad \cdot \quad \cdot \quad \cdot \qquad \cdot \\ C_1 \left(\delta_J^{(1)} - \delta_J^{(o)} \right) + C_2 \left(\delta_J^{(2)} - \delta_J^{(o)} \right) + \ldots\ldots + C_J \left(\delta_J^{(J)} - \delta_J^{(o)} \right) = - \delta_J^{(o)} \end{array}\right\}$$

$$\text{or} \quad \sum_{m=1}^{J} C_m \left(\delta_n^{(m)} - \delta_n^{(o)} \right) = - \delta_n^{(o)} \quad , \; n = 1, 2, \ldots, J$$

The final polynominal is then written

$$\bar{F}(y) = \bar{a}_o + \bar{a}_2 y^2 + \bar{a}_4 y^4 + \ldots + a_{2j} y^{2j}$$

where $\bar{a}_{2j} = a_{2j} + C_j \cdot \Delta a_{2j}$; Δa_{2j} is the jth perturbation .

$j = 1, 2, 3, \ldots\ldots, J$

and $$\bar{a}_o = a_o - \left[\bar{\delta}_o^{(o)} + \sum_{j=1}^{J} C_j \left(\bar{\delta}_o^{(j)} - \bar{\delta}_o^{(o)} \right) \right]$$

A final sweep through the Transonic-Subsonic region uses $\bar{F}(y)$ to describe the detached shock. The points along the reference line are scaled (see below) and

written on binary tape B 3 along with the free stream conditions and the body equations, and the properties within the Subsonic region are printed as output.

The value, K (see page 19), is calculated for this final reference line, and the position of each point is adjusted as follows:

$$x_{new} = K x_{old} + (x_B - K \bar{\bar{x}}) ; \; y_{new} = K y_{old}$$

The "final" shock polynominal is modified as indicated on page 19, and the final pass through the elliptic region is then completed.

CARD	COL.	DATA	FORMAT
4, 5, . . . , A-1	2-10	a	F
	12-20	b	F
	22-30	c	F
	32-40	d	F
	42-50	e	F
	52-60	x_t	F
	62-70	α	F
A	1-72	Blank	
A + 1	1	Stagnation Point Code = 1	I
	2-10	x_o	F
	11	Point 1 Code = 1 or 2	I
	12-20	x_1	F
	21	Point 2 Code = 1 or 2	I
	22-30	x_2	F
	31	Point 3 Code = 1 or 2	I
	32-40	x_3	F
	41	Point 4 Code = 1 or 2	I
	42-50	x_4	F
	51	Point 5 Code = 1 or 2	I
	52-60	x_5	F
	61	Point 6 Code = 1 or 2	I
	62-70	x_6	F
A+2, A+3	Identical in format to card A + 1		
(if required)	Pertains to points 7 through 20, in sequence		

CARD	COL.	DATA	FORMAT
B	2-10	y_o	F
	12-20	y_1	F
	22-30	y_2	F
	32-40	y_3	F
	42-50	y_4	F
	52-60	y_5	F
	62-70	y_6	F
B+1, B+2		Identical in format to card B.	
(if required)		Pertains to points 7 through 20, in sequence	
C	1, 2	Number of intervals of mesh spacing, $\Delta\tau_1$	I
	3-10	$\Delta\tau_1$	F
	11, 12	Number of intervals of mesh spacing, $\Delta\tau_2$	I
	13-20	$\Delta\tau_2$	F
	21, 22	Number of intervals of mesh spacing, $\Delta\tau_3$	I
	23-30	$\Delta\tau_3$	F
	41, 42	Number of intervals of mesh spacing, Δy_1	I
	43-50	Δy_1	F
	51-52	Number of intervals of mesh spacing, Δy_2	I
	53-60	Δy_2	F
	61-62	Number of intervals of mesh spacing, Δy_3	I
	63-70	Δy_3	F
C + 1	1-10	The x-coordinates of the "iteration points"	F
	11-20	along the prescribed profile in ascending order	
	. . .	for the second series of sweeps. A maximum	
	61-70	of 7 points.	

CARD	COL.	DATA	FORMAT
C + 2	1-10	The y-coordinates corresponding to	F
	11-20	the previous card	
	.		
	.		
	.		
	61-70		

only. The corresponding y-coordinates are on cards (s) B (and B+1 and B+2). Note that the stagnation point must always be prescribed as an "iteration point".

To assure an accurate solution, it is advisable to prescribe at least two points adjoining the assumed sonic point on the body, as geometry points. For a spherical nose, these points should be located where the slope of the body is approximately 40° and 50° respectively. Should the body exhibit a more rapid change of curvature than does a sphere, in the neighborhood of the sonic point, then additional geometry points should be clustered in this region.

The geometry of the body should be "normalized" so that the assumed sonic point has the coordinate, $y^{*} \equiv h_s \leq 1.0$ (see sketch, page 8).

The input card, C, prescribes the τ - y mesh used in the subsonic region. As indicated, up to 3 different mesh intervals in each direction may be prescribed. Since the analysis becomes increasingly unstable as the mesh is refined, it is necessary to maintain as coarse a mesh as possible. For a spherical nose, a 5 x 5 τ -y mesh yielded very good results. In general, even for the more complex nose geometries, an 8 x 8 τ -y mesh should be a rough upper limit of mesh density. The program cannot accommodate a mesh more refined than 15 x 15.

Columns 3-10 indicate the τ mesh interval adjacent to the bow shock ($\tau = 1$), and cols. 43-50 refer to the y mesh increment adjacent to the axis of symmetry. Refer to Fig. II and the section on sample inputs and outputs for further details.

Cards C+1 and C+2 prescribe a new set of "iteration" points which are to be satisfied by the perturbation technique at the conclusion of the second series of sweeps through the transonic and subsonic flow regions. These points need not be identical to those used initially; the number of points may also differ.

Thus the number of input cards necessary for a given run varies from roughly 10 to an upper limit of 24; in most cases the number will not exceed 14.

The option of using varying mesh intervals was included so that a relatively dense mesh may be prescribed in those portions of the subsonic region where the velocity gradients are high, without impairing the stability (and accuracy) of the solution. A recommended mesh for a spherical nose is:

5 intervals @ $\Delta y_1 = 0.2$

5 intervals @ $\Delta \tau_1 = 0.2$

For those nose geometries which exhibit a very rapid change of curvature in the neighborhood of the sonic point (e.g. the Apollo configuration) it will be necessary to utilize 3 mesh intervals in each direction to obtain accurate results.

Note that the last "body card" (card A) should be blank. Thus, these may be up to 12 body profiles, followed by a blank card, followed by the nose geometry, etc. The value of x_t for all body profiles must be non-zero. The value of $\bar{x}_o$ should be positive (≥ 0) on card A + 1.

Experience has indicated that no more than 3 "iteration" points (including the stagnation point) should be prescribed for the first series of sweeps (cards A+1, A+2, and A+3). If the nose is spherical, these same three points should be prescribed on cards C+1 and C+2. If the nose is not spherical, a total of four points may be prescribed on cards C+1 and C+2. While it is possible to prescribe more than four points, the equations on page 32 tend to become singular, and the resulting solution is poor - thus the practical upper limit is four iteration points. (The example listed on page S2 is unfortunate since it represents an early test case which conflicts with the above rule.)

To locate these iteration points properly along the body profile, the following approximate criteria are recommended:

If we define

$\bar{S}$ as the distance from the axis to the assumed sonic point, along the profile of the body, then for 3 iteration points,

$$S_1 = 0$$
$$S_2 = {}^2/_3\ \bar{S}$$
$$S_3 = \bar{S}$$

For 4 iteration points

$$S_1 = 0$$
$$S_2 = {}^1/_2\ \bar{S}$$
$$S_3 = {}^3/_4\ \bar{S}$$
$$S_4 = \bar{S}$$

Thus for a spherical nose of unit radius, $\bar{S} = {}^{\pi}/_4$

$S_1 = 0,\ x_1 = y_1 = 0$ (stagnation point)

$S_2 = {}^{\pi}/_6,\ x_1 = 0.134\ ,\ y_1 = 0.5$

$S_3 = {}^{\pi}/_4,\ x_1 = 0.293,\ y_1 = 0.707$, for 3 points.

Job 5201.

Total No. of Pages iv and 173
Copy No. (4/) of (100)

TECHNICAL REPORT NO. 340

DESCRIPTION OF IBM 709/90/94 COMPUTER PROGRAMS AND ANALYSIS FOR FLOW FIELDS ABOUT BODIES OF REVOLUTION IN HYPERSONIC FLIGHT

By
E. Lieberman

Prepared For

New York Ordnance
Picatinny Arsenal
Dover, New Jersey

Under Contract No. DA-30-069-ORD-2984

Prepared By

General Applied Science Laboratories, Inc.
Merrick and Stewart Avenues
Westbury, L.I., New York

Approved By: Antonio Ferri
President

May, 1963

ACKNOWLEDGEMENTS

The flow field analysis contained herein is primarily the work of Dr. Robert Vaglio-Laurin. The major portions were extracted from previously published articles which are listed as references 2 and 3. Certain sections, however, appear in this report for the first time.

The author wishes to express his thanks to Miss Gertrude Weilerstein for her coding and write-up of the conical flow analysis and for her editing of this report. Mr. James DeGroat contributed to the coding of the SUPERSONIC program, and a refinement to the Subsonic analysis resulted from a discussion with Dr. Gino Moretti.

TABLE OF CONTENTS

TABLE OF CONTENTS

- Continued -

DESCRIPTION OF IBM 709/90/94 COMPUTER PROGRAMS AND ANALYSIS FOR FLOW FIELDS ABOUT BODIES OF REVOLUTION IN HYPERSONIC FLIGHT

By
E. Lieberman

INTRODUCTION

This report embodies all the necessary information required, for the use of the subject programs. It is assumed that the user has a general background in the physics described herein, and it is recommended that the analysis be carefully studied before any attempt is made to utilize these programs. While a knowledge of computers is not essential, it is suggested that aid should be sought where necessary to ensure that the input data cards are correctly punched, and that the operating procedures are properly executed.

The large section on Flow Diagrams is included for the purpose of completeness and is intended to serve as a guide, only for those expert programmers who have the coding available, and who wish to study the coding in some detail.

Description of Programs

The programs described in this report make it possible to generate the entire flow field about axisymmetric bodies of revolution in hypersonic flight. These "second generation" programs (see Ref. 1) can accommodate virtually any geometrical configuration, including those having very blunt noses and after-bodies with expansion and reentrant corners. The gas considered is in chemical equilibrium and includes the effects of gas dissociation and vibrational excitation.

These programs have been coded for the IBM 709/7090/7094 large scale digital computers having a 32 K (32,768 words) core capacity, and a minimum of 4 tape units on each of 2 Data Synchronizer channels. An on-line card punch is not necessary. Due to the logical nature of the analysis coupled with storage problems, it was deemed necessary to code the major portion of the program in the FAP language. Every effort was made to minimize the cost of using these programs; the entire flow field can be generated in as little as 5 minutes on the IBM 7090 computer. However, for some configurations, depending upon the free stream conditions, bluntness of nose region, and length of after-body, this machine time could increase to as much as 20 minutes; average running time is approximately 10 minutes.

To attain the utmost in efficiency and flexibility, a total of 3 program decks were formed. They are:

1. TRANSONIC-SUBSONIC program
2. SUPERSONIC program
3. FLOW FIELD program

1. TRANSONIC-SUBSONIC Program

This program accepts as input data, the free stream conditions, coordinates of points which prescribe the geometry of the nose region of the body, and a description of the mesh used in the numerical procedure of computing the flow properties in the elliptic region. These subsonic flow properties, together with the flow properties at points along a second family characteristic (reference) line which is in the transonic flow region just downstream of the sonic line, constitute the output of this program. This output is written on two magnetic tapes: one is a BCD tape which is listed on peripheral equipment, and the other is a binary tape which may be retained for subsequent use by the SUPERSONIC program. The procedure followed by the program is outlined below:

1. By satisfying continuity conditions in the nose region of the body, the approximate geometry of the detached (bow) shock is obtained and expressed in the form, $x = a_o + a_2 y^2 + a_4 y^4$. For some nose configurations, this form of the "basic" shock polynomial will be inadequate, resulting in envelopes in the transonic flow region. The term $a_8 y^8$ is then added parametrically to overcome this situation.

2. The program then marches up the bow shock and constructs a mesh of characteristic lines row by row, spanning the area between bow shock and body, in that (transonic) region of the flow field just downstream of the sonic line (fig. IV). The reference line is located and transformed into the τ-y plane.

3. With the geometry of the bow shock, and the transformed properties along the reference line, available, the calculations proceed by an inverse method, to determine the properties within the subsonic region. The calculated profile of the nose between the axis of symmetry and the point on the body common to the reference line, is compared with the given profile. Deviations in the x-direction, between the two profiles, are calculated and stored.

4. One by one, the coefficients of the "basic" shock polynominal obtained in step 1, are perturbed. After each perturbation, the program sweeps through the transonic and subsonic regions, as described in steps 2 and 3, calculating and storing the resulting deviations. There are as many coefficients perturbed and resulting sweeps, as there are prescribed "iteration" points in the nose region.

5. At the conclusion of this procedure, it is possible to solve for the corrections to be applied to the coefficients of the "basic" shock polynomial to form a "final" polynomial, such that agreement is attained between the calculated and the prescribed nose profiles. Using this "final" polynomial to describe the geometry of the bow shock, the program sweeps once more through the transonic and the subsonic regions, calculating the final properties along the reference line, and within the subsonic region.

6. The free stream conditions, final reference line, and body profile equations, are written on binary tape for subsequent use if desired.

2. SUPERSONIC Program

This program accepts as input data, the free stream conditions, properties along a reference line, and equations which prescribe the geometry of the body profile, from the reference line, downstream. The flow properties along the bow shock, along the body, and within the flow field at points on the mesh of characteristics, constitute the output of the program. An "up-dated" binary tape is also written. The procedure followed by the program is outlined below.

1. March up first family characteristic lines (slope = tan $(\theta + \mu)$) from the reference line to the bow shock, starting near the intersection of the reference line and bow shock, and gradually extending the domain until region A is completed (see fig. I).

2. March down second family characteristic lines (slope = tan$(\theta - \mu)$) from the final first family line in region A to the body, starting near the intersection of this first family line and the body. Eventually, region B of the flow field is completed.

3. The remainder of the flow field is denoted as region C. This region is constructed by first computing a point on the bow shock by utilizing the first two points on the previous second family line, and then marching down a second family line from this shock point, to the body.

4. The logic used in regions B and C, permit the program to detect discontinuities in the body profile. Thus an expansion corner - which produces a Prandtl - Meyer fan - or a reentrant corner - which is the origin of a secondary

shock - may be prescribed at any point downstream of the reference line.

5. The program can accommodate any combination of expansion corners and reentrant corners subject to the restriction that no second family characteristic line can cross more than two secondary shocks prior to intersecting the body. The program recognizes that a secondary shock may "die" within the interior of the flow field, and the logic adjusts itself accordingly. Intersection of two secondary shocks within the flow field, or of a secondary shock and the bow shock, will be correctly calculated and the mesh adjusted, only if one of the two intersecting shock is very much "weaker" than the other, at the point of intersection. If the two shocks are of substantially the same strength, then the resulting shear layer creates a discontinuity in the mesh downstream of the point of intersection, and this condition lies outside the scope of this program. Another condition which could arise is the case of a strong secondary shock causing the flow downstream to become subsonic, in which case, the method of characteristics does not apply.

Another restrictive condition is a situation where the slope of a second family line is essentially the same as the slope of a portion of the body profile. This would create a large gap in the mesh of characteristics which could cause the program to abort. While there are logical mechanisms built into the coding to control the mesh to some extent, an intrinsic condition such as that just described, can not be remedied.

6. Bodies with conical noses fall within the scope of this program; of course, only the supersonic flow field exists for these configurations. A subroutine which is included as part of the SUPERSONIC program, calculates properties along a horizontal reference line, and thus serves as a prologue to the

major portion of the program.

3. FLOW FIELD Program

This program is a CHAIN job consisting of two LINKS. Essentially, the first link is the TRANSONIC-SUBSONIC program, while the second link is the SUPERSONIC program. The automatic linkage of the two parts is accomplished by utilizing a feature of the IB FORTRAN Monitor System and the transfer of common data is done via the binary tape previously described.

The input to this program is identical to the input required by the TRANSONIC-SUBSONIC program, and the output is the sum total of the two components of the FLOW FIELD program.

The above description merely presents the overall scope of application of the subject programs. All necessary details are presented in the following sections.

While these programs have been tested for a wide range of flight conditions and body configurations, it is certain that not all possible conditions and permutations of branching have been encountered. In addition, due to the limitations of time and cost, some of the more "marginal" features of the SUPERSONIC program (LINK 2), such as shock intersections (which in general lies outside the scope of this program as indicated previously), and certain variations of "dying" secondary shocks, have not been as vigorously tested as the major components of the program.

CALCULATION OF COEFFICIENTS OF "BASIC" POLYNOMIAL TO APPROXIMATE DETACHED SHOCK

A rough guess of the detachment distance, δ_o, is found as follows:

The radius of curvature of the body at the "sonic" point (where slope is unity) is calculated numerically and denoted by R_s^*.

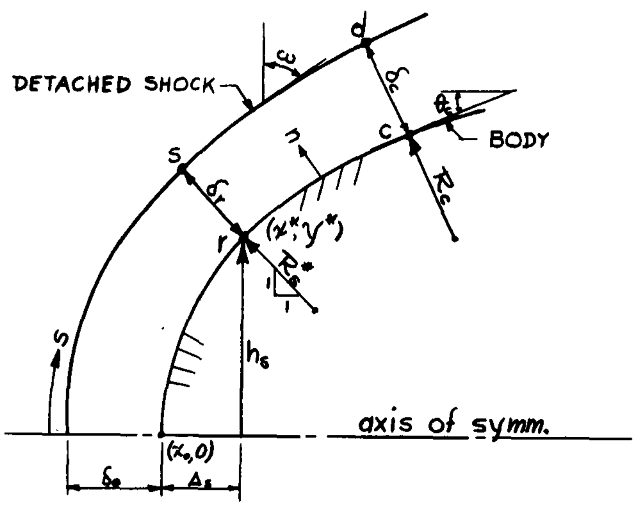

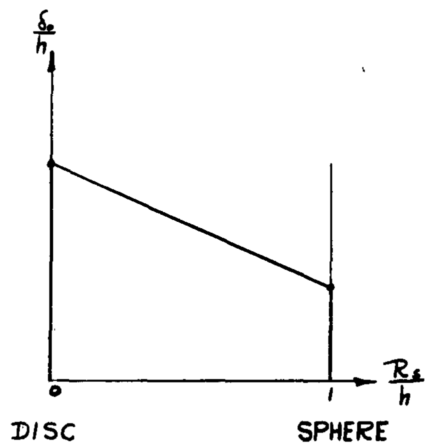

Next, cross a normal shock to obtain the density, ρ_2, and γ_n, behind it and calculate,

Sphere: $$\frac{\delta_o}{h} = \frac{2}{3} \left[\frac{\rho_2}{\rho_\infty} - 1 \right]^{-1}$$ and

Disc: $$\frac{\delta_o}{h} = 1.03 \left[\frac{\rho_2}{\rho_\infty} - 1 \right]^{-1/2}$$

where $h = h_s + R_s^* (1 - \cos 45^\circ)$. Note that $h_s = y^*$

Then, for the given body, R_s^*/h may be calculated and the corresponding value of δ_o / h may be found by linearly interpolating between those values calculated for the disc and for the sphere, as indicated in the sketch. Thus, multiplication by h yields the initial estimate of the detachment distance, δ_o, for this body. Implied in this approach, is the assumption that the point (x^*, y^*) closely approximates the sonic point on the body.

Next, we improve the approximation of δ_o, iteratively, as follows:

Compute

$$\left.\begin{aligned}
\bar{B} &= (1 + u_{w_o}) \widetilde{P}_{w_o} u_{w_o} \delta_o \left(1 + \frac{2}{3} \frac{\delta_o}{R_{b_o}} \right) \\
\bar{C} &= H_{w_o} \left(1 + \frac{\delta_o}{R_{b_o}} \right)^2 - H_o - \frac{\delta_o}{2} \left[(g_o + g_w) + \frac{1}{3} \frac{\delta_o}{R_{b_o}} (g_o + 2 g_w) \right] \\
&\quad - \frac{\delta_o}{2} \left(\frac{\gamma - 1}{\gamma + 1} \right) \frac{1}{R_{b_o}} \left[\widetilde{\Pi}_o \left(1 + \frac{\delta_o}{3 R_{b_o}} \right) + \widetilde{\Pi}_{w_o} \left(1 + \frac{2}{3} \frac{\delta_o}{R_{b_o}} \right) \right] \\
&\quad - \frac{\delta_o}{R_{b_o}} \widetilde{P}_{w_o} u_{w_o}^2 \left(1 + \frac{2}{3} \frac{\delta_o}{R_{b_o}} \right)
\end{aligned}\right\} \quad (1)$$

where R_{b_o} is the radius of the body at the axis of symmetry, calculated numerically,

and

$$\widetilde{P}_{w_o} = \frac{\gamma - 1}{\gamma + 1}\left[\frac{\gamma}{\gamma + 1} + \alpha - \left\{\left[\frac{1}{\gamma + 1} - \alpha\right]^2 - 2\beta\right\}^{1/2}\right]^{-1}$$

$$\alpha = \frac{\gamma}{\gamma_\infty}\left[(\gamma + 1) M_\infty^2\right]^{-1}, \quad \beta = \frac{1}{\gamma_\infty M_\infty^2}\left(\frac{\gamma - 1}{\gamma + 1}\right)\left[\frac{\gamma_\infty}{\gamma_\infty - 1} - \frac{\gamma}{\gamma - 1}\right]$$

$$\widetilde{\Pi}_{w_o} = \frac{1}{\gamma_\infty M_\infty^2} + 1 - \left(\frac{\gamma - 1}{\gamma + 1}\right)\frac{1}{P_{w_o}}$$

$$\left.\begin{aligned}
& U_o = \left(\frac{\gamma - 1}{\gamma + 1}\right)\frac{1}{\widetilde{P}_{w_o}}, \quad u_{w_o} = -U_o \\
& H_{w_o} = \widetilde{P}_{w_o} u_{w_o}^2 + \left(\frac{\gamma - 1}{\gamma + 1}\right)\widetilde{\Pi}_{w_o}, \quad g_{w_o} = \frac{\widetilde{\Pi}_{w_o}}{R_{b_o}}\left(\frac{\gamma - 1}{\gamma + 1}\right)
\end{aligned}\right\} \qquad (2)$$

$$c = 1 + \frac{2}{(\gamma_\infty - 1) M_\infty} \qquad \Phi_b = \widetilde{\Pi}_{w_o}\widetilde{P}_{w_o}^{-\gamma}$$

$$\tau_o = \left[\left(\frac{\gamma + 1}{2\gamma}\right) c\right]^{\frac{1}{\gamma - 1}}, \quad \widetilde{\Pi}_o = \tau_o^{\gamma}\,\Phi_b^{-\left(\frac{1}{\gamma - 1}\right)}$$

$$H_o = \left(\frac{\gamma - 1}{\gamma + 1}\right)\widetilde{\Pi}_o, \quad g_o = \frac{H_o}{R_{b_o}}, \quad \gamma = \gamma_n$$

Then $\left(\frac{d\omega}{ds}\right)_o = -\frac{\bar{C}}{\bar{B}}$ (3) and we may calculate the radius of curvature of the detached shock at the axis, R_{sh_o},

$$(R_{sh_o})^{-1} = \left(\frac{d\omega}{ds}\right)_o\left(1 + \frac{\delta_o}{R_{b_o}}\right)^{-1} \qquad (3a)$$

Solve the following two equations for the coordinates of points s:

$$x_s = x^* + y^* - y_s$$

$$y_s^2 + 2 R_{sh_o} y_s = 2 R_{sh_o} (x^* + y^* - \bar{x}_o + \delta_o) \tag{4}$$

Note that the first two terms of the detached shock polynominal are

$$a_o = \bar{x}_o - \delta_o \text{ and } a_2 = (2 R_{sh_o})^{-1}$$

Then

$$\delta_r = \frac{x_r - x_s}{\cos 45^o} \quad ; \quad x_r \equiv x^* \ , \quad y_r \equiv y^*$$

To compute the mass flow across the shock layer, δ_r , it is necessary to compute the pressure, $\widetilde{P}_w$, and velocity, v_w , behind the shock at point s. In addition these properties ($\widetilde{P}_b^*$, v_b^*) must also be computed at the sonic point on the body.

$$v_b^* = \left[\left(\frac{\gamma - 1}{\gamma + 1} \right) c \right]^{1/2} \quad , \quad \tau_b^* = \left[\left(\frac{\gamma + 1}{2 \gamma} \right) (c - v_b^{*2}) \right]^{\left(\frac{1}{\gamma - 1} \right)}$$

$$\widetilde{P}_b^* = \tau_b^* \Phi_b^{-\left(\frac{1}{\gamma - 1} \right)}$$

Then with $\tan \omega = \left(\frac{dx}{dy} \right)_s = \frac{y_s}{R_{sh_o}}$, and with $\theta = 45^o$,

$$\widetilde{P}_w = \left(\frac{\gamma - 1}{\gamma + 1} \right) \left[\frac{\gamma}{\gamma + 1} + \alpha (1 + \tan^2 \omega) - \left\{ \left[\frac{1}{\gamma + 1} - \alpha (1 + \tan^2 \omega) \right]^2 - 2 \beta (1 + \tan^2 \omega) \right\}^{1/2} \right]^{-1}$$

$$U = 1 - \left(1 - \left(\frac{\gamma - 1}{\gamma + 1} \right) \frac{1}{\widetilde{P}_w} \right) (1 + \tan^2 \omega)^{-1}$$

$$\left.\begin{aligned} V &= \tan\omega\left(1 - \left(\frac{\gamma - 1}{\gamma + 1}\right)\frac{1}{\widetilde{P}_w}\right)\left(1 + \tan^2\omega\right)^{-1} \\ v_w &= U\cos\theta + V\sin\theta \end{aligned}\right\} \quad (5)$$

It is necessary to compute the rate of change of mass flow in the direction normal to the body at the sonic point, and then assume that the variation of **mass flow is closely approximated by a parabolic across the shock δ_r.** Then

$$\left(\frac{\partial \widetilde{\Pi}}{\partial n}\right)_r = \left(\frac{\gamma + 1}{\gamma - 1}\right)\frac{\widetilde{P}_b^* \, v_b^{*2}}{R_b} \quad (6)$$

where n is the normal to the body at point r

R_b is the radius of curvature of the body at point $r = R_s^*$

From shock relations,

$$\left.\begin{aligned} &\left(\frac{1}{\omega}\frac{d\widetilde{P}_{w_o}}{d\omega}\right) = 2\left(\frac{\gamma + 1}{\gamma - 1}\right)\widetilde{P}_{w_o}^2\left[\alpha - \left\{\alpha\left(\frac{1}{\gamma + 1} - \alpha\right) - \beta\right\}\left\{\left[\frac{1}{\gamma + 1} - \alpha\right]^2 - 2\beta\right\}^{-1/2}\right] \\ &\left(\frac{\partial \widetilde{P}}{\partial n}\right)_r = \frac{\widetilde{P}_b^*}{\gamma\,\Pi_r}\left\{\left(\frac{\partial \widetilde{\Pi}}{\partial n}\right)_r - 4a_2^2\,\widetilde{P}_{w_o}^{-(\gamma+1)}\,\widetilde{P}_b^{*(\gamma+1)} \cdot v_b^* \cdot y_r \cdot \right. \\ &\qquad \left. \cdot\left\{2 + \left(\frac{\gamma + 1}{\gamma - 1}\right)\frac{1}{\widetilde{P}_{w_o}}\left(\frac{1}{\omega}\frac{d\widetilde{P}_{w_o}}{d\omega}\right)\left[\left(\frac{\gamma - 1}{\gamma + 1}\right)\frac{1}{\widetilde{P}_{w_o}} - \gamma\,\widetilde{\Pi}_{w_o}\right]\right\}\right\} \end{aligned}\right\} \quad (7)$$

where $\widetilde{\Pi}_r = \Phi_b^{-\left(\frac{1}{\gamma - 1}\right)}\,\tau_b^{*\gamma}$

From Bernoulli's equation we solve for $\left(\frac{\partial v}{\partial n}\right)_r$

$$\left.\begin{aligned}
&\left(\frac{2\gamma}{\gamma+1}\right)\frac{1}{\widetilde{P}_b^*}\left[\left(\frac{\partial \widetilde{\Pi}}{\partial n}\right)_r - \frac{\widetilde{\Pi}_r}{\widetilde{P}_b^*}\left(\frac{\partial \widetilde{P}}{\partial n}\right)_r\right] + 2\,v_b^*\left(\frac{\partial v}{\partial n}\right)_r = 0 \\
&\text{and} \\
&\left[\frac{\partial(\widetilde{P}\;v)}{\partial n}\right]_r = \widetilde{P}_b^*\left(\frac{\partial v}{\partial n}\right)_r + v_b^*\left(\frac{\partial \widetilde{P}}{\partial n}\right)_r = \frac{A_1}{\delta_r}
\end{aligned}\right\}\quad(8)$$

Then assume the variation along δ_r .

$$\widetilde{P}\,v = \widetilde{P}_b^*\;v_b^* + A_1\left(\frac{n}{\delta}\right) + A_2\left(\frac{n}{\delta}\right)^2$$

Then $A_2 = \widetilde{P}_{w_s} v_{w_s} - \widetilde{P}^*_b v^*_b - A_1$

Integrating across this shock layer, the mass flow, M , is calculated.

$$M = \frac{\widetilde{P}^*_b v^*_b}{2 \cos 45^o} \left\{ \left[y_r + \delta_r \cos 45^o \right]^2 - y_r^2 \right\} + A_1 \delta_r \left[\frac{y_r}{2} + \frac{\delta_r \cos 45^o}{3} \right] + A_2 \delta_r \left[\frac{y_r}{3} + \frac{\delta_r \cos 45^o}{4} \right] \quad (9)$$

Compare $\quad M \overset{?}{=} \left(\frac{\gamma - 1}{\gamma + 1} \right) \frac{y_s^2}{2}$

If $M \lessgtr \left(\frac{\gamma - 1}{\gamma + 1} \right) \frac{y_s^2}{2}$ then $\delta_o = \delta_o \pm \Delta \delta_o$

where $\Delta \delta_o$ is a prescribed small increment. Return to eq. (1) with this new value of δ_o , compute new coefficients a_o and a_2 and check M again using (9). Continue this iteration, adjusting δ_o as required, until continuity at the shock layer, δ_r , is satisfied. Then test

$\frac{\Delta s}{h_s} \lessgtr 0.5$ If < 0.5, the basic shock polynomial must be refined by adding an $a_4 y^4$ term. The other condition lies outside the scope of this program.

The coefficients a_o and a_2 are held fixed while a_4 is determined by satisfying continuity across the shock layer, δ_c . Using γ across the normal shock, initially set

$$\mu_c = \frac{3\pi}{4} - \theta_c - \frac{1}{2} \sqrt{\frac{\gamma + 1}{\gamma - 1}} . \tan^{-1} \left\{ \frac{\left[1 - \left(2 \left(\frac{\widetilde{\Pi}_c}{\Pi_r} \right)^{\left(\frac{\gamma - 1}{\gamma} \right)} - 1 \right)^2 \right]^{1/2}}{2 \left(\frac{\widetilde{\Pi}_c}{\Pi_r} \right)^{\left(\frac{\gamma - 1}{\gamma} \right)} - 1} \right\}$$

where $\frac{\widetilde{\Pi}_c}{\Pi_r}$ is approximated by $2 \sin^2 \theta_c$.

Then iterate on μ_c, solving for $\widetilde{P}_c$ and v_c in the process

$$\left(\frac{\widetilde{\Pi}_c}{\widetilde{\Pi}_r}\right)^{\frac{\gamma-1}{\gamma}} = 1/2\left\{1+\cos\left[2\sqrt{\frac{\gamma-1}{\gamma+1}}\left(\frac{3\pi}{4}-\theta_c-\mu_c\right)\right]\right\} \tag{10}$$

since $\theta_r + \mu_r = \frac{\pi}{4} + \frac{\pi}{2} = \frac{3\pi}{4}$

$$\widetilde{P}_c = \widetilde{P}_b^{\,*}\left(\frac{\widetilde{\Pi}_c}{\widetilde{\Pi}_r}\right)^{1/\gamma}, \quad v_c^{\,2} = c - \frac{2\gamma}{\gamma+1}\,\frac{\widetilde{\Pi}_c}{\widetilde{P}_c} \tag{11}$$

and $\mu_c = \sin^{-1}\left\{\dfrac{\left[\gamma\left(\frac{\gamma-1}{\gamma+1}\right)\frac{\widetilde{\Pi}_c}{\widetilde{P}_c}\right]^{1/2}}{v_c}\right\} = \tan^{-1}\left\{\dfrac{\left[\gamma\left(\frac{\gamma-1}{\gamma+1}\right)\frac{\widetilde{\Pi}_c}{\widetilde{P}_c}\right]^{1/2}}{\left[v_c^{\,2}-\gamma\left(\frac{\gamma-1}{\gamma+1}\right)\frac{\widetilde{\Pi}_c}{\widetilde{P}_c}\right]^{1/2}}\right\}$

Compare this value of μ_c with that used in (10); return to (10) with this value if no agreement is reached and repeat until $\left|\mu_c^{(n+1)} - \mu_c^{(n)}\right| \leqslant 10^{-4}$

It is now possible to calculate the value a_4 of the shock polynomial, $x = a_o + a_2 y^2 + a_4 y^4$, by satisfying continuity across the shock layer, δ_c. At point d

$$x_d - a_o - a_2 y_d^{\,2} - a_4 y_d^{\,4} = 0 \tag{12}$$

Setting $\delta_c = \delta_r$ initially, then with x_c, y_c, θ_c, given (inputs),

$$\left.\begin{aligned}
y_d &= y_c + \delta_c \cos\theta_c \\
x_d &= x_c - \delta_c \sin\theta_c \\
a_4 &= -\frac{1}{y_d^{\,4}}\left[a_2 y_d^{\,2} + a_o - x_d\right] \\
\left(\frac{dx}{dy}\right)_d &= \tan\omega_d = 2a_2 y_d + 4a_4 y_d^{\,3}
\end{aligned}\right\} \tag{13}$$

Compute $\widetilde{P}_w$ and v_w from (5) and then the mass flow across the shock layer, δ_c, may be computed. It is necessary to compute the rate of change of mass flow in the direction normal to the body at point c, and then assume that the variation of mass flow is closely approximated by a cubic law across the shock layer, δ_c. Then

$$\left(\frac{\partial \widetilde{\Pi}}{\partial_n}\right)_c = \left(\frac{\gamma+1}{\gamma-1}\right) \frac{\widetilde{P}_c v_c^2}{R_c} \tag{14}$$

where n is the normal to the body at point c.

R_c is the radius of curvature of the body at point c, given (input).

$\widetilde{P}_c$, v_c are calculated from (11).

From shock relations,

$$\left.\begin{aligned}
&\left(\frac{1}{\omega}\ \frac{d\widetilde{P}_{w_o}}{d\omega}\right) = 2\left(\frac{\gamma+1}{\gamma-1}\right) \widetilde{P}_{w_o}^{\,2} \left[a - \left\{ a\left(\frac{1}{\gamma+1} - a\right) - \beta \right\} \left\{ \left[\frac{1}{\gamma+1} - a\right]^2 - 2\beta \right\}^{-1/2} \right] \\
&\left(\frac{\partial \widetilde{P}}{\partial n}\right)_c = \frac{\widetilde{P}_c}{\gamma \widetilde{\Pi}_c} \left[\left(\frac{\partial \widetilde{\Pi}}{\partial n}\right)_c - 4a_2^{\,2}\ \widetilde{P}_{w_o}^{\,-(\gamma+1)}\ \widetilde{P}_c^{\,(\gamma+1)} \cdot v_c y_c \right. \\
&\qquad \left. \cdot \left\{ 2 + \left(\frac{\gamma+1}{\gamma-1}\right) \frac{1}{\widetilde{P}_{w_o}} \left(\frac{1}{\omega}\ \frac{d\widetilde{P}_{w_o}}{d\omega}\right) \left[\left(\frac{\gamma-1}{\gamma+1}\right) \frac{1}{\widetilde{P}_{w_o}} - \gamma \widetilde{\Pi}_{w_o} \right] \right\} \right]
\end{aligned}\right\} \tag{15}$$

From Bernoulli's equation, we solve for $\left(\frac{\partial v}{\partial n}\right)_c$

$$\left.\begin{aligned}
&\left(\frac{2\gamma}{\gamma+1}\right)\frac{1}{\tilde{P}_c}\left[\left(\frac{\partial\tilde{\Pi}}{\partial n}\right)_c - \frac{\tilde{\Pi}_c}{\tilde{P}_c}\left(\frac{\partial\tilde{P}}{\partial n}\right)_c\right] + 2v_c\left(\frac{\partial v}{\partial n}\right)_c = 0\\
&\text{and}\\
&\left[\frac{\partial(\tilde{P}v)}{\partial n}\right]_c = \tilde{P}_c\left(\frac{\partial v}{\partial n}\right)_c + v_c\left(\frac{\partial\tilde{P}}{\partial n}\right)_c = \frac{A_1}{\delta_c}
\end{aligned}\right\} \tag{16}$$

Then assuming the variation along δ_c,

$\tilde{P}v = \tilde{P}_c v_c + A_1\left(\frac{n}{\delta}\right) + A_3\left(\frac{n}{\delta}\right)^3$, solve for A_3

$$A_3 = \tilde{P}_{w_d} v_{w_d} - \tilde{P}_c v_c - A_1$$

Integrating across the shock layer,

$$M = \int_0^\delta \tilde{P}v\ (y_c + n\cos\theta_c)\ dn \qquad \text{or}$$

$$M = \int_0^1 \left[\tilde{P}_c v_c + A_1\left(\frac{n}{\delta}\right) + A_3\left(\frac{n}{\delta}\right)^3\right]\left[y_c + \delta_c\left(\frac{n}{\delta}\right)\cos\theta_c\right]\delta_c\, d\left(\frac{n}{\delta}\right) \qquad \text{or}$$

$$M = \frac{\tilde{P}_c v_c}{2\cos\theta_c}\left\{\left[y_c + \delta_c\cos\theta_c\right]^2 - y_c^2\right\} + A_1\delta_c\left[\frac{y_c}{2} + \frac{\delta_c\cos\theta_c}{3}\right] + A_3\delta_c\left[\frac{y_c}{4} + \frac{\delta_c\cos\theta_c}{5}\right] \tag{17}$$

Compare $M \overset{?}{=} \left(\frac{\gamma-1}{\gamma+1}\right)\frac{y_d^2}{2}$

If $M \gtrless \left(\frac{\gamma-1}{\gamma+1}\right) \frac{y_d^2}{2}$ then $\delta_c = \delta_c \pm \Delta\delta_c$

where $\Delta\delta_c$ is a prescribed, small increment. Return to (13), (5), then (14) through (17), and iterate on δ_c until continuity is satisfied. After convergence, the value of a_4 from (10) is held fixed, and from a system analogous to (12), $y_s = y_r + \delta_r \cos 45^\circ$, and since $\tan\theta_r \doteq 1$,

$$a_4 y_s^4 + a_2 y_s^2 + y_s - y_r + a_0 - x_r = 0 \tag{18}$$

Solve (18) iteratively for y_s, adjusting δ_r until (18) is satisfied. Then, $\tan\omega_s = 2a_2 y_s + 4a_4 y_s^3$

Compute (5) through (9), testing continuity and adjusting δ_0 if not satisfied; execute eqs. (1) through (3a). Then with $a_0 = \bar{x}_0 - \delta_0$ and $a_2 = (2R_{sh_0})^{-1}$, return to (18) for δ_r and y_s. Continue this iteration on δ_0 until continuity is satisfied.

When continuity is satisfied across the shock layer, δ_r, hold a_0 and a_2 fixed, and return to (12) to iterate again on δ_c, revising a_4 in the process. And so the double iteration to determine those values of a_0, a_2, and a_4 which define a basic shock polynomial continues until

$$M_{\left(\begin{smallmatrix} r,s \\ c,d \end{smallmatrix}\right)} = \left(\frac{\gamma-1}{\gamma+1}\right) \frac{y_{\left(\begin{smallmatrix} s \\ d \end{smallmatrix}\right)}^2}{2} (1 \pm 0.025) ,$$

i.e. continuity is satisfied within 2.5% across both shock layer considered, simultaneously.

For certain nose configurations which differ significantly from spheres, it is necessary to prescribe the downstream portion of the shock geometry with great precision to successfully generate a reference line and avoid the possibility of an envelope within the flow field. In such cases it is necessary to add to the basic

shock polynomial, the term $a_8 y^8$. Since the coefficient, a_8, is extremely small (and negative), this term has virtually no effect upon the mass flow calculations, and is merely used, parametrically, as a device to successfully execute the transonic region of the flow field.

Note that the preceeding analysis is based upon the assumptions of linear mass flow variation between shock and body at the axis, a parabolic variation across the shock layer, r s, and a cubic variation at the downstream section, c d. These assumptions are consistant with the physics; as one proceeds around the "shoulder", in the downstream direction this variation assumes still higher orders.

TRANSONIC ANALYSIS

After establishing the coefficients of the polynomial which prescribes the shape of the detached shock in the nose region, the program "marches up" this shock from the axis until it finds the first supersonic point. It then continues its march downstream, generating properties behind the shock at 53 additional points, constructing a mass flow-entropy table in the process.

With this information, a mesh of characteristics is constructed, extending from shock to body as indicated in Fig. IV. The reference line is that second family characteristic line which extends from the shock and terminates at the supersonic body point which is farthest upstream (closest to the axis).

At the conclusion of the Transonic analysis, the program executes a routine which transforms the properties along the reference line from the physical plane to the τ-y plane which is used by the Subsonic analysis. Some small inconsistencies arise due to the fact that γ varies from point to point in the Transonic region, while it is assumed constant in the Subsonic analysis. These inconsistencies are minimized by assigning as the γ used in the Subsonic region, the average of the values at the body point and at the axis behind the detached shock (across a normal shock). These inconsistencies are adjusted along the length of the reference line, and it has been found that they have no noticeable effect on the results.

TRANSONIC ANALYSIS

The properties behind the detached shock at 54 points are calculated in the same manner as those in the Supersonic program (see page 37). The only difference is that the value of ϵ at every point is calculated from the derivative of the shock polynomial, $F_y(y)$, rather than by computing $\Delta\epsilon$, as is necessary in the supersonic program.

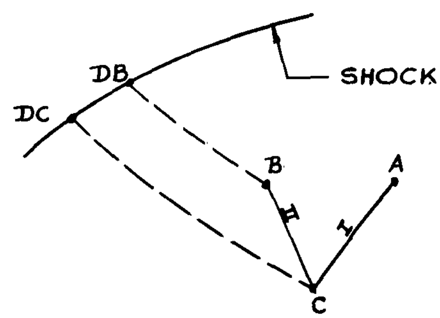

INTERIOR POINT

The properties of points A, B, and coordinates of DB are known; the properties of point C, and the coordinates of point DC are required.

Points DB and DC are defined as those shock points having the same entropy as points B and C, respectively.

$$x_c = \frac{y_B - y_A - x_B \tan(\theta-\mu)_B + x_A \tan(\theta+\mu)_A}{\tan(\theta+\mu)_A - \tan(\theta-\mu)_B}$$

$$y_c = y_A + (x_c - x_A)\tan(\theta+\mu)_A$$

$$y_{DC} = \left[y_{DB}^2 - \frac{\rho_B W_B}{\rho_\infty W_\infty} \frac{(y_C^2 - y_B^2)\sin\mu_B}{\sin(\theta-\mu)_B} \right]^{1/2}$$

$$x_{DC} = F(y_{DC})$$

If $y_{DC} < 0$, then point C lies within the domain of the body - see analysis of Body Point, below.

Compute the mass flow at point DC and enter the entropy table to extract $\left(\frac{S}{R}\right)_{DC}$. Then

$$\left(\frac{S}{R}\right)_C = \left(\frac{S}{R}\right)_{DC}$$

The remaining properties are calculated in the same manner as an interior point for the Supersonic program (page 43).

BODY POINT

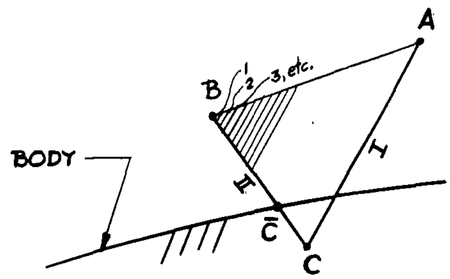

Since the test $y_{DC} < 0$ identifies point C as being within the domain of the body, it is necessary to iterate to locate a point on the surface of the body, which corresponds to $y_{DC} = 0$.

The program divides the line BA into 40 segments, establishes the properties of points 1, 2, 3, ... by interpolation, and successively calculates new points "C", using point B and points 1, 2, 3, ... until $y_{DC} < 0$ once again. By interpolating, the properties of point $\bar{C}$, on the surface of the body are determined within very close tolerances.

SUBSONIC ANALYSIS

At the completion of the transonic region, the reference line is defined, and the program then transforms the properties of all points on the reference line, from the physical x-y plane to the τ-y plane. The properties along the reference line required by the Subsonic analysis are U, V, τ and y.

$$U = \frac{W}{W_\infty}\cos\theta \quad , \quad V = \frac{W}{W_\infty}\sin\theta \quad , \quad y = y$$

and τ is found by integrating along the reference line from the shock ($\tau = 1$) towards the body according to the following formula. Refer to Fig. II.

$$\tau_n = \tau_{ns} \frac{\delta\left[\frac{y_n + y_{ns}}{2} - (y_n - y_{ns})\right] + \left[(R\cdot U)_n + (R\cdot U)_{ns}\right](y_n - y_{ns}) - (x_n - x_{ns})\left[(R\cdot V)_n + (R\cdot V)_{ns}\right]}{\delta\left[\frac{(y_n + y_{ns})}{2} + (y_n - y_{ns})\right]}$$

where $\delta = \dfrac{\gamma - 1}{\gamma + 1}$, $R_n = \delta \dfrac{\rho_n}{\rho_\infty}$, $\gamma = 1/2\,(\gamma_b + \gamma_n)$

γ_b is the value at the body on the reference line

γ_n is the value behind a normal shock (detached shock at the axis)

Since τ_{body} will not equal zero identically, the "noise" is distributed uniformly along the reference line as follows:

$$\tau_n = \frac{\tau_n^* - \tau_b}{1 - \tau_b}$$

where τ_n^* is the value calculated by the integration scheme, above.

τ_b is the value calculated at the body ($\neq 0$)

τ_n is the adjusted value at each point, n, on the reference line.

τ_b is assumed very small compared to unity ($<< 0.1$), and test runs have indicated that this assumption is correct.

SUBSONIC ANALYSIS

At each interior mesh line of constant τ, we set up and solve a system of linear equations in the unknown velocity components, U and V. Since the analysis is non-linear, the coefficients of the system being functions of the unknowns, it is necessary to approximate the unknowns first, using differencing techniques, compute these coefficients, and then solve the system to obtain the variation of U and V (as well as the other desired properties) along the mesh line, from the axis of symmetry to the reference line. To refine and improve the stability of the solution, the procedure is repeated once more, utilizing the more accurate values of U and V resulting from the first solution. Notably, the derivatives with respect to τ are significantly refined. Refer to Fig. II.

$$\left.\begin{aligned}
&\tan \phi_{ns} = \frac{y_n - y_{ns}}{\tau_n - \tau_{ns}} \\
&\left(\frac{dU}{d\tau}\right)_{ns} = \left[\frac{\partial U}{\partial \tau} + \frac{\partial U}{\partial y} \tan \phi\right]_{ns} \\
&\left(\frac{dV}{d\tau}\right)_{ns} = \left[\frac{\partial V}{\partial \tau} + \frac{\partial V}{\partial y} \tan \phi\right]_{ns} \\
&\text{For a first approximation of the unknowns } U_n \text{ and } V_n, \\
&U_n = U_{ns} + \left(\frac{dU}{d\tau}\right)_{ns} \left(\tau_n - \tau_{ns}\right) \\
&V_n = V_{ns} + \left(\frac{dV}{d\tau}\right)_{ns} \left(\tau_n - \tau_{ns}\right)
\end{aligned}\right\} \quad (1)$$

Substitute the above Un and Vn into the following Equation (2)

$$
\left.\begin{aligned}
A_1 &= V\left\{1+\frac{(\delta-1)}{(\delta+1)}\ \frac{\tau U}{f}\left[\frac{(c-U^2-V^2)}{(1+\delta)f}\right]^{-\frac{(1+\delta)}{2\delta}}\right\}\\
A_2 &= \tau-\left(\frac{U}{\delta}\right)\left[\frac{(c-U^2-V^2)}{(1+\delta)f}\right]^{\frac{1-\delta}{2\delta}}\\
B_1 &= -U+\tau\left[\frac{(c-U^2-V^2)}{(1+\delta)f}\right]^{\frac{\delta-1}{2\delta}}\left\{\delta+\left[\frac{(\delta-1)}{(\delta+1)}\right]V^2\left[\frac{(c-U^2-V^2)}{(1+\delta)}\right]^{-1}\right\}\\
B_2 &= -\frac{V}{\delta}\left[\frac{(c-U^2-V^2)}{(1+\delta)f}\right]^{\frac{1-\delta}{2\delta}}\\
C_1 &= \frac{-(\delta-1)}{2(1+\delta)}\ \frac{y}{f}\cdot U\cdot V\cdot\left[\frac{(c-U^2-V^2)}{(1+\delta)f}\right]^{-\frac{(\delta+1)}{2\delta}}\\
C_2 &= -\frac{y}{2}\\
D_1 &= -\frac{y}{2}\left[\frac{(c-U^2-V^2)}{(1+\delta)f}\right]^{\frac{(\delta-1)}{2\delta}}\left\{\delta+\frac{(\delta-1)}{(\delta+1)}\ V^2\left[\frac{(c-U^2-V^2)}{(1+\delta)}\right]^{-1}\right\}\\
D_2 &= 0\\
E_1 &= \frac{-V\delta}{2}\left[\frac{(c-U^2-V^2)}{(1+\delta)f}\right]^{\frac{(\delta-1)}{2\delta}}\\
E_2 &= \frac{(\delta-1)}{2\delta}\left[\frac{(c-U^2-V^2)}{(1+\delta)f}\right]^{\frac{(\delta+1)}{2\delta}}\cdot\frac{\partial f}{\partial T}\\
R &= \left[\frac{(c-U^2-V^2)}{(1+\delta)f}\right]^{\frac{(1-\delta)}{2\delta}}\\
P &= f\left[\frac{(c-U^2-V^2)}{(1+\delta)f}\right]^{\frac{(1+\delta)}{2\delta}}
\end{aligned}\right\}\qquad (2)
$$

where $f \equiv f(\tau y^2) = P^* R^{*(-\gamma)}$, $\delta = \frac{\gamma - 1}{\gamma + 1}$, $c = \left[\frac{2}{(\gamma_\infty - 1)} \cdot \frac{1}{M_\infty^2} \right] + 1$

$$P^* = \frac{1}{\gamma_\infty M_\infty^2} + \left[\frac{1}{(\gamma+1)(1+g)} - a \right] + \left[a^2 - \frac{\frac{2a}{(\gamma+1)} + 2\beta}{(1+g)} + \frac{1}{(\gamma+1)^2 (1+g)^2} \right]^{1/2}$$

$$\frac{\delta}{R^*} = \left[\frac{\gamma}{(\gamma+1)} + a(1+g) \right] - \left[\frac{1}{(\gamma+1)^2} - \left(\frac{2a}{(\gamma+1)} + 2\beta \right)(1+g) + a^2 (1+g)^2 \right]^{1/2}$$

$$\frac{\partial f}{\partial \tau} = \frac{P^* \gamma}{\delta} \left(\frac{1}{R^*} \right)^{\gamma-1} \frac{\partial g}{\partial \tau} \left\{ a + \left[\left(\frac{a}{(\gamma+1)} + \beta \right) - a^2 (1+g) \right] \left[\frac{1}{(\gamma+1)^2} - \left(\frac{2a}{(\gamma+1)} + 2\beta \right)(1+g) + a^2 (1+g)^2 \right]^{-1/2} \right\}$$

$$+ \left(\frac{1}{R^*} \right)^{\gamma} \frac{1}{(1+g)^2} \frac{\partial g}{\partial \tau} \left\{ -\frac{1}{(\gamma+1)} + \left[\left(\frac{a}{(\gamma+1)} + \beta \right) - \frac{1}{(\gamma+1)^2 (1+g)} \right] \left[a^2 - \frac{\left(\frac{2a}{(\gamma+1)} + 2\beta \right)}{(1+g)} + \frac{1}{(\gamma+1)^2 (1+g)^2} \right]^{-1/2} \right\}$$

$$g = \sum_{m=2,4\ldots}^{m_1} C_m \tau^{\left(\frac{m}{2}\right)} y^m \quad \text{and} \quad \frac{\partial g}{\partial \tau} = \sum_{m=2,4\ldots}^{m_1} \frac{m}{2} C_m \tau^{\left(\frac{m}{2} - 1\right)} y^m$$

where $g = g(\tau, y)$, consisting of the terms of the polynomial, F_y^2, with the τ term inserted as indicated.

$F(y)$ is polynomial defining shock curve

$F_y = dF/dy$

$$a = \left(\frac{\gamma}{\gamma+1} \right) \frac{1}{\gamma_\infty M_\infty^2}$$

$$\beta = \frac{(\gamma-1)}{(\gamma+1)} \left[\left(\frac{\gamma_\infty}{(\gamma_\infty - 1)} - \frac{\gamma}{(\gamma-1)} \right) \frac{1}{\gamma_\infty M_\infty^2} \right]$$

$$\left.\begin{aligned} \overline{C}_{in} &= C_{in} - A_{in} \tan \phi_{ns} \\ \overline{D}_{in} &= D_{in} - B_{in} \tan \phi_{ns} \end{aligned}\right\} \quad i = 1, 2$$

At point n, two equations are obtained ($1 \le n \le p-1$)

$$a_{in} U_n + c_{in}(U_{(n+1)} - U_{(n-1)}) + b_{in} V_n + d_{in}(V_{(n+1)} - V_{(n-1)}) + e_{in} = 0 \qquad (3)$$

i = 1, 2; in the unknowns U and V

where $a_{in} = 2A_{in}$

$b_{in} = 2B_{in}$

$$c_{in} = \overline{C}_{in} \frac{(\tau_n - \tau_{ns})}{(y_{(n+1)} - y_{(n-1)})}$$

$$d_{in} = \overline{D}_{in} \frac{(\tau_n - \tau_{ns})}{(y_{(n+1)} - y_{(n-1)})}$$

$$e_{in} = -2(A_{in} U_{ns} + B_{in} V_{ns}) - (A_{in}(\overline{\frac{dU}{d\tau}}) + B_{in}(\overline{\frac{dV}{d\tau}}) - E_{in})(\tau_n - \tau_{ns})$$

when n = 1, then $U_{n-1} = U\Big]_{y=o}$ is found:

$$U\left[(c-U^2)/(1+\delta)\, f(0)\right]^{\frac{(1-\delta)}{2\delta}} = \tau\delta$$

and $\partial V/\partial\tau\Big]_{y=o} = \left(\frac{\partial U}{\partial y}\right)_o = V_o = 0$

At the axis,

$$U_{y=o} = \tau\delta\left[\frac{(c-U^2)}{(1+\delta)f(0)}\right]^{\frac{\delta-1}{2\delta}} \quad \text{iteratively}$$

initially set $U = \frac{\tau}{10}$

For the first solution, $\overline{\frac{dU}{d\tau}} = \left(\frac{dU}{d\tau}\right)_{ns}$ and $\overline{\frac{dV}{d\tau}} = \left(\frac{dV}{d\tau}\right)_{ns}$.

However, for the second, "refined" solution, $\frac{dU}{d\tau} = 1/2\left[\left(\frac{dU}{d\tau}\right)_{ns} + \left(\frac{dU}{d\tau}\right)_{n}\right]$

and $\frac{dV}{d\tau} = 1/2\left[\left(\frac{dV}{d\tau}\right)_{ns} + \left(\frac{dV}{d\tau}\right)_{n}\right]$ where $\left(\frac{dU}{d\tau}\right)_{n}$ and $\left(\frac{dV}{d\tau}\right)_{n}$ are calculated

from the results of Eqs. (5) evaluated at the end of the first solution.

Equation (3) forms a system of 2(p-1) linear algebraic equations which are solved simultaneously yielding the values of U_n, V_n ($1 \le n \le p-1$). Using these values the following expressions are evaluated:

$$\left.\begin{aligned} \left(\frac{\partial U}{\partial y}\right)_n &= \frac{U_{(n+1)} - U_{(n-1)}}{y_{(n+1)} - y_{(n-1)}} \\ \left(\frac{\partial V}{\partial y}\right)_n &= \frac{V_{(n+1)} - V_{(n-1)}}{y_{(n+1)} - y_{(n-1)}} \end{aligned}\right\} \quad 1 \le n \le p-1 \tag{4}$$

$$\left.\begin{aligned} A_1\left(\frac{\partial U}{\partial \tau}\right) + B_1\left(\frac{\partial V}{\partial \tau}\right) + C_1\left(\frac{\partial U}{\partial y}\right) + D_1\left(\frac{\partial V}{\partial y}\right) + E_1 = 0 \\ A_2\left(\frac{\partial U}{\partial \tau}\right) + B_2\left(\frac{\partial V}{\partial \tau}\right) + C_2\left(\frac{\partial U}{\partial y}\right) + E_2 = 0 \end{aligned}\right\} \tag{5}$$

Solve (5) for $\left(\frac{\partial U}{\partial \tau}\right)_n$ and $\left(\frac{\partial V}{\partial \tau}\right)_n$

The solution of the 2 (p-1) linear simultaneous equations, and Eq. (4) and (5) above, yield the necessary parameters at every point, n, n = 1, 2, ..., p-1.

Using the values of U_n, V_n, $\left(\frac{\partial U}{\partial T}\right)_n$, and $\left(\frac{\partial V}{\partial T}\right)_n$, just calculated, return to Eqs. (2), (3), (4), and (5). Then the following is calculated, and the program "marches" to the next mesh line.

To affect the transformation from T to the physical x:

Within the flow field,

$$dx = -\frac{1}{R \cdot V}\left[\left(y\frac{\delta}{2}\right)dT + (T \cdot \delta - R \cdot U)\, dy\right]$$

in difference form:

$$x_n = x_{ns} - \left\{\frac{1}{(R \cdot V)_n + (R \cdot V)_{ns}}\left[\frac{(y_n + y_{ns})\,\delta}{2}(T_n - T_{ns}) + \left[(T_n + T_{ns})\,\delta - (R_n \cdot U_n + R_{ns} \cdot U_{ns})\right](y_n - y_{ns})\right]\right\}$$

At the axis,

$$dx = -\frac{\frac{U}{2T}}{\frac{\partial V}{\partial y}}\, dT$$

In difference form:

$$x_n = x_{ns} - \frac{\left(\frac{U}{2T}\right)_{ns} + \left(\frac{U}{2T}\right)_n}{\left(\frac{\partial V}{\partial y}\right)_{ns} + \left(\frac{\partial V}{\partial y}\right)_n}(T_n - T_{ns}) = x_{ns} - \frac{(U_n + U_{ns})\quad(T_n - T_{ns})}{(T_n + T_{ns})\left(\frac{\partial V}{\partial y_{ns}} + \frac{\partial V}{\partial y_n}\right)} \qquad (6)$$

Knowing the values of x along the shock, the values of x along line 1 may be computed, and this procedure repeated until the body is described.

BEHIND SHOCK WAVE

$$U = 1 - \left[\frac{1}{(\gamma+1)(1+F_y^2)} - \alpha\right] - \left[\alpha^2 - \frac{\frac{2\alpha}{(\gamma+1)} + 2\beta}{(1+F_y^2)} + \frac{1}{(1+F_y^2)^2(\gamma+1)^2}\right]^{1/2}$$

$$V = F_y\left[\frac{1}{(\gamma+1)(1+F_y^2)} - \alpha\right] + F_y\left[\alpha^2 - \frac{\frac{2\alpha}{(\gamma+1)} + 2\beta}{(1+F_y^2)} + \frac{1}{(1+F_y^2)^2(\gamma+1)^2}\right]^{1/2}$$

$$\frac{\partial U}{\partial y} = \frac{2F_y F_{yy}}{(1+F_y^2)^2}\left\{\frac{1}{(\gamma+1)} - \frac{\left[\left(\frac{\alpha}{\gamma+1}+\beta\right) - \frac{1}{(\gamma+1)^2(1+F_y^2)}\right]}{\left[\alpha^2 - \frac{\frac{2\alpha}{\gamma+1} + 2\beta}{(1+F_y^2)} + \frac{1}{(\gamma+1)^2(1+F_y^2)^2}\right]^{1/2}}\right\}$$

$$\frac{\partial V}{\partial y} = F_{yy}(1-U) - F_y\frac{\partial U}{\partial y} \quad \text{where } F_{yy} = \frac{d^2F(y)}{dy^2}$$

Solve the following 2 sim. equ. for $\frac{\partial U}{\partial \tau}$ and $\frac{\partial V}{\partial \tau}$

$$\left.\begin{aligned} A_1\frac{\partial U}{\partial \tau} + B_1\frac{\partial V}{\partial \tau} + C_1\frac{\partial U}{\partial y} + D_1\frac{\partial V}{\partial y} + E_1 &= 0 \\ A_2\frac{\partial U}{\partial \tau} + B_2\frac{\partial V}{\partial \tau} + C_2\frac{\partial U}{\partial y} + E_2 &= 0 \end{aligned}\right\}$$

where A_i, B_i, C_i, D_i, E_i ($i = 1, 2$) are found from (2).

These properties are calculated at mesh points along the mesh line, $\tau = 1$.

ITERATION ON DETACHED SHOCK POLYNOMIAL

After the "basic" shock polynomial, which is of the form, $x = F(y) = a_o + a_2 y^2 + a_4 y^4 + a_8 y^8$, has been generated (see page 8), the program sweeps through the Transonic and Subsonic regions, calculating as an end result, the profile of the body in the vicinity of the nose. The profile calculated will not, in general, agree with the prescribed body geometry. The deviations in the x - direction along the body, at the prescribed interation points (see section on Input Format, page 77), i, are calculated as $\delta_i^{(o)}$. The superscript (o), identifies these δ_i as being caused by the "basic" shock polynomial. See sketch below.

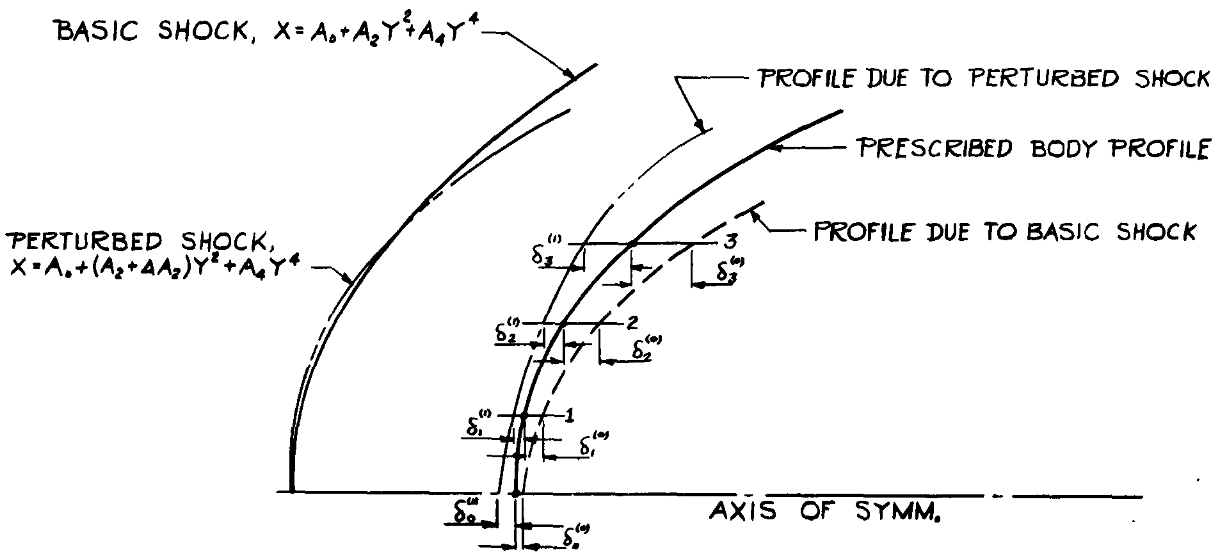

If a total of J points are prescribed as iteration points (excluding the stagnation point - J = 3 in above sketch), the program executes J additional sweeps through the Transonic-Subsonic regions. For each sweep, one coefficient of the "basic" shock polynomial is perturbed and the resulting deviations calculated. Thus for the jth sweep, j= 1, 2, ... , J, the detached shock polynomial is of the form $F(y) = a_o + a_2 y^2 + a_4 y^4 + a_8 y^8 + \Delta a_{2j} y^{2j}$, and the deviations are prescribed as $\delta_i^{(j)}$, i = 1, 2, ... , J. Note that a_8 may be zero.

After J sweeps have been completed, a system of simultaneous equations may be written in the unknowns, C_j, as follows:

$$\left\{ \begin{array}{l} C_1 \delta_1^{(1)} + C_2 \delta_1^{(2)} + C_3 \delta_1^{(3)} + \ldots\ldots + C_J \delta_1^{(J)} = -\delta_1^{(0)} \\ C_1 \delta_2^{(1)} + C_2 \delta_2^{(2)} + C_3 \delta_2^{(3)} + \ldots\ldots + C_J \delta_2^{(J)} = -\delta_2^{(0)} \\ C_1 \delta_J^{(1)} + C_2 \delta_J^{(2)} + C_3 \delta_J^{(3)} + \ldots\ldots + C_J \delta_J^{(J)} = -\delta_J^{(0)} \end{array} \right\}$$

The final polynomial is then written

$$\bar{F}(y) = \bar{a}_o + \bar{a}_2 y^2 + \bar{a}_4 y^4 + \ldots + a_{2j} y^{2J}$$

where $\bar{a}_{2j} = a_{2j} + C_j \cdot \Delta a_{2j}$; Δa_{2j} is the jth perturbation.

$j = 1, 2, 3, \ldots\ldots, J$

and $$\bar{a}_o = a_o - \left[\delta_o^{(0)} + \sum_{j=1}^{J} C_j \left[\delta_o^{(j)} - \delta_o^{(0)} \right] \right]$$

A final sweep through the Transonic-Subsonic region uses $\bar{F}(y)$ to describe the detached shock. The points along the reference line are written on binary tape B 3 along with the free stream conditions and the body equations, and the properties within the Subsonic region are printed as output.

SUPERSONIC ANALYSIS

The flow properties at points along that reference line generated during the final sweep through the Transonic region, represent the initial conditions for calculation of the Supersonic flow field. In addition, the free stream conditions and the geometry of the after-body are required.

With this information, a mesh of characteristic lines is constructed, and the flow properties at each mesh point are calculated. To conserve machine time (and paper), the flow properties at every other interior point in region C (see fig. 1) is written on magnetic tape for subsequent listing. However, if a secondary shock is encountered, thereafter all points are written.

Preliminary Properties:

$$W_\infty = M_\infty a_\infty = M_\infty \sqrt{\gamma_\infty \cdot R \cdot T_\infty}$$

$$K_1 = 2\, Cp_\infty T_\infty + W_\infty^2$$

where $R = 1716$, $Cp_\infty = 6006$, $\gamma_\infty = 1.4$

$$T_t = \frac{K_1}{2\, Cp_\infty} - \frac{\gamma_\infty - 1}{\gamma_\infty} \frac{\theta'}{e^{\theta'/T_t} - 1}$$

solve by iteration where T_t initially $= \dfrac{K_1}{2\, Cp_\infty}$; $\theta' = 5500$

$$E_\infty = \frac{e^{\theta'/T_\infty}}{e^{\theta'/T_\infty} - 1}, \qquad \Gamma_\infty = \frac{\gamma_\infty}{\gamma_\infty - 1}$$

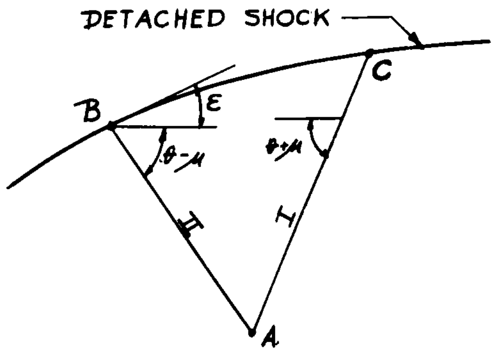

Point on Detached Shock

The following properties are known at Points A & B:

$x, y, P', \theta, \frac{S}{R}, h', \rho', \gamma, \mu, m, W$

In addition, ϵ_B and Γ_B are known.

The object is to generate the same properties at point C, as at point B.

To determine the change in curvature of the shock between points B and C, certain derivatives must be evaluated at point B:

Calling $F_y = \cot \epsilon_B$

$$\rho_B = 0.002498 \; e^{2.302585\, \rho'_B}, \quad p_B = 2116.4 \; e^{P'_B}$$

$$u = W_\infty \left[\frac{1 - (1 - \frac{\rho_\infty}{\rho_B})}{(1 + F_y^2)} \right], \quad v = W_\infty F_y \frac{(1 - \frac{\rho_\infty}{\rho_B})}{(1 + F_y^2)}$$

$$\frac{dp}{d\epsilon} = \rho_\infty W_\infty^2 (1 + F_y^2)^{-1} \left[\frac{d}{d\epsilon} \left(1 - \frac{\rho_\infty}{\rho_B}\right) + 2 \left(1 - \frac{\rho_\infty}{\rho_B}\right) F_y \right]$$

$$\frac{du}{d\epsilon} = - \frac{1}{\rho_\infty W_\infty} \frac{dp}{d\epsilon}, \quad \frac{dv}{d\epsilon} = - \left(\frac{du}{d\epsilon} + \frac{v(1 + F_y^2)}{F_y^2} \right) F_y$$

$$\left(\frac{d\theta}{d\epsilon}\right)_B = \frac{u\dfrac{dv}{d\epsilon} - v\dfrac{du}{d\epsilon}}{u^2 + v^2}$$

$$\left(\frac{dP'}{d\epsilon}\right)_B = \frac{1}{p_B}\frac{dp}{d\epsilon}$$

Then

$$\Delta\epsilon = \frac{1}{\left(\dfrac{\sin 2\mu}{2\gamma}\right)_A \left(\dfrac{dP'}{d\epsilon}\right)_B + \left(\dfrac{d\theta}{d\epsilon}\right)_B} \left\{ \left(\frac{\sin 2\mu}{2\gamma}\right)_A (P'_A - P'_B) + \theta_A - \theta_B \right.$$

$$\left. + \left[\frac{\sin\mu \sin\theta}{y\cos(\theta+\mu)}\right]_A \left[\frac{\left[y - x\tan(\theta+\mu)\right]_A - \left[y - x\tan\epsilon\right]_B}{\tan(\theta+\mu)_A - \tan\epsilon_B} + x_A\right] \right\}$$

$$x_c = \frac{y_B - y_A + x_A \tan(\theta+\mu) - x_B \tan\epsilon_B\left(1 + \dfrac{\Delta\epsilon}{\sin 2\epsilon_B}\right)}{\tan(\theta+\mu) - \tan\epsilon_B\left(1 + \dfrac{\Delta\epsilon}{\sin 2\epsilon_B}\right)}$$

$$y_c = y_A + (x_c - x_A)\tan(\theta+\mu)_A$$

$$\epsilon_c = \epsilon_B + \Delta\epsilon$$

$m_c = \rho_\infty W_\infty \left[y_c^2 - \epsilon\, y_1^2\right]$ to be stored in table. (see page 67)

The above equations for x_c, y_c, and $\Delta\epsilon$ do not apply if $(\theta+\mu)_A = 90^\circ \pm 1^\circ$. See page 42 .

Now, iterate on Γ to calculate the remaining properties behind the shock at point C.

<u>Iteration on Γ :</u>

Initially, set $\Gamma_c = \Gamma_B$

Then, $F_y = \cot \epsilon_c$

$$\alpha = \frac{\Gamma_c}{\gamma_\infty(\Gamma_c + 1)M_\infty^2}, \qquad \beta = \frac{1}{\Gamma_c + 1}\left[\frac{\Gamma_c - 1}{\gamma_\infty - 1} - \frac{\Gamma_c}{\gamma_\infty}\right]\frac{1}{M_\infty^2}$$

$$B = \left\{\left(\frac{1}{\Gamma_c + 1}\right)^2 - 2\left(\frac{\alpha}{\Gamma_c + 1} + \beta\right)\left(1 + F_y^2\right) + \alpha^2\left(1 + F_y^2\right)^2\right\}^{1/2}$$

$$\left(1 - \frac{\rho_\infty}{\rho_c}\right) = \frac{1}{\Gamma_c + 1} - \alpha\left(1 + F_y^2\right) + B$$

$$\rho_c = \frac{\rho_\infty}{1 - (1 - \frac{\rho_\infty}{\rho_c})}$$

$$p_c = p_\infty + \rho_\infty W_\infty^2 \left(1 - \frac{\rho_\infty}{\rho_c}\right)\left(1 + F_y^2\right)^{-1}$$

$$h_c = \frac{\Gamma_c}{\left(\Gamma_c - 1\right)}\frac{p_c}{\rho_c}$$

$$h_c' = \frac{h_c}{4.506 \cdot 10^6}, \qquad P_c' = \ln\left(\frac{p_c}{2116.4}\right)$$

$$\rho_c' = \frac{1}{2.302585}\ln\left(\frac{\rho_c}{0.002498}\right)$$

Test for either dissociated gas analysis, page 38 , or vibrational excitation gas analysis page 39 .

Dissociated Gas Analysis - Detached Shock Point

$$\left(\frac{S}{R}\right)_c = \sum_{i=0}^{4} \sum_{j=0}^{5} Aij \; (P'_c)^i \; (h'_c)^j$$

$$\Delta \rho' = \frac{\left(\frac{S}{R}\right)_c - \sum_{m=0}^{4} \sum_{n=0}^{5} Bmn \left(\rho'_c\right)^m \left(h'_c\right)^n}{\sum_{m=0}^{4} \sum_{n=0}^{5} m \, . \, Bmn \left(\rho'_c\right)^{(m-1)} \left(h'_c\right)^n}$$

$$\Delta \Gamma = -2.30259 \left(\frac{\rho_\infty}{\rho_c}\right) (\Gamma_c + 1) \; \Delta\rho'_c \left\{ \frac{1}{\Gamma_c + 1} + \frac{\alpha}{\Gamma_c} (1 + F_y^2) \right.$$

$$+ \frac{1}{B} \left[\frac{1}{(\Gamma_c + 1)^2} + (1 + F_y^2) \left(\frac{\alpha}{(\Gamma_c + 1)} \frac{(1 - \Gamma_c)}{\Gamma_c} + \frac{2\beta}{(\Gamma_c - 1)} + \frac{1}{\gamma_\infty M_\infty^2 (\Gamma_c - 1)} \right) \right.$$

$$\left.\left. - \frac{\alpha^2}{\Gamma_c} (1 + F_y^2)^2 \right] \right\}^{-1}$$

$$\Gamma_c = \Gamma_c + \Delta \Gamma$$

Iterate on Γ_c until $|\Delta \Gamma| < 10^{-6}$

Continued on page 40 .

VIBRATIONAL EXCITATION GAS ANALYSIS - DETACHED SHOCK POINT

$$T_c = \frac{h_c}{C_{p_\infty}} - \frac{\gamma_\infty - 1}{\gamma_\infty} \quad \frac{\theta'}{\left(e^{\theta'/T_c} - 1\right)}$$

Iterate for T_c , with T_c initially $= \dfrac{h_c}{C_{p_\infty}}$

If $\theta'/T_c > 70$, then $T_c = \dfrac{h_c}{C_{p_\infty}}$

$$\Delta\rho'_c = \frac{1}{2.30259} \; \ell n \left(\frac{T^*}{T_c}\right) \text{ where } T^* = \frac{p_c}{\rho_c R}.$$

$$\Delta\Gamma = -2.30259 \frac{\rho_\infty}{\rho_c} (\Gamma_c + 1)\, \Delta\rho'_c \left\{ \frac{1}{\Gamma_c + 1} + \frac{\alpha}{\Gamma_c} (1 + F_y^2) \right.$$

$$\left. + \frac{1}{B}\left[\frac{1}{(\Gamma_c + 1)^2} + (1+F_y^2)\left(\frac{\alpha}{\Gamma_c + 1} \quad \frac{(1-\Gamma_c)}{\Gamma_c} + \frac{2\beta}{\Gamma_c - 1} + \frac{1}{\gamma_\infty M_\infty^2 (\Gamma_c - 1)}\right) - \frac{\alpha^2}{\Gamma_c}(1+F_y^2)^2\right]\right\}^{-1}$$

$$\Gamma_c = \Gamma + \Delta\Gamma$$

Iterate on Γ until $|\Delta\Gamma| < 10^{-6}$

Continued on page 40 .

The final values of P'_c , p_c , ρ'_c , ρ_c , h'_c , h_c are now calculated, using either dissociated gas analysis or vibrational excitation gas analysis, depending upon the physics at the particular shock point. Note that $\left(\frac{S}{R}\right)_c$ has been calculated for the dissociated gas analysis only; and has been stored in table. Now we may compute θ_c :

$$u_c = W_\infty \left[1 - \frac{\left(1 - \frac{\rho_\infty}{\rho_c}\right)}{\left(1 + F_y^2\right)} \right], \quad v_c = \frac{W_\infty F_y \left(1 - \frac{\rho_\infty}{\rho_c}\right)}{\left(1 + F_y^2\right)}$$

$$\theta_c = \tan^{-1} \left(\frac{v}{u}\right)_c$$

It is now necessary to calculate the parameter, $\frac{d}{d\epsilon}\left(1 - \frac{\rho_\infty}{\rho_c}\right)$. This parameter must be calculated at point C, at this time, so that it may be used during the course of calculating the next point on the detached shock. This parameter is required to obtain $\frac{dp}{d\epsilon}$ (see page 35).

This is done by differencing this point C, with a shock point with an inclination, $\epsilon_c - 1^\circ$, point 2. The iteration on Γ is repeated for point 2 to obtain ρ_2 . Then

$$\frac{d}{d\epsilon}\left[1 - \left(\frac{\rho_\infty}{\rho_c}\right)\right] = \frac{\left(1 - \frac{\rho_\infty}{\rho_2}\right) - \left(1 - \frac{\rho_\infty}{\rho_c}\right)}{\Delta \epsilon_2} \quad ; \quad \Delta \epsilon_2 = -1^\circ$$

Then compute W_c , M_c , γ_c , and μ_c as for an interior point (gas dissociation), page 45 , or (vibration excitation) continue on page 41 .

VIBRATIONAL EXCITATION GAS ANALYSIS FOR DETACHED SHOCK POINT

$$\left(\frac{S}{R}\right)_c = \left(\frac{S}{R}\right)_\infty + \frac{\gamma_\infty}{\gamma_\infty - 1}\,\ell n\frac{T_c}{T_\infty} + \ell n\frac{p_\infty}{p} + \theta'\left[\frac{E_c}{T_c} - \frac{E_\infty}{T_\infty}\right] + \ell n\left[\frac{e^{\theta'/T_\infty} - 1}{e^{\theta'/T_c} - 1}\right]$$

$$\text{where } E_c = \frac{e^{\theta'/T_c}}{e^{\theta'/T_c} - 1}$$

This value of entropy is to be stored in the table.

If $\frac{\theta'}{T_c} > 70$, set $E_c = 1$ and $\frac{1}{e^{(\theta'/T_c)} - 1} = 0$; $\gamma_c = \gamma_\infty$

If $\frac{\theta'}{T_\infty} > 70$, set $E_\infty = 1$

In either case, $\ell n\left[\frac{e^{\theta'/T_\infty} - 1}{e^{\theta'/T_c} - 1}\right] = \frac{\theta'}{T_\infty} - \frac{\theta'}{T_c}$

$$\gamma_c = 1 + \frac{\gamma_\infty - 1}{1 + (\gamma_\infty - 1)\left[\left(\frac{\theta'}{T_c}\right)^2 \frac{E_c}{\left(e^{\theta'/T_c} - 1\right)}\right]}$$

$$M_c^{\,2} = \frac{2}{\gamma_c T_c}\left[\frac{\gamma_\infty}{\gamma_\infty - 1}(T_t - T_c) + \theta'\left(\frac{1}{e^{(\theta'/T_t)} - 1} - \frac{1}{e^{(\theta'/T_c)} - 1}\right)\right]$$

$W_c = a_c M_c$ where a_c is found as for an interior point

$$\mu_c = \sin^{-1}\left(\frac{1}{M_c}\right)$$

SHOCK POINT CALCULATIONS WHEN $(\theta + \mu) = 90^{\circ} \pm 1^{\circ}$

$$x_c = x_A$$

$$\Delta\epsilon = \frac{\left(\frac{\sin 2\mu}{2\gamma}\right)_A \left(P'_A - P'_B\right) + (\theta_A - \theta_B) - (y_c - y_A)\left(\frac{\sin\mu \sin\theta}{y}\right)_A}{\left(\frac{\sin 2\mu}{2\gamma}\right)_A \left(\frac{dP'}{d\epsilon}\right)_B + \left(\frac{d\theta}{d\epsilon}\right)_B}$$

$$y_c = y_B + (x_A - x_B)\tan\epsilon_B \left[1 + \frac{\Delta\epsilon}{\sin 2\epsilon_B}\right]$$

Note that in the expression for $\Delta\epsilon$, the last term in the numerator contains y_c. As a first approximation compute $\Delta\epsilon$, omitting this term, then compute y_c, then re-compute $\Delta\epsilon$, using this value of y_c.

Calculation of Interior Point

The following properties are known at points A and B:

$x, y, P', \theta, \frac{S}{R}, h', \rho', \gamma, \mu, m, \dddot{W}$.

The object is to generate these properties at point C.

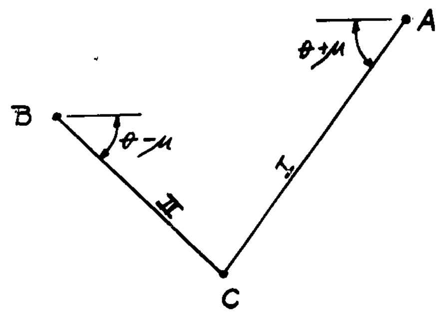

$$x_c = \frac{y_B - y_A - x_B \tan(\theta-\mu)_B + x_A \tan(\theta+\mu)_A}{\tan(\theta+\mu)_A - \tan(\theta-\mu)_B}$$

$$y_c = y_A + (x_c - x_A)\tan(\theta+\mu)_A$$

$$P'_c = \frac{1}{\left(\frac{\sin 2\mu}{2\gamma}\right)_A + \left(\frac{\sin 2\mu}{2\gamma}\right)_B} \left[\left(\frac{\sin 2\mu}{2\gamma} P'\right)_A + \left(\frac{\sin 2\mu}{2\gamma} P'\right)_B \right.$$

$$\left. + \theta_A - \theta_B - \left[\frac{\sin\mu \sin\theta}{y \cos(\theta+\mu)}\right]_A (x_c - x_A) - \left[\frac{\sin\mu \sin\theta}{y\cos(\theta-\mu)}\right]_B (x_c - x_B)\right]$$

$$\theta_c = \theta_A - \left(\frac{\sin 2\mu}{2\gamma}\right)_A (P'_c - P'_A) - \left[\frac{\sin\mu \sin\theta}{y\cos(\theta+\mu)}\right]_A (x_c - x_A)$$

The above equations do not apply if $(\theta + \mu)_A = 90 \pm 1^\circ$

For the equations governing this condition, see page 48.

$$m_c = {}^1/_2\,(m_{c_1} + m_{c_2})$$

where

$$m_{c_1} = m_A + \rho_A W_A \sin\mu_A \cdot {}^1/_2\,(y_A + y_c)\left[(x_c - x_A)^2 + (y_c - y_A)^2\right]^{1/2}$$

$$m_{c_2} = m_B - \rho_B W_B \sin\mu_B \cdot {}^1/_2\,(y_B + y_c)\left[(x_c - x_B)^2 + (y_c - y_B)^2\right]^{1/2}$$

Enter the table of mass flow vs. entropy with the above value of m_c, and extract the corresponding value of $\left(\frac{S}{R}\right)_c$.

Test for either dissociated gas analysis, page 45, or non-dissociated vibration excitation gas analysis, page 46.

Dissociated Gas Analysis

Let $h'_{*c} = \frac{1}{2} \left(h'_A + h'_B \right)$ and $\rho'_{*c} = \frac{1}{2} \left(\rho'_A + \rho'_B \right)$

then
$$\Delta h' = \frac{\left[\frac{S}{R} - \sum_{i=0}^{4} \sum_{j=0}^{5} Aij \left(P' \right)^i \left(h'_* \right)^j \right]_c}{\left[\sum_{i=0}^{4} \sum_{j=0}^{5} j \cdot Aij \left(P' \right)^i \left(h'_* \right)^{(j-1)} \right]_c}$$

$$\Delta \rho' = \frac{\left[\frac{S}{R} - \sum_{m=0}^{4} \sum_{n=0}^{5} Bmn \left(\rho'_* \right)^m \left(h'_* \right)^n \left(1 + \frac{n \, \Delta h'}{h'_*} \right) \right]_c}{\left[\sum_{m=0}^{4} \sum_{n=0}^{5} m \cdot Bmn \left(\rho'_* \right)^{(m-1)} \left(h'_* \right)^n \right]_c}$$

and $h'_c = h'_{*c} + \Delta h'$, $\rho'_c = \rho'_{*c} + \Delta \rho'$

$$h_c = 4.506 \cdot 10^6 \; h'_c$$

$$p_c = 2116.4 \; e^{P'_c}$$

$$\rho_c = 0.002498 \; e^{2.302585 \, \rho'_c}$$

$$a_c^2 = \left(h_c - e_c \right) \frac{h_c}{e_c}$$

where $e_c = \left(h_c - \frac{p_c}{\rho_c} \right)$

$$W_c = \sqrt{K_1 - 2 h_c} \; , \quad M_c = \frac{W_c}{a_c}$$

$$\mu_c = \sin^{-1} \left(\frac{1}{M_c} \right) \; , \quad \gamma_c = \frac{a_c^2 \, \rho_c}{p_c}$$

Continue on page 47.

Non-Dissociated Vibrational Excitation Gas Analysis

Let $p^* = 1/2\,(p_A + p_B)$, $\rho^* = 1/2\,(\rho_A + \rho_B)$, $T^* = \dfrac{p^*}{R\rho^*}$

Then $T_c = T^* + \Delta T$

where

$$\Delta T = T^* \frac{\left(\frac{S}{R}\right)_c - \left(\frac{S}{R}\right)_\infty + \Gamma_\infty \ell n\left(\frac{T_\infty}{T^*}\right) + \ell n\left(\frac{p_c}{p_\infty}\right) + \ell n\left[\frac{e^{\theta'/T^*}-1}{e^{\theta'/T_\infty}-1}\right] + \theta'\left(\frac{E_\infty}{T_\infty} - \frac{E^*}{T^*}\right)}{\Gamma_\infty + \left(\frac{\theta'}{T^*}\right)^2 E^*\ (E^*-1)}$$

where $E^* = \dfrac{e^{\theta'/T^*}}{e^{\theta'/T^*}-1}$ and $\Gamma_\infty = \dfrac{\gamma_\infty}{\gamma_\infty - 1}$

If $\dfrac{\theta'}{T^*} > 70$, $E^* = 1$ and $\ell n\left[\dfrac{e^{\theta'/T^*}-1}{e^{\theta'/T_\infty}-1}\right] = \dfrac{\theta'}{T^*} - \dfrac{\theta'}{T_\infty}$

Then $\rho_c = \dfrac{p_c}{RT_c}$ and $\rho'_c = \dfrac{1}{2.302585}\ \ell n\left(\dfrac{\rho_c}{0.002498}\right)$

$$h_c = C_{p_\infty}\left[T_c + \frac{\theta'}{\Gamma_\infty\,(e^{\theta'/T_c}-1)}\right] \quad \text{and } h'_c = \frac{h_c}{4.506 \cdot 10^6}$$

$$\gamma_c = 1 + \frac{\gamma_\infty - 1}{1 + (\gamma_\infty - 1)\left[\left(\frac{\theta'}{T}\right)^2 \frac{e^{\theta'/T_c}}{\left(e^{\theta'/T_c}-1\right)^2}\right]}$$

If $\dfrac{\theta'}{T_c} > 70$, $h_c = C_{p_\infty} \cdot T_c$ and $\gamma_c = \gamma_\infty$

$$M_c^2 = \frac{2}{\gamma_c T_c}\left[\Gamma_\infty\ (T_t - T_c) + \theta'\left(\frac{1}{e^{\theta'/T_t}-1} - \frac{1}{e^{\theta'/T_c}-1}\right)\right]$$

$\mu_c = \sin^{-1}\left(\dfrac{1}{M_c}\right)$, $W_c = \sqrt{K_1 - 2h_c}$

An improved value of the mass flow may now be calculated.

$$m_c = \frac{1}{2} (m_{c_1} + m_{c_2})$$

where

$$m_{c_1} = m_A + \frac{1}{2} \left\{ \rho_A W_A \sin \mu_A + \rho_c W_c \sin \mu_c \right\} \frac{(y_A + y_c)}{2} \left[(x_c - x_A)^2 + (y_c - y_A)^2 \right]^{1/2}$$

$$m_{c_2} = m_B - \frac{1}{2} \left\{ \rho_B W_B \sin \mu_B + \rho_c W_c \sin \mu_c \right\} \frac{(y_B + y_c)}{2} \left[(x_c - x_B)^2 + (y_c - y_B)^2 \right]^{1/2}$$

This completes the analysis of an interior point

Interior Point Calculations when $(\theta + \mu) = 90^\circ \pm 1^\circ$

$$x_c = x_A$$

$$y_c = y_B + (x_c - x_B) \tan(\theta - \mu)_B$$

$$P'_c = \frac{1}{\left(\frac{\sin 2\mu}{2\gamma}\right)_A + \left(\frac{\sin 2\mu}{2\gamma}\right)_B} \left[\left(\frac{\sin 2\mu}{2\gamma} P'\right)_A + \left(\frac{\sin 2\mu}{2\gamma} P'\right)_B + \theta_A - \theta_B - (y_c - y_A) \left(\frac{\sin \mu \sin \theta}{y}\right)_A - (x_c - x_B) \left(\frac{\sin \mu \sin \theta}{y \cos(\theta - \mu)}\right)_B \right]$$

$$\theta_c = \theta_A - \left(\frac{\sin 2\mu}{2\gamma}\right)_A (P'_c - P'_A) - (y_c - y_A) \left(\frac{\sin \mu \sin \theta}{y}\right)_A$$

POINT ON BODY

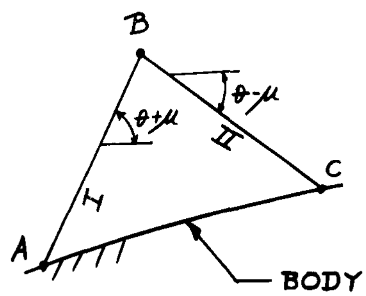

The general equation of second degree is: $ax^2 + by^2 + cx + dy + e = 0$

This equation may be used to prescribe the sequential segments which make up the body profile.

$$x_c = \frac{2D}{-B \mp \sqrt{B^2-4AD}}, \text{ for } A \neq 0 \; ; \; x = -\frac{D}{B} \text{ for } A = 0$$

$$y_c = y_B + (x_c - x_B) \tan(\theta - \mu)_B$$

where
$$A = a + b \tan^2(\theta - \mu)_B$$

$$B = \tan(\theta - \mu)_B \left\{ 2b \left[y_B - x_B \tan(\theta - \mu)_B \right] + d \right\} + c$$

$$D = b \left[y_B - x_B \tan(\theta - \mu)_B \right]^2 + d \left[y_B - x_B \tan(\theta - \mu)_B \right] + e$$

$$\theta_c = \tan^{-1}\left[-\frac{2ax_c + c}{2by_c + d} \right]$$

$$P'_c = P'_B + \frac{\theta_c - \theta_B - \left[\frac{\sin\mu \sin\theta}{y\cos(\theta-\mu)} \right]_B (x_c - x_B)}{\left[\frac{\sin 2\mu}{2\gamma} \right]_B}$$

$$\left(\frac{S}{R}\right)_c = \left(\frac{S}{R}\right)_A$$

Test for either dissociated gas analysis, page 45, or vibrational excitation gas analysis, page 46

EXPANSION CORNER

When an expansion corner is detected, the program adjusts the mesh of characteristic lines, so that a second-family line intersects the body very close to the corner. The exterior angle, α, is divided into 15 components, i. e., $\Delta\theta = \frac{\alpha}{15}$. The procedure then follows a step-wise integration around the corner to form the vertex of the expansion fan.

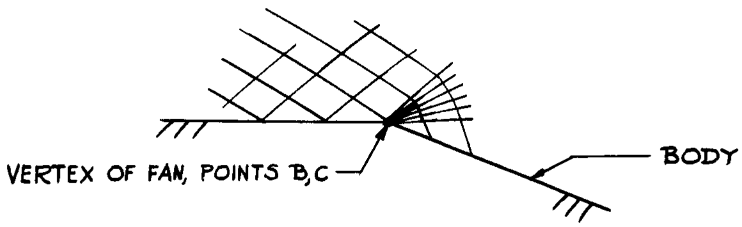

Given that point B is the "previous" point on the corner, the properties of point C, the "next" point, are found as follows:

$$x_c = x_B, \qquad y_c = y_B, \qquad \left(\frac{S}{R}\right)_c = \left(\frac{S}{R}\right)_B$$

$$\theta_c = \theta_B + \Delta\theta$$ (Note that α and $\Delta\theta$ are negative for an expansion corner.)

$$P'_c = P'_B + \left(\frac{2\gamma}{\sin 2\mu}\right)_B \Delta\theta + \left\{\frac{2\gamma}{\sin 2\mu\cos\mu}\left[\frac{(\gamma+1)}{2\sin 2\mu\cos\mu} - \sin\mu\right] - \frac{1}{2}\left(\frac{2\gamma}{\sin 2\mu}\right)^2\right\}_B (\Delta\theta)^2$$

Test for either dissociated gas analysis page 45, or vibrational excitation gas analysis, page 46, to complete the calculation of the remaining properties at point C.

SECONDARY SHOCK CALCULATION

When the program detects a re-entrant corner, the mesh is adjusted so that a second family line terminates very close to the corner. Refer to Figure III a, page 95 . Points A and D refer to the upstream and the downstream properties at the corner, respectively. Point A is calculated in the usual manner, utilizing the properties of points F and J.

To cross the shock at the corner, it is necessary to estimate the angle of inclination of the shock , ϵ_o. Defining $F_\eta = \cot^{-1}(\epsilon_o - \theta_A)$, we solve the cubic,

$$F_\eta^3 + \tan\delta\left(1 + \frac{\gamma_d + 1}{2} M_u^2\right) F_\eta^2 + (1 - M_u^2) F_\eta + \tan\delta\left(1 + \frac{\gamma_d - 1}{2} M_u^2\right) = 0$$

where the subscripts u, d, pertain to upstream and downstream properties at a shock point, respectively. Thus, at the corner, u pertains to point A, d to point D. This cubic implies that $\gamma_d = \gamma_u$, thus it yields an approximate value for F_η. The flow deviation, $\delta = \alpha = \theta_D - \theta_A$.

It is now possible to cross the shock to obtain the downstream properties at the corner. This analysis is similar to that used to cross the detached shock (page 37) except that upstream conditions must be substituted for free stream properties. The iteration is performed on γ_d rather than on Γ. At the corner (only) an additional iteration is performed on F_η, since, as indicated above, the cubic yields only an approximate value.

Iteration on γ_d

Initially, set $\gamma_d = \gamma_u$

$$\alpha = \frac{\gamma_d}{\gamma_u} \frac{1}{(\gamma_d + 1)\ M_u^2} \qquad \beta = \frac{\gamma_d - 1}{\gamma_d + 1} \left(\frac{\gamma_u}{\gamma_u - 1} - \frac{\gamma_d}{\gamma_d - 1} \right) \frac{1}{\gamma_u M_u^2}$$

$$B = \left\{ \left(\frac{1}{\gamma_d + 1} \right)^2 - 2 \left(\frac{\alpha}{\gamma_d + 1} + \beta \right) \left(1 + F_\eta^2 \right) + \alpha^2 \left(1 + F_\eta^2 \right)^2 \right\}^{1/2}$$

$$\left(1 - \frac{\rho_u}{\rho_d} \right) = \frac{1}{\gamma_d + 1} - \alpha \left(1 + F_\eta^2 \right) + B$$

$$\rho_d = \frac{\rho_u}{1 - \left(1 - \dfrac{\rho_u}{\rho_d} \right)} \qquad p_d = p_u + \rho_u W_u^2 \frac{\left(1 - \dfrac{\rho_u}{\rho_d} \right)}{\left(1 + F_\eta^2 \right)}$$

$$h_d = \left(\frac{\gamma_d}{\gamma_d - 1} \right) \frac{p_d}{\rho_d} \qquad h'_d = \frac{h_d}{4.506 \cdot 10^6}$$

$$\rho'_d = \frac{1}{2.302585} \ln \left(\frac{\rho_d}{0.002498} \right)$$

$$P'_d = \ln \left(\frac{p_d}{2116.4} \right) \qquad (1)$$

Test for either dissociated gas analysis or vibrational excitation gas analysis.

Dissociated Gas Analysis

$$\left(\frac{S}{R} \right)_d = \sum_{i=0}^{4} \sum_{j=0}^{5} A_{ij} \left(P'_d \right)^i \left(h'_d \right)^j$$

$$\Delta \rho'_d = \frac{\left(\frac{S}{R}\right)_d - \sum_{m=0}^{4} \sum_{n=0}^{5} Bmn \left(\rho'_d\right)^m \left(h'_d\right)^n}{\sum_{m=0}^{4} \sum_{n=0}^{5} m \cdot Bmn \left(\rho'_d\right)^{m-1} \left(h'_d\right)^n} \qquad \text{(2a)}$$

Continue with equ. (3)

Vibrational Excitation Gas Analysis

$$T_d = \frac{h_d}{C_{p_\infty}} - \frac{\left(\gamma_\infty - 1\right)}{\gamma_\infty} \frac{\theta'}{e^{(\theta'/T)} - 1} \qquad \text{Iterate for } T$$

$$T^* = \frac{Pd}{\rho_d R}, \quad \Delta \rho'_d = \frac{1}{2.302585} \ln \left(\frac{T^*}{T_d}\right) \qquad \text{(2b)}$$

After obtaining $\Delta \rho'_d$ using either (2a) or (2b),

$$\Delta \gamma_d = -K_c \frac{\rho_u}{\rho_d} (\gamma_d + 1) \Delta \rho'_d \left\{ \frac{1}{\left(\gamma_d + 1\right)} + \frac{\alpha}{\gamma_d} (1 + F_\eta^2) + \frac{1}{B} \left[\frac{1}{(\gamma_d + 1)^2} + (1 + F_\eta^2) \cdot \right.\right.$$

$$\left.\left. \left(\frac{\alpha}{(\gamma_d + 1)} \frac{(1 - \gamma_d)}{\gamma_d} + \frac{2\beta}{\gamma_d - 1} + \frac{1}{\gamma_u M_u^2 (\gamma_d - 1)} \right) - \frac{\alpha^2}{\gamma_d} (1 + F_\eta^2)^2 \right] \right\}^{-1} \qquad (3)$$

Then $\gamma_d = \gamma_d + \Delta \gamma_d$, $K_c = 2.30259$

The iteration on γ_d converges when $\left|\Delta\gamma_d\right| < 10^{-6}$

For the corner only, equ. (4) is executed; for all other secondary shock points, the analysis is continues with equ. (5).

$$\Delta F_\eta = \left\{ \tan\delta \left[(1+F_\eta^2) - \left(\frac{1}{\gamma_d+1} - \alpha\,(1+F_\eta^2) + B \right) \right] - \frac{F_\eta}{\gamma_d+1} + \alpha(1+F_\eta^2)\,F_\eta - BF_\eta \right\} \cdot$$
$$\left\{ \frac{1}{\gamma_d+1} - \alpha\,(1+F_\eta^2) + B - 2F_\eta \tan\delta + 2(F_\eta + \tan\delta) \left[\frac{F_\eta}{B} \left(\alpha^2 (1+F_\eta^2) - \beta - \frac{\alpha}{\gamma+1} \right) - \alpha F_\eta \right] \right\}^{-1} \tag{4}$$

$$F_\eta = F_\eta + \Delta F_\eta$$

The iteration continues by returning to equ. (1), and converges when $\left|\Delta F_\eta\right| < 10^{-5}$

$$\left.\begin{aligned} u &= W_u \left[1 - \frac{(1 - \frac{\rho_u}{\rho_d})}{(1+F_\eta^2)} \right] \qquad v = W_u\,F_\eta \frac{(1 - \frac{\rho_u}{\rho_d})}{(1+F_\eta^2)} \\ \theta_d &= \tan^{-1} \left(\frac{v}{u}\right) \end{aligned}\right\} \tag{5}$$

Test for either dissociation gas analysis, equ. (6a) , or vibrational excitation gas analysis, equ. (6b).

$$\left.\begin{aligned} & W_d = \sqrt{K_1 - 2h_d} \qquad M_d = \frac{W_d}{a}, \qquad \mu_d = \sin^{-1}\left(\frac{1}{M_d}\right) \\ & \text{where } a^2 = (h_d - e_d)\,\frac{h_d}{e_d}, \qquad e_d = h_d - \frac{p_d}{\rho_d} \\ & \gamma_d^* = \frac{a^2\,\rho_d}{p_d} \end{aligned}\right\} \tag{6a}$$

$$\left(\frac{S}{R}\right)_d = \left(\frac{S}{R}\right)_\infty + \left(\frac{\gamma_\infty}{\gamma_\infty - 1}\right) \ell n \left(\frac{T_d}{T_\infty}\right) + \ell n \frac{p_\infty}{p_d} + \theta' \left[\frac{e^{\theta'/T_d}}{T_d (e^{\theta'/T_d} - 1)} - \frac{e^{\theta'/T_\infty}}{T_\infty (e^{\theta'/T_\infty} - 1)} \right] + \ell n \left[\frac{e^{\theta'/T_\infty} - 1}{e^{\theta'/T_d} - 1} \right]$$

If $\frac{\theta'}{T_d} > 70$, $\frac{e^{\theta'/T_d}}{e^{\theta'/T_d} - 1} = 1$ and $\ell n \frac{e^{\theta'/T_\infty} - 1}{e^{\theta'/T_d} - 1} = \frac{\theta'}{T_\infty} - \frac{\theta'}{T_d}$

$$M_d = \frac{2}{\gamma_d T_d} \left[\frac{\gamma_\infty}{\gamma_\infty - 1} (T_t - T_d) + \theta' \left(\frac{1}{e^{\theta'/T_t} - 1} - \frac{1}{e^{\theta'/T_d} - 1} \right) \right]$$

$$\mu_d = \sin^{-1} \left(\frac{1}{M_d}\right) \qquad W_d = M_d \cdot a \qquad (6b)$$

where $a = (h_d - e_d) \frac{h_d}{e_d}$, $e_d = h_d - \frac{p_d}{\rho_d}$

$$\gamma_d^* = 1 + \frac{(\gamma_\infty - 1)}{1 + (\gamma_\infty - 1) \left[\left(\frac{\theta'}{T_d}\right)^2 \frac{e^{\theta'/T_d}}{(e^{\theta'/T_d} - 1)^2} \right]}$$

In either case, γ_d^* is written as output and used in the calculation of properties of points downstream of the secondary shock.

<u>Calculation of Point on Secondary Shock above Corner</u>

After crossing the secondary shock at the re-entrant corner, a new second family line is generated, originating at the detached shock and terminating at point C (see Fig. IIIa). Note that A - C is a first family line which is a part of the mesh upstream of the secondary shock, i.e. the properties at points A and C are those which would exist if the secondary shock were not present. Then,

$$x_{B'} = \frac{y_A - x_A \tan \epsilon_o - y_B + x_B \tan (\theta - \mu)_B}{\tan(\theta - \mu)_B - \tan \epsilon_o}$$

$$y_{B'} = y_B + (x_{B'} - x_B) \tan(\theta - \mu)_B$$

The upstream properties at B' are found by interpolating between points B and C.

Using the downstream properties at the corner, θ_D, and μ_D, a first family is generated connecting B' with the body, at point G.

$$x_G = \frac{2D}{-B \mp \sqrt{B^2 - 4AD}} \quad \text{for } A \neq 0; \; x_G = -\frac{D}{B} \quad \text{for } A = 0$$

$$y_G = y_{B'} + (x_G - x_{B'}) \tan(\theta + \mu)_D$$

where $A = a + b\tan^2(\theta+\mu)_D$

$$B = \tan(\theta+\mu)_D \left\{ 2b\left[y_{B'} - x_{B'}\tan(\theta+\mu)_D \right] + d \right\} + c$$

$$D = b\left[y_{B'} - x_{B'}\tan(\theta+\mu)_D \right]^2 + d\left[y_{B'} - x_{B'}\tan(\theta+\mu)_D \right] + e$$

$$\theta_G = \tan^{-1}\left[-\frac{2a\,x_G + c}{2b\,y_G + d} \right]$$

Note that the coefficients, a, b, c, d, e, refer to the body profile immediately downstream of the corner, A-G-E.

The remaining properties at point G are assumed equal to those properties at point D.

Point $\tilde{B}_1$ is located by the intersection of a line drawn from the corner having an angular inclination of $(\epsilon_o + \frac{\Delta}{2})$, and the second family line joining points B and C. The value of Δ is chosen to be -1°. Then,

$$x_{\tilde{B}_1} = \frac{y_A - x_A\tan(\epsilon_o + \frac{\Delta}{2}) - y_B + x_B\tan(\theta-\mu)_B}{\tan(\theta-\mu)_B - \tan(\epsilon_o + \frac{\Delta}{2})}$$

$$y_{\tilde{B}_1} = y_B + (x_{\tilde{B}_1} - x_B)\tan(\theta-\mu)_B$$

The upstream properties at $\tilde{B}_1$ are found by interpolating between points B and C.

Point B_1 is located by the intersection of the first family line, B' G, and the line having the inclination, $(\epsilon_o + \frac{\Delta}{2})$, $A\tilde{B}_1$.

$$x_{B_1} = \frac{y_A - x_A\tan(\epsilon_o + \frac{\Delta}{2}) - y_G + x_G\tan(\theta+\mu)_G}{\tan(\theta+\mu)_G - \tan(\epsilon + \frac{\Delta}{2})}$$

$$y_{B_1} = y_G + (x_{B_1} - x_G)\tan(\theta+\mu)_G$$

The upstream properties at B_1 are found by interpolating between $\tilde{B}_1$ and A.

If the secondary shock were straight from the corner to its intersection with the first family line through G, then B' would be a point on the secondary shock. On the other hand, if the secondary shock changed in curvature by the amount Δ, between the corner and its intersection with the first family line through G, then B_1 would be a point on the secondary shock. The actual intersection of the secondary shock and the aforementioned first family line, point $\bar{B}$, lies somewhere in the neighborhood of these two points, B' and B_1.

To locate point $\bar{B}$, and to calculate the downstream properties at this point, the following procedure is followed.

1. Assume that B' lies on the shock, and "cross the shock" to get downstream properties at B'

2. Assume that B_1 lies on the shock, and "cross the shock" to get downstream properties at B_1

3. With this information, the location and properties of the actual point on the shock, $\bar{B}$, may be calculated.

To get the downstream properties at point B', set $F_\eta = \cot^{-1}(\epsilon_o - \theta_{B'})$, and iterate on γ_d (equ. 1 - 3), omitting equation (4) since F_η is prescribed. The remaining downstream properties are found by equations (5-6).

Similarly, to get the downstream properties at point B_1, set $F_\eta = \cot^{-1}(\epsilon_o + \Delta - \theta_{B_1})$ and proceed as above.

Now,

$$\frac{dP'}{d\epsilon} = \frac{P'_{B_{1_d}} - P'_{B'_d}}{\Delta} \qquad \frac{d\theta}{d\epsilon} = \frac{\theta_{B_{1_d}} - \theta_{B'_d}}{\Delta} \tag{7}$$

$$\frac{dh'}{d\epsilon} = \frac{h'_{B_{1_d}} - h'_{B'_d}}{\Delta}$$

The actual change in curvature between points D' and $\bar{B}$ is

$$\Delta\epsilon = \left(\frac{\sin 2\mu}{2\gamma}\right)_G \left(P'_G - P'_{B'_d}\right) + \theta_G - \theta_{B'_d} + \left[\frac{\sin\mu\sin\theta}{y\cos(\theta+\mu)}\right]_G \left[x_G + \frac{y_G - x_G\tan(\theta+\mu)_G - y_D + x_D\tan\epsilon_o}{\tan(\theta+\mu)_G - \tan\epsilon_o}\right]$$

$$\cdot \left[\left(\frac{\sin 2\mu}{2\gamma}\right)_G \frac{dP'}{d\epsilon} + \frac{d\theta}{d\epsilon}\right]^{-1} \qquad (7)\ \text{cont.}$$

$$\left.\begin{aligned}
x_{\bar{B}} &= \frac{y_D - x_D(\tan\epsilon_o)\left(1 + \frac{\Delta\epsilon}{\sin 2\epsilon_o}\right) - y_G + x_G\tan(\theta+\mu)_G}{\tan(\theta+\mu)_G - \tan\epsilon_o\left(1 + \frac{\Delta\epsilon}{\sin 2\epsilon_o}\right)} \\
y_{\bar{B}} &= y_G + (x_{\bar{B}} - x_G)\tan(\theta+\mu)_G \\
P'_{\bar{B}} &= P'_{B'_d} + \left(\frac{dP'}{d\epsilon}\right)\Delta\epsilon \\
h'_{\bar{B}} &= h'_{B'_d} + \left(\frac{dh'}{d\epsilon}\right)\Delta\epsilon \qquad \theta_{\bar{B}} = \theta_{B'_d} + \left(\frac{d\theta}{d\epsilon}\right)\Delta\epsilon \\
\epsilon_{\bar{B}} &= \epsilon_o + \Delta\epsilon
\end{aligned}\right\} \qquad (8)$$

Test for dissociation gas analysis, or for vibrational excitation gas analysis.

For dissociation gas analysis, use equs. (2a), and (6a) to generate the remaining properties at point $\bar{B}$. For vibrational excitation gas analysis, use equs. (2b), and (6b) to generate the remaining properties of point $\bar{B}$.

Note that these are downstream properties at $\bar{B}$.

After computing the downstream properties of $\bar{B}$, the body point, E, downstream of the secondary shock is calculated in the usual manner, page 49 . In this case, point $\bar{B}$ acts as point B; and point D as point A(page 49 .). The line $\bar{B}$ E is a second family line.

The program then returns to the detached shock, to generate a new (upstream) second family line.

CALCULATION OF SUBSEQUENT POINTS ON THE SECONDARY SHOCK

Refering to Fig. IIIb, the point D on the secondary shock has been computed, as well as point E on the body. The second family line terminating at point C has been generated.

To determine point $\bar{B}$, a procedure similar to that used to calculate point D is followed. With $\epsilon_o = \epsilon_D$, point B' is calculated in a manner identical to that described for the shock point D, above the corner.

Point G is the intersection of the first family line from B' (using θ_D and μ_D), and the downstream second family line, DE.

$$x_G = \frac{y_D - y_{B'} - x_D \tan(\theta - \mu)_D + x_{B'} \tan(\theta + \mu)_D}{\tan(\theta + \mu)_D - \tan(\theta - \mu)_D}$$

$$y_G = y_{B'} + (x_G - x_{B'}) \tan(\theta + \mu)_D$$

The remaining properties at G are interpolated between points D and E.

The points $\tilde{B}_1$ B_1, and $\bar{B}$ are calculated in exactly the same manner as described for the shock point above the corner, pages 56 to 59 .

The second family line downstream of the secondary shock, is now generated. The interior point, F, is calculated using points $\bar{B}$ and E, in the usual manner, where $\bar{B}$ acts as point B, and E acts as point A (page 43). The body point, H, is found using point F and E.

In this manner, the secondary shock is constructed along with the rest of the flow field. Note that the second family lines downstream of the secondary shock, are slightly offset with respect to the upstream second family lines.

INTERSECTION OF TWO SHOCKS
WITHIN FLOW FIELD

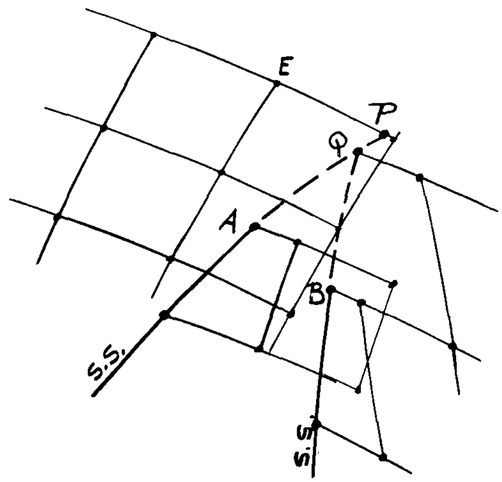

When there is only 1 interior point on the second-family line downstream of the first secondary shock then we must test whether point Q lies below point P or

Test $y_Q \lessgtr y_P$

where

$$x_Q = \frac{y_A - x_A \tan \epsilon_A - y_B + x_B \tan \epsilon_B}{\tan \epsilon_B - \tan \epsilon_A} \quad ; \quad y_Q = y_B + (x_Q - x_B) \tan \epsilon_B$$

$$x_P = \frac{y_A - x_A \tan \epsilon_A - y_E + x_E \tan (\theta - \mu)_E}{\tan (\theta - \mu)_E - \tan \epsilon_A} \quad ; \quad y_P = y_E + (x_P - x_E) \tan (\theta - \mu)_E$$

If $y_Q > y_P$, no intersection takes place and the 2 s. s. must be extended at least one more point.

If $y_Q < y_P$, then the shock intersect as shown.

The conditions upstream at point Q is assumed to be those upstream at point A (stored in PNTF, which is B') : $W_{Q_u} = W_F$

It is necessary to get an approximate value of the inclination of the resultant secondary shock of Q:

$$F_\eta^3 + \tan\delta_o \left(1 + \frac{\gamma_{Q_u} + 1}{2} M_{Q_u}^2\right) F_\eta^2 + (1 - M_{Q_u}^2)\; F_\eta + \tan\delta_o \left(1 + \frac{\gamma_{Q_u} - 1}{2} M_{Q_u}^2\right) = 0$$

where $\delta_o = \theta_B - \theta_F$ initially

Then

$$\epsilon = \theta_F + \cot^{-1} F_\eta \tag{1}$$

Subscripts: Q_d , downstream at point Q

Q_u , upstream at point Q

B , downstream at point B

A , downstream at point A

F , upstream at point A

n , for n^{th} iteration on δ

Now, for the given value of δ, we may cross the shock in the usual manner:

$$\alpha = \frac{\gamma_{Q_d}}{\gamma_{Q_u}} \quad \frac{1}{(\gamma_{Q_u} + 1)\, M_\infty^2} \qquad \beta = \frac{\gamma_{Q_d} - 1}{\gamma_{Q_d} + 1}\left(\frac{\gamma_{Q_u}}{\gamma_{Q_u} - 1} - \frac{\gamma_{Q_d}}{\gamma_{Q_d} - 1}\right) \frac{1}{\gamma_{Q_u}\, M^2_{Q_u}}$$

$$\left(1 - \frac{\rho_{Q_u}}{\rho_{Q_d}}\right) = \frac{1}{\gamma_{Q_d} + 1} - \alpha\,(1 + F_\eta^2) + \left\{\left[\frac{1}{\gamma_{Q_d} + 1} - \alpha\,(1 + F_\eta^2)\right]^2 - 2\beta\,(1 + F_\eta^2)\right\}^{1/2}$$

$$\rho_{Q_d} = \frac{\rho_{Q_u}}{1 - \left(1 - \frac{\rho_{Q_u}}{\rho_{Q_d}}\right)} \tag{2}$$

$$p_{Q_d} = p_{Q_u} + \rho_{Q_u} W^2_{Q_u} \left(1 - \frac{\rho_{Q_u}}{\rho_{Q_d}}\right) (1 + F_\eta^2)^{-1}$$

$$h_{Q_d} = \frac{\gamma_{Q_d}}{\gamma_{Q_d} - 1} \quad \frac{p_{Q_d}}{\rho_{Q_d}}$$

Now test Real gas (3a) or vibration excitation (3b)

$$\left.\begin{aligned}
\rho'_{Q_d} &= \frac{1}{2.302585}\, \ell n \frac{\rho_{Q_d}}{2.498.10^{-3}}, \quad P'_{Q_d} \doteq \ell n \frac{p_{Q_d}}{2.1164 \cdot 10^3} \\
h'_{Q_d} &\doteq \frac{h_{Q_d}}{4.506 \cdot 10^6}, \quad \left(\frac{S}{R}\right)_{Q_d} = \sum_{i=0}^{4} \sum_{j=0}^{5} A_{ij}\, (P'_{Q_d})^i\, (h'_{Q_d})^j \\
\Delta \rho'_{Q_d} &= \frac{\left(\frac{S}{R}\right)_{Q_d} - \sum_{m=0}^{4} \sum_{n=0}^{5} B_{mn}\, (\rho'_{Q_d})^m (h'_{Q_d})^n}{\sum_{m=0}^{4} \sum_{n=0}^{5} m B_{mn}\, (\rho'_{Q_d})^{m-1}\, (h'_{Q_d})^n}
\end{aligned}\right\} \text{(3a)}$$

$$
\begin{gathered}
T = \frac{h_{Q_d}}{C_{p_\infty}} - \frac{\gamma_\infty - 1}{\gamma_\infty} \; \frac{\theta'}{e^{\theta'/T} - 1} \quad \text{by iteration} \quad T\text{in} = \frac{h_{Q_d}}{C_{p_\infty}} \\
\left(\frac{S}{R}\right)_{Q_d} = \left(\frac{S}{R}\right)_\infty + \frac{\gamma_\infty}{\gamma_\infty - 1} \ell n \left(\frac{T}{T_\infty}\right) + \ell n \left(\frac{p_\infty}{p_{Q_d}}\right) + \theta' \left[\frac{e^{\theta'/T}}{T\,(e^{\theta'/T} - 1)} - \frac{e^{\theta'/T_\infty}}{T\,(e^{\theta'/T_\infty} - 1)} \right] + \ell n \left[\frac{e^{\theta'/T_\infty} - 1}{e^{\theta'/T} - 1} \right] \\
\Delta \rho'_{Q_d} = \frac{1}{2.302585} \ell n \left(\frac{p_{Q_d}}{\rho_{Q_d} R T} \right) , \quad \rho'_{Q_d} = \frac{1}{2.302585} \ell n \left(\frac{\rho_{Q_d}}{2.498 \cdot 10^{-3}} \right) \\
P'_{Q_d} = \ell n \left(\frac{p_{Q_d}}{2.1164 \cdot 10^{3}} \right) , \quad h'_{Q_d} = \frac{h_{Q_d}}{4.506 \cdot 10^{6}}
\end{gathered}
\tag{3b}
$$

Then after using either (3a) or (3b),

$$
\begin{gathered}
\Delta \gamma_{Q_d} = -2.302585 \, (\gamma_{Q_d} + 1) \left(\rho_{Q_u} / \rho_{Q_d} \right) \Delta \rho'_{Q_d} \Bigg[\frac{1}{\gamma_{Q_d} + 1} + \frac{\alpha}{\gamma_{Q_d}} (1 + F_\eta^2) \\
+ \frac{1}{B} \left\{ \left(\frac{1}{\gamma_{Q_d} + 1} \right)^2 + (1 + F_\eta^2) \left[\frac{\alpha}{\gamma_{Q_d} + 1} \; \frac{1 - \gamma_{Q_d}}{\gamma_{Q_d}} + \frac{\beta}{\gamma_{Q_d} - 1} \left(2 + \frac{1}{\beta \gamma_{Q_u} M^2_{Q_u}} \right) \right] - \frac{\alpha^2}{\gamma_{Q_d}} (1 + F_\eta^2)^2 \right\} \Bigg]^{-1} \\
\text{where} \quad B^2 = \frac{1}{(\gamma_{Q_d} + 1)^2} - 2 \left(\frac{\alpha}{\gamma_{Q_d} + 1} \right) + \beta \, (1 + F_\eta^2) + \alpha^2 (1 + F_\eta^2)^2 \\
\text{and} \quad \gamma_{Q_d} = \gamma_{Q_d} + \Delta \gamma_{Q_d}
\end{gathered}
\tag{4}
$$

With this new value of γ_{Q_d}, repeat eqs. (2) thru (4) until $\Delta \gamma_{Q_d} \leq 10^{-6}$

With the final iterated value of γ_{Q_d}, calculate the correction to F_η corresponding to this value of δ:

$$\Delta F_\eta = \frac{\tan\delta\left\{(1+F_\eta^2) - \left[\frac{1}{\gamma_D+1} - \alpha(1+F_\eta^2) + B\right]\right\} - \frac{F_\eta}{\gamma_D+1} + \alpha(1+F_\eta^2)F_\eta - BF_\eta}{\frac{1}{\gamma_D+1} - \alpha(1+F_\eta^2) + B - 2F_\eta\tan\delta + 2(F_\eta+\tan\delta)\left[\frac{F_\eta}{B}\left(\alpha^2(1+F_\eta^2) - \beta - \frac{\alpha}{\gamma_D+1}\right) - \alpha F_\eta\right]} \tag{5}$$

and $F_\eta = F_\eta + \Delta F_\eta$

With this new value of F_η repeat eqs. (2) thru (5), iterating on both γ_{Q_d} and F_η as indicated until $|\Delta F_\eta| \le 10^{-5}$.

With the final iterated values of γ_{Q_d} and F_η, test for real gas or vibration excitation and compute μ, accordingly, as usual.

Then compute a new value for δ:

$$\delta_{n+1} = \delta_o - \left[\left(\frac{\sin\mu\,\cos\mu}{\gamma}\right)_{Q_d}\left(P'_{Q_d} - P'_B\right)\right]_n \tag{6}$$

With this new value of $\delta_n = \delta_{n+1}$, test below:

$$\left|\frac{\delta_n - \delta_o + \left[\left(\frac{\sin\mu\,\cos\mu}{\gamma}\right)_{Q_d}\left(P'_{Q_d} - P'_B\right)\right]_n}{\delta_n}\right| \lesseqgtr 0.0025$$

If the test fails (> 0.0025) return to (1), etc.

If test is satisfied, the properties of the resultant shock at Q, downstream, have been calculated. Use (1) to calculate inclination of this shock of Q

Intersection of Bow Shock with Secondary Shock

The analysis is identical with that outlined for 2 secondary shocks except that eq... (1) becomes

$$\epsilon_Q = \cot^{-1} F_\eta \equiv \cot^{-1} F_y$$

and the subscripts, Q_u and F are replaced by ∞ which indicates free stream conditions, and $\theta_F \equiv \theta_{Q_u} = 0$. Thus $\delta_o = \theta_B$, initially.

CALCULATION OF ENTROPY WITHIN THE FLOW FIELD.

As indicated in the preceding analysis, the mass flow at each point in the mesh of characteristics is calculated. The entropy is explicitly calculated only at points along the detached shock and along all secondary shocks. At each shock point, the calculated value of entropy and the corresponding mass flow are entered into a table. Since the relationship between mass flow and entropy is different behind a secondary shock, than it is behind the detached shock, up to three sets of mass flow-entropy tables must be constructed - one for points downstream of the detached shock and upstream of the first secondary shock; one for those points between the first and second secondary shocks; one for those points downstream of the second secondary shock.

These tables are logically adjusted and modified every time a change in the character of the flow field takes place: secondary shocks dying, intersecting, originating at a corner, or intersecting the detached shock. After the mass flow is calculated at each interior point, the program correlates the position of this point within the flow field, with its correct entropy table, and extracts the corresponding value of entropy by interpolation within this table. Since the mass flow is calculated iteratively at the interior points, these values are of high precision, and thus the values of entropy extracted from the tables are correspondingly very accurate.

CONICAL FLOW ANALYSIS

Given the free stream parameters and the body equation for the conical nose, the attached conical shock angle is obtained by interation, and a horizontal reference line consisting of 20 points is generated from the shock to the body.

From the body equation $cx + dy + e = 0$, the body angle is obtained.

$$\eta_c = \tan^{-1}(-c/d) \tag{1}$$

An initial guess of the shock angle is given by

$$\eta_{initial} = 1.2(\eta_c) \tag{2}$$

and Γ is assumed = 1.25

Iteration for Shock Angle

With Γ and $F_y = \cot \eta$ properties behind the shock are obtained using the equations given on pages through . The conical flow equations (7) through (15) below are used to obtain the value of a body angle $(\eta_B)_i$ for the given shock angle (η_i).

For the first iteration on the shock angle

$$\begin{aligned} \delta_i &= \eta_c - \eta_{B_i} \\ \eta_{i+1} &= \eta_i + \delta_i \end{aligned} \tag{3}$$

The iteration is repeated with $\eta_i = \eta_{i+1}$

On all subsequent iterations,

$$\delta_i = \eta_c - \eta_{B_i}$$

$$\Delta_i = \eta_{B_i} - \eta_{B_{i-1}} \tag{4}$$

$$\text{DDELTA} = (\delta_i)(\delta_{i-1}) / \Delta_i$$

and

$$\eta_{i+1} = \eta_i + \text{DDELTA} \tag{5}$$

The calculation is repeated until

$$|\text{DDELTA}| \leq .01^\circ \tag{6}$$

For the final shock angle $\eta_s = \eta_i + \text{DDELTA}$ the properties behind the shock are obtained.

Conical Flow Equations

Given η_c, the shock angle η and the properties behind the shock

$$\Delta\eta = (\eta_c - \eta) / 10 \tag{7}$$

If $\Delta\eta \geq 1^\circ$, then $\Delta\eta \equiv 1.^\circ$ and $\text{DETA} = |\Delta\eta / 100|$

$$\frac{v_r}{W_\infty} = (u \cos\eta + v \sin\eta) \frac{1}{W_\infty} \tag{8}$$

$$\frac{v_t}{W_\infty} = (-u \sin\eta + v \cos\eta)\frac{1}{W_\infty} \tag{9}$$

At
$$\frac{v_t}{W_\infty} = 0 \; ; \; \eta \equiv \eta_B$$

and an iterative procedure is used to obtain η_B starting with the shock angle η from the following equations

$$\left(\frac{v_t}{W_\infty}\right)_{\eta_j} = \left(\frac{v_t}{W_\infty}\right)_{\eta_{j-1}} \cos\Delta\eta + \left(\frac{R}{W_\infty} - \frac{v_r}{W_\infty}\right)_{\eta_{j-1}} \sin\Delta\eta \tag{10}$$

$$\left(\frac{v_r}{W_\infty}\right)_{\eta_j} = \left(\frac{v_t}{W_\infty}\right)_{\eta_{j-1}} \sin\Delta\eta - \left(\frac{R}{W_\infty} - \frac{v_r}{W_\infty}\right)_{\eta_{j-1}} \cos\Delta\eta + \left(\frac{R}{W_\infty}\right)_{\eta_{j-1}} \tag{11}$$

with

$$\left(\frac{R}{W_\infty}\right) = -\left(\frac{v_t}{W_\infty}\cot\eta + \frac{v_r}{W_\infty}\right)\left[1 - \frac{\left(v_t/W_\infty\right)^2}{\left(a/W_\infty\right)^2}\right]^{-1} \tag{12}$$

$$\left(\frac{a^2}{W_\infty^2}\right) = (\Gamma - 1)\left(\frac{h}{W_\infty^2}\right) \tag{13}$$

$$\left(\frac{h}{W_\infty^2}\right) = \frac{1}{2}\left[1 - \left(\frac{v_r}{W_\infty}\right)^2 - \left(\frac{v_t}{W_\infty}\right)^2\right] + \frac{h_\infty}{W_\infty^2} \tag{14}$$

when $\left(\frac{v_t}{W_\infty}\right)_j > 0$

$$\Delta\eta = \Delta\eta / 10 \text{ until}$$

$$|\Delta\eta| \leq \text{DETA}$$

η_B is then interpolated for

$$\eta_B = - \frac{\left(\frac{v_t}{W_\infty}\right)_j \Delta\eta}{\left[\left(\frac{v_t}{W_\infty}\right)_{j-1} - \left(\frac{v_t}{W_\infty}\right)_j\right]} + \eta_{j+1} \tag{15}$$

Points along the Reference Line

Once the final shock angle (η_s) and the properties behind the shock are obtained, a horizontal reference line consisting of 20 points is calculated. Γ and S/R are maintained constant and equal to the shock point values. The x - coordinate of the last point on the reference line (body point) is $3/4$ of the distance to x_t .

Thus,

$$x(20) = \frac{3}{4} (x_t - \bar{x}_o) \tag{16}$$

$$y(J) = \left[(c)\ x(20) + e \right] / d \qquad 1 \le J \le 20 \tag{17}$$

$$x(1) = \cot \eta_s \ y(1) + \bar{x}_o \tag{18}$$

$$\Delta x = 4/71 \left[x(20) - x(1) \right] \tag{19}$$

$$x(2) = x(1) + \Delta x / 4 \tag{20}$$

$$x(3) = x(2) + \Delta x / 2 \tag{21}$$

$$x(J) = x(J-1) + \Delta x \qquad 4 \le J \le 19 \tag{22}$$

Values of $\eta(J)$ corresponding to x (J) can be obtained from

$$\eta(J) = \tan^{-1} \left[y(J) / (x(20) - \bar{x}_o) \right] \tag{23}$$

The values at each subsequent point J are obtained in the following manner.

$$\Delta\eta = \left[\eta(J) - \eta(J-1) \right] / 5 \tag{24}$$

If $\Delta\eta \ge .01^\circ$, $\Delta\eta = \Delta\eta / 2$

Equations (10) through (14) are iterated upon from $\eta(J-1)$ until $\eta(J)$ is reached and the values of h/W_∞^2 , v_t / W_∞ , v_r / W_∞ , a^2 / W_∞^2 obtained, at each point (J)

$$u = \left(\frac{v_r}{W_\infty} \cos \eta - \frac{v_t}{W_\infty} \sin \eta \right) W_\infty \tag{25}$$

$$v = \left(\frac{v_r}{W_\infty} \sin \eta + \frac{v_t}{W_\infty} \cos \eta \right) W_\infty \tag{26}$$

$$\theta = \tan^{-1} (v/u) \tag{27}$$

$$M^2 = \left[\left(\frac{v_r}{W_\infty} \right)^2 + \left(\frac{v_t}{W_\infty} \right)^2 \right] \Big/ \left(\frac{a}{W_\infty} \right)^2 \tag{28}$$

$$\mu = \sin^{-1} (1/M) \tag{29}$$

Use either (30a) for gas dissociation or (30b) for vibrational excitation.

Assume $\rho'(J) = \rho'(J-1)$ initially to obtain

$$\Delta \rho' = \frac{S/R - \sum_{m=0}^{4} \sum_{n=0}^{5} B_{mn} (\rho_i')^m (h')^n}{\sum_{m=0}^{4} \sum_{n=0}^{5} m \, B_{mn} (\rho_i')^{m-1} (h')^n}$$

Iterate using $\rho'_{i+1} = \rho'_i + \Delta\rho'$

then obtain

$$p = \frac{\Gamma - 1}{\Gamma} \rho h$$

(30a)

$$
\left.
\begin{aligned}
T_{initial} &= \frac{h}{c_p} \\
T &= \frac{h}{c_{p_\infty}} - \frac{\gamma_\infty - 1}{\gamma_\infty} \frac{\theta'}{\left(e^{\theta'/T} - 1\right)} \quad \text{by iteration} \\
\ell n \; {}^{p}/{}_{p_\infty} &= \frac{\gamma_\infty}{\gamma_\infty - 1} \; {}^{T}/{T_\infty} + \theta' \left[\frac{e^{\theta'/T}}{T\left(e^{\theta'/T} - 1\right)} - \frac{e^{\theta'/T_\infty}}{T_\infty\left(e^{\theta'/T_\infty} - 1\right)} \right] \\
&\quad - \ell n \left[\frac{e^{\theta'/T} - 1}{e^{\theta'/T_\infty} - 1} \right] + \left({}^{S}/{}_{R}\right)_\infty - {}^{S}/{}_{R}
\end{aligned}
\right\} (30b)
$$

and

$$
\rho = \frac{p}{h} \; \frac{\Gamma}{\Gamma - 1}
$$

INPUT FORMATS

In this section, the input formats for each of the three program decks - Flow Field, Transonic-Subsonic, and Supersonic - will be described in detail. Refer to the section on Nomenclature for allied information.

The term "card", refers to the standard IBM data processing card consisting of 12 rows and 80 columns. Since columns 73 - 80 are not read by the computer, any identifying information may be punched in these columns. The term, "format", refers to the mode of input. Symbolically, these modes may be defined as follows:

I	integer	± XX	(no decimal point)
F	fixed point	± XX. XXX	(decimal point required)
E	floating point	± X. XXX ± YY	(YY is the exponent to the base 10: $\pm X.XXX \cdot 10^{(YY)}$)

For the E and F modes, the decimal point may , of course, be shifted from the position indicated in the above examples and the maximum number of significant figures is governed by the field width assigned for each "word" of data. The plus (+) sign may be omitted in all cases, except for the sign immediately preceeding the exponent for the E mode. An additional format is the Hollerith mode which consists of alpha-numerical information, and for our purposes, will be utilized exclusively for an identification input card, which will subsequently be printed as a title at the head of the output listing.

FLOW FIELD PROGRAM

Due to the size of this binary deck, an option has been incorporated into the coding to permit the user to either read in the input data cards via the IB Monitor input tape or via the on-line card reader. It is recommended that the latter option be utilized, since this will allow the user to permanently store the object deck on magnetic tape, thus avoiding frequent handling of the cards. Refer to the section on Operating Instructions for further details.

CARD	COL.	DATA	FORMAT
1	1	1	I
	2-72	Hollerith information - title	
2	1-10	M_∞	F
	11-20	T_∞	F
	21-30	$(S/R)_\infty$	F
	31-40	ρ_∞	E
	41-50	p_∞	E
3	1-10	x^*	F
	11-20	y^*	F
	21-30	x_c	F
	31-40	y_c	F
	41-50	θ_c	F
	51-60	R_c	F

CARD	Col.	DATA	FORMAT
4, 5, . . . , A	2-10	a	F
	12-20	b	F
	22-30	c	F
	32-40	d	F
	42-50	e	F
	52-60	x_t	F
	62-70	α	F
A + 1	1	Stagnation Point Code = 1	I
	2-10	x_o	F
	11	Point 1 Code = 1 or 2	I
	12-20	x_1	F
	21	Point 2 Code = 1 or 2	I
	22-30	x_2	F
	31	Point 3 Code = 1 or 2	I
	32-40	x_3	F
	41	Point 4 Code = 1 or 2	I
	42-50	x_4	F
	51	Point 5 Code = 1 or 2	I
	52-60	x_5	F
	61	Point 6 Code = 1 or 2	I
	62-70	x_6	F
A+2, A+3	Identical in format to card A + 1		
(if required)	Pertains to points 7 through 20, in sequence		

CARD	COL.	DATA	FORMAT
B	2-10	y_o	F
	12-20	y_1	F
	22-30	y_2	F
	32-40	y_3	F
	42-50	y_4	F
	52-60	y_5	F
	62-70	y_6	F
B+1, B+2		Identical in format to card B.	
(if required)		Pertains to points 7 through 20, in sequence	
C	1, 2	Number of intervals of mesh spacing, $\Delta\tau_1$	I
	3-10	$\Delta\tau_1$	F
	11, 12	Number of intervals of mesh spacing, $\Delta\tau_2$	I
	13-20	$\Delta\tau_2$	F
	21, 22	Number of intervals of mesh spacing, $\Delta\tau_3$	I
	23-30	$\Delta\tau_3$	F
	41, 42	Number of intervals of mesh spacing, Δy_1	I
	43-50	Δy_1	F
	51, 52	Number of intervals of mesh spacing, Δy_2	I
	53-60	Δy_2	F
	61, 62	Number of intervals of mesh spacing, Δy_3	I
	63-70	Δy_3	F

Card 1 may be used for a title of identification since it is written as the first line of output. The free stream conditions are punched on card 2.

Card 3 contains the coordinates, (x^*, y^*), of the assumed sonic point on the body, i.e. where the slope of the body is unity. The remaining data consists of coordinates of a downstream point, (x_c, y_c), where the slope of the body is tan θ_c , and where the radius of curvature of the body is R_c . In general, $20^o < \theta_c < 25^o$; the input value of θ_c is in radians.

Cards 4 through A contain the coefficients of the equations describing sequential sections of the body profile: $a x^2 + b y^2 + c x + d y + e = 0$. The domain of validity for each section is defined by its terminal value, x_t . The exterior angle between this section and the following one is α ; a positive non-zero value of α defines a reentrant corner at $x = x_t$. If α is negative, an expansion corner is defined and, of course, $\alpha = 0$ indicates that the body is continuous at $x = x_t$. A maximum of 12 body profiles may be prescribed.

The following cards prescribed the coordinates of up to 21 points which define the geometry of the nose region of the body, and also indicate which of these points are to be satisfied by the iterative procedure employed by the Transonic-Subsonic program to achieve an accurate configuration of the bow shock. A maximum of 10 of these "iteration points", including the stagnation point, may be prescribed.

The x-coordinates of these points, in sequential order, from the axis of symmetry, downstream, are punched on card A (and cards A+1 and A+2, if necessary), along with codes which indicate whether a specific point is to be satisfied by iteration. A code = 1 prescribes an "iteration point"; a code of 2 indicates that this point will be used for the purpose of describing the nose geometry

only. The corresponding y-coordinates are on card (s) B (and B+1 and B+2) Note that the stagnation point must always be prescribed as an "iteration point".

To assure an accurate solution, it is advisable to prescribe at least two points adjoining the assumed sonic point on the body, as "iteration"points. For a spherical nose, these points should be located where the slope of the body is approximately 40° and 50° respectively. Should the body exhibit a more rapid change of curvature than does a sphere, in the neighborhood of the sonic point, then additional iteration points should be clustered in this region. At least 5 points, including the sonic point, should be prescribed as "iteration" body points in the region from the axis of symmetry to the assumed sonic point.

The final input card, C , prescribes the τ-y mesh used in the subsonic region. As indicated, up to 3 different mesh intervals in each direction may be prescribed. Since the analysis becomes increasingly unstable as the mesh is refined, it is necessary to maintain as coarse a mesh as possible. For a spherical nose, a 5 x 4 τ-y mesh yielded very good results. In general, even for the more complex nose geometries, a 10 x 12 τ-y mesh should be a rough upper limit of mesh density. The program cannot accommodate a mesh more refined than 15 x 15.

Columns 3 - 10 indicate the τ mesh interval adjacent to the bow shock ($\tau = 1$), and cols. 43 - 50 refer to the y mesh increment adjacent to the axis of symmetry. Refer to Fig. II and the section on sample inputs and outputs for further details.

Thus the number of input cards necessary for a given run varies from roughly 8 to an upper limit of 22; in most cases the number will not exceed 12.

The option of using varying mesh intervals was included so that a relatively dense mesh may be prescribed in those portions of the subsonic region where the velocity gradients are high, without impairing the stability (and accuracy) of the solution. A recommended mesh for a spherical nose is:

4 intervals @ $\Delta y_1 = 0.15$ and 4 @ $\Delta y_2 = 0.1$

4 intervals @ $\Delta \tau_1 = 0.15$ and 4 @ $\Delta \tau_2 = 0.1$

These proportions result in a relatively coarse (8 x 8) mesh which is sufficiently detailed in those areas characterized by high velocity gradients.

For those nose geometries which exhibit a very rapid change of curvature in the neighborhood of the sonic point (e.g. the Apollo configuration), it will be necessary to utilize 3 mesh intervals in each direction to obtain accurate results.

Note that the last "body card" (card A) should be blank. Thus, there may be up to 12 body profiles, followed by a blank card, followed by the nose geometry, etc. The value of x_t for all body profiles must be non-zero.

TRANSONIC-SUBSONIC PROGRAM

The input format is identical in all respects to that used for the Flow Field program. Since only the nose region is considered, it is not necessary to prescribe the body profiles for the after-body (cards 4, 5, . . .), since the program will not utilize this information. Thus only one or two body cards which prescribe the body profile in the vicinity of the assumed sonic point, will be necessary.

Refer to the description of input format for the Flow Field program for all necessary details. Since this object deck is half the size of the Flow Field deck, it may not be advantageous to utilize the option to read data cards, on-line.

SUPERSONIC PROGRAM

Option 1

Option 1 is employed when it is necessary to punch all input data on cards. This situation occurs whenever the binary tape, generated by the Transonic - Subsonic program, is not available. Before generating the supersonic flow field mesh, the program will write all inputs on binary tape mounted on unit B3, in exactly the same format as that required by options 2 and 3 of this program, for subsequent use, if desired.

CARD	COL.	DATA	FORMAT
1	1	0	I
	2-72	Hollerith information - title	
2	1	1	I
3	1-10	M_∞	F
	11-20	p_∞	F
	21-30	T_∞	F
	31-40	$(S/R)_\infty$	F
	41-50	ϵ_o	F
	51-60	ρ_∞	E
4, 5, ..A	1-10	a	F
	11-20	b	F
	21-30	c	F

CARD	COL.	DATA	FORMAT
	31-40	d	F
	41-50	e	F
	51-60	x_t	F
	61-70	α	F
A + 1	1-72	Blank	
A+2, A+3, . . . , B	1-8	x	F
	9-16	y	F
	17-24	P'	F
	25-32	θ	F
	33-40	S/R	F
	41-48	h'	F
	49-56	ρ'	F
	57-64	γ	F
	65-72	μ	F
B + 1	1-72	Blank	

Card 1 is an identification card which is printed as output. The option is prescribed on card 2. Card 3 contains the free stream conditions and the angle (in radians) of inclination with respect to the x axis of the bow shock at the reference line (ϵ_o). Cards 4 through A contain the geometrical data of sequential sections of the body profile; a maximum of 12 is permitted. Properties of sequential points along the reference line from detached shock to body are punched in cards A+2 through B. While a maximum of 21 points will be accepted, no more than a dozen, or so, is necessary in most cases.

Conical Nose

Option 1 also includes the case of a body having a conical nose. In this case, the program computes the points along a reference line having a constant value of y. Data cards 1 through A + 1 are identical to those previously described; cards A + 2 through B + 1 do not apply. Note that the values of a and b on card 4 must be zero since the first body profile is conical.

Since this reference line is written on the binary tape on unit B 3, subsequent runs may be executed using options 2 and/or 3.

Note that ϵ_0 on card 2 must be left blank since it is not known as an input.

Option 2

Option 2 is employed when the binary tape written by the Transonic - Subsonic program is available, and the supersonic portion of the flow field has not been completely generated. This situation could occur if the Transonic - Subsonic program were run, or if the Flow Field program were manually terminated at the completion of Link 1 due to scheduling problems, or if a machine failure occured during execution of Link 2, or any similiar cause. When this option is chosen, the program will behave essentially like Link 2 of the Flow Field program; binary tape B3 will be read and the supersonic flow field mesh will then be constructed.

CARD	COL.	DATA	FORMAT
1	1	0	I
	2-72	Hollerith information - title	
2	1	2	I

Card 1 may be used for identification since it is printed as output. The option is prescribed on card 2.

Option 3

Option 3 is employed when the binary tape written by the Transonic-Subsonic program is available, and it is desired to alter the geometry of the after-body of the vehicle under consideration, and generate the corresponding super-sonic flow field for an entire family of body shapes without incurring the cost of repeating the transonic-subsonic calculations. The new body equations will be written on the binary tape B-3 to replace the old ones.

CARD	COLS.	DATA	FORMAT
1	1	0	I
	2-72	Hollerith information - title	
2	1	3	I
3, 4, . . , A	1-10	a	F
	11-20	b	F
	21-30	c	F
	31-40	d	F
	41-50	e	F
	51-60	x_t	F
	61-70	α	F
A + 1	1-72	Blank	

Card 1 may be used for identificaticatication since it is printed as output. The option is prescribed on card 2. Cards 3 through A contain the geometrical data of sequential sections of the body profile; a maximum of 12 is permitted.

OPERATING INSTRUCTIONS

These computer programs are designed for use with the standard IBM FORTRAN Monitor Systems which are commonly used with the IBM 709/7090/7094 digital computers. Since the FLOW FIELD program is a CHAIN job consisting of two LINKS, any variation of the above systems which does not accommodate CHAIN jobs, cannot be utilized. The TRANSONIC-SUBSONIC and SUPERSONIC programs are not CHAIN jobs and thus are not subject to the above restriction.

An IOU table subroutine is included as part of the object decks; this avoids those difficulties associated with varying logical tape assignments from one computer installation to another. The following tape units are common to all programs:

A 1	IBM FORTRAN System Tape
A 2	Program INPUT Tape
A 3	Program OUTPUT Tape - to be listed.
A 4	Intermediate Monitor tape - used to stack LINKS of CHAIN job for FLOW FIELD program
B 1	Intermediate Monitor Tape
B 2	Intermediate Monitor Tape
B 3	Binary Tape utilized by all these programs
B 4	"Clock" Tape - utilized by Monitor System

FLOW FIELD and TRANSONIC - SUBSONIC PROGRAMS

Input Option No. 1

If desired, the object decks may be stacked with those of other programs and loaded onto tape via the IBM 1401 as part of a "Monitor Run". In this case, the data (input) cards are placed immediately behind the DATA control card and become a part of the object deck for a given run. Of course, this program alone may be loaded onto tape as indicated above, or via the on-line card reader, if desired. The tape is mounted on unit A 2 as the INPUT tape. This procedure is standard at most computer installations; the lone disadvantage is that the binary program cards must be handled each time a run is to be executed.

The following sense switch setting is required for this input option:

Sense Switch 5: UP

Input Option No. 2

Since the object deck of the FLOW FIELD program is rather large and thus somewhat cumbersome to handle, the user may elect to store this deck permanently on magnetic tape. This tape is then mounted on unit A 2 as the INPUT tape, and the following simple procedure executed:

1. Clear memory and read in via the on-line card reader, the FORTRAN START card.
2. After the Monitor starts functioning (a few seconds), FEED out this START card.

3. Place the data cards in the hopper of on-line card reader and depress the reader START key until the READY light goes on.

The following sense switch setting is required for this input option:

Sense Switch 5: DOWN

Output Options:

Since writing BCD tape is relatively costly, the program is designed to restrict the amount of output and generate only the final results of the calculations. In some instances, the user may elect to generate additional, intermediate, information so that he may follow the development of the computations in greater detail. These options pertain only to the TRANSONIC - SUBSONIC portion (LINK 1) of the FLOW FIELD program; the SUPERSONIC portion (LINK 2) makes no reference to sense switch settings.

Output Option No. 1

The program will write on output tape A 3 only the final results of the calculations. These include the calculations of the final, iterated, shock polynomial, the final reference line, and the final results of the properties within the subsonic (elliptic) region of the flow field. In addition, the program will generate a binary tape on unit B 3 which is used as input media by LINK 2 of the FLOW FIELD program. This tape may also be saved for subsequent use by the SUPERSONIC program. The following sense switch settings are required for this output option:

Sense Switch 1: UP

Sense Switch 2: UP

Output Option No. 2

In addition to the output described for option no. 1 the program will write on output tape A 3, the properties behind the bow shock at points in the transonic region, the properties of points along the reference line, and the properties within the elliptic region, for each sweep through the transonic-subsonic regions in the process of iterating to obtain the final shock polynomial. In addition, the coefficients of the basic, perturbed, and final shock polynomials are written, as well as statements identifying envelopes in the transonic region (if any). The following sense switch settings are required for this output option:

Sense Switch 1: UP

Sense Switch 2: DOWN

Output Option No. 3

In addition to the output described for both options 1 and 2, the program will write on output tape A 3, the properties at points within the transonic region for each sweep through the transonic-subsonic region. This writing consumes a substantial amount of machine time; thus this option should be utilized very sparingly. The following sense switch settings are required for this output option:

Sense Switch 1: DOWN

Sense Switch 2: DOWN

Any combination of sense switch settings involving switches 1, 2, or 5 may be selected according to the needs of a particular run. Note that sense switches 3, 4, and 6 are not interrogated by the program.

SUPERSONIC PROGRAM

As indicated above, this program does not interrogate sense switch settings, and does not incorporate any input and/or output options as is present for the other two programs. This program is designed to function as a monitor job; the data cards are placed behind the DATA control card and become a part of the object deck for a given run. This deck is then loaded onto magnetic tape via the IBM 1401 computer, or via the on-line card reader - this may also be accomplished as part of a larger monitor run.

There are three variations in the use of this program; these are described in detail in the section on input formats and are classified as execution options. For options 2 and 3, the program requires a binary input tape mounted on unit B 3; this tape must have been previously generated by either the FLOW FIELD program or the TRANSONIC-SUBSONIC program or generated by a previous run of the SUPERSONIC program - see below. Option number 1 requires that a blank tape be mounted on unit B 3 for binary output purposes. The user must indicate whether he wishes to retain the use of the tape on unit B 3 for future runs with the SUPERSONIC program.

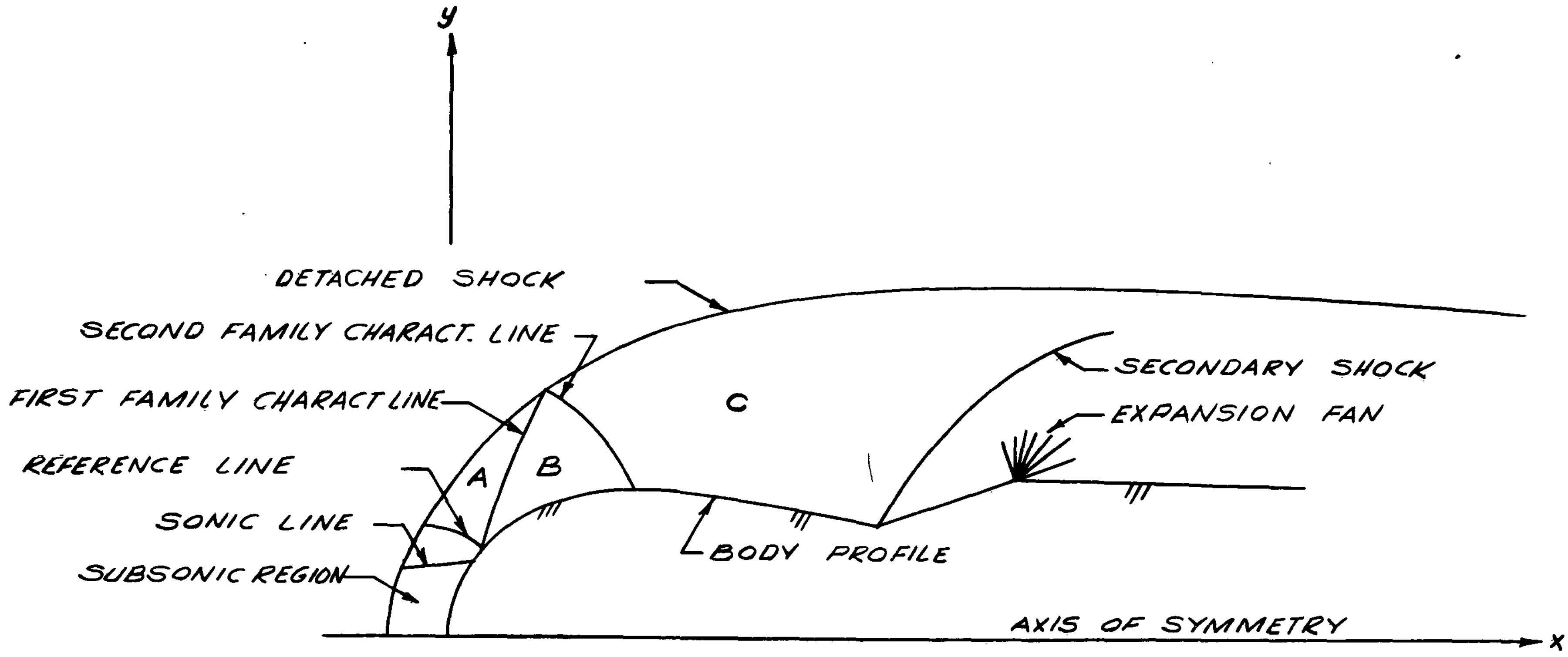

FIG. I SCHEMATIC OF FLOW FIELD

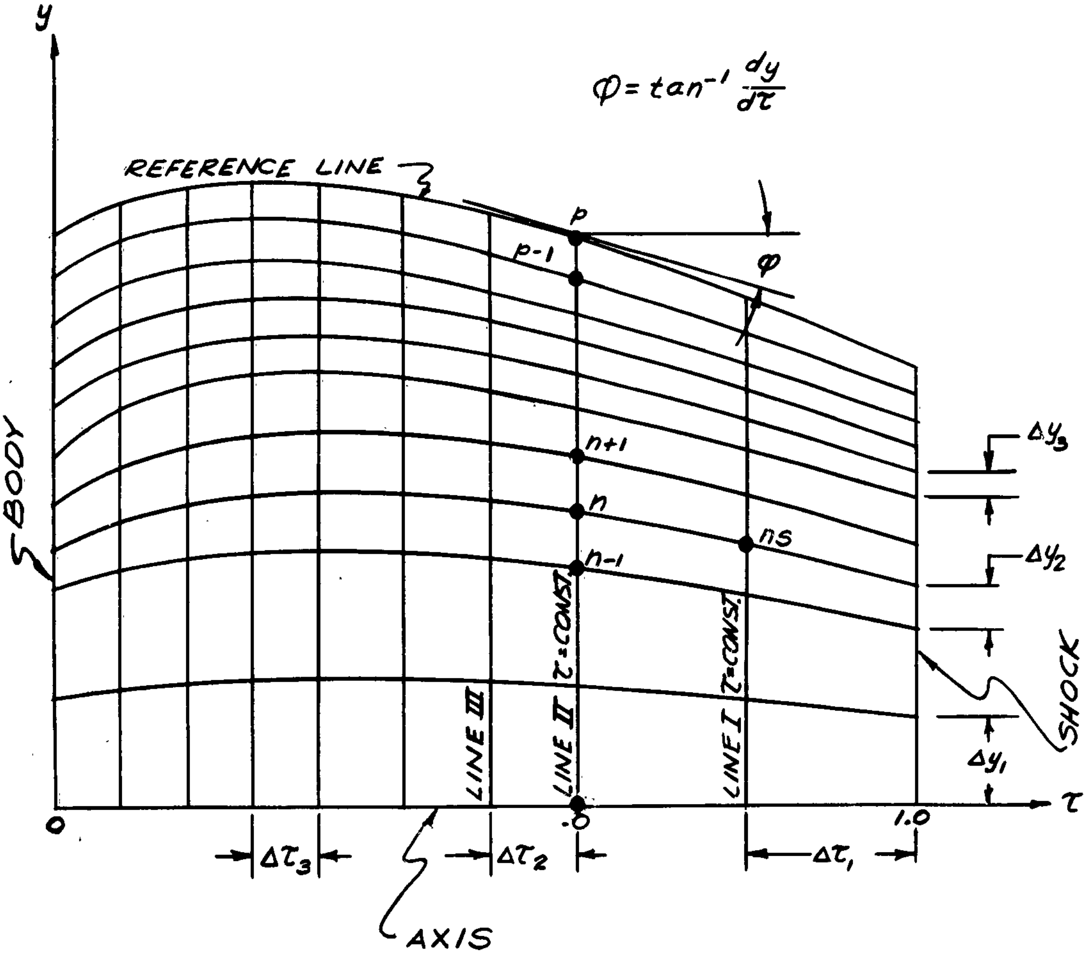

FIG. II TRANSFORMED τ-y PLANE SUBSONIC REGION

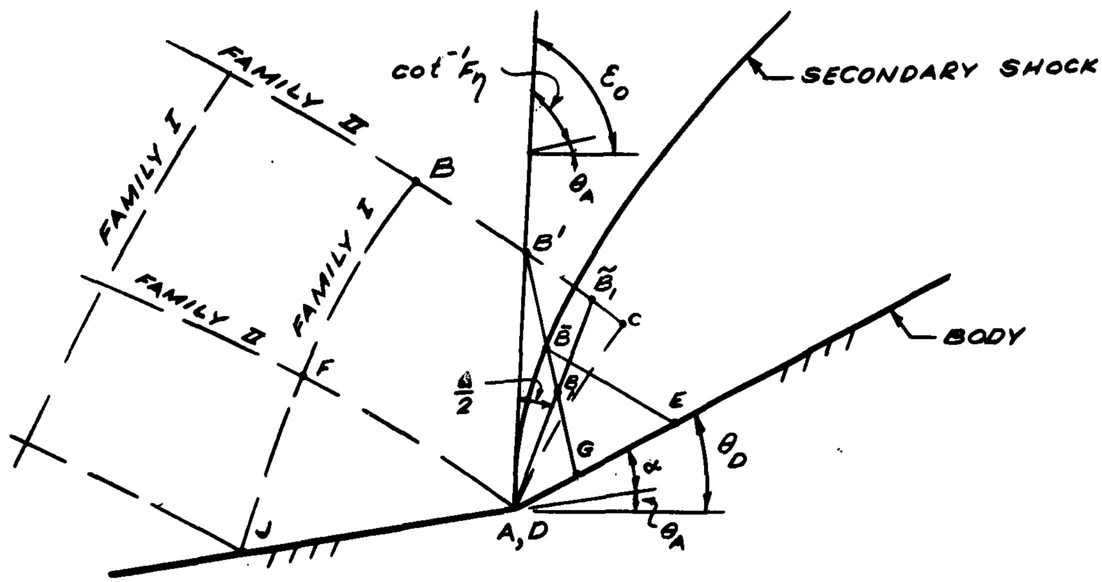

FIG. III a

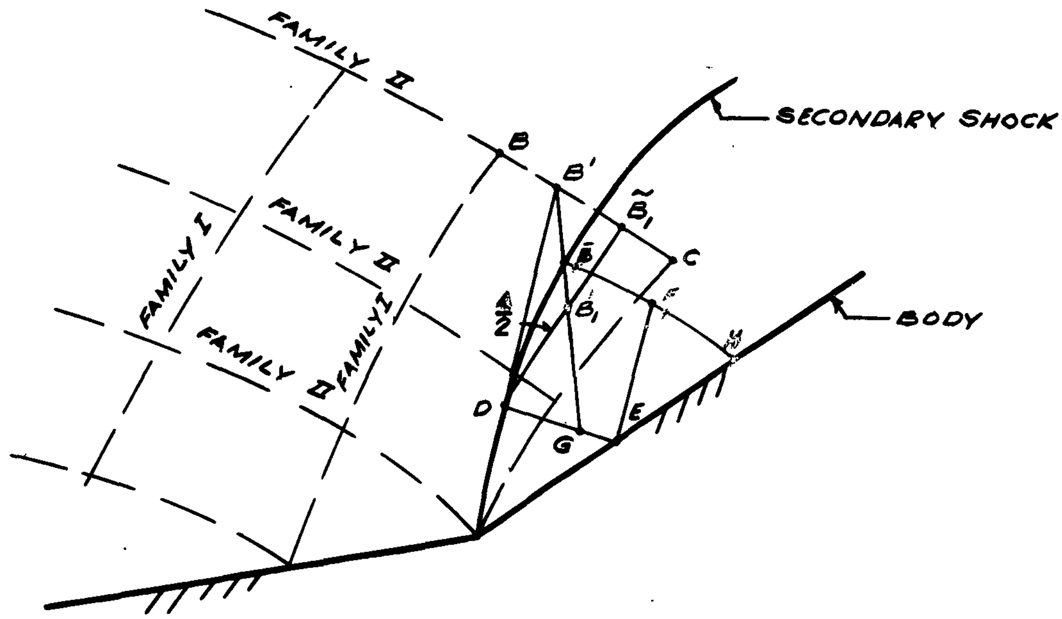

FIG. IIIb

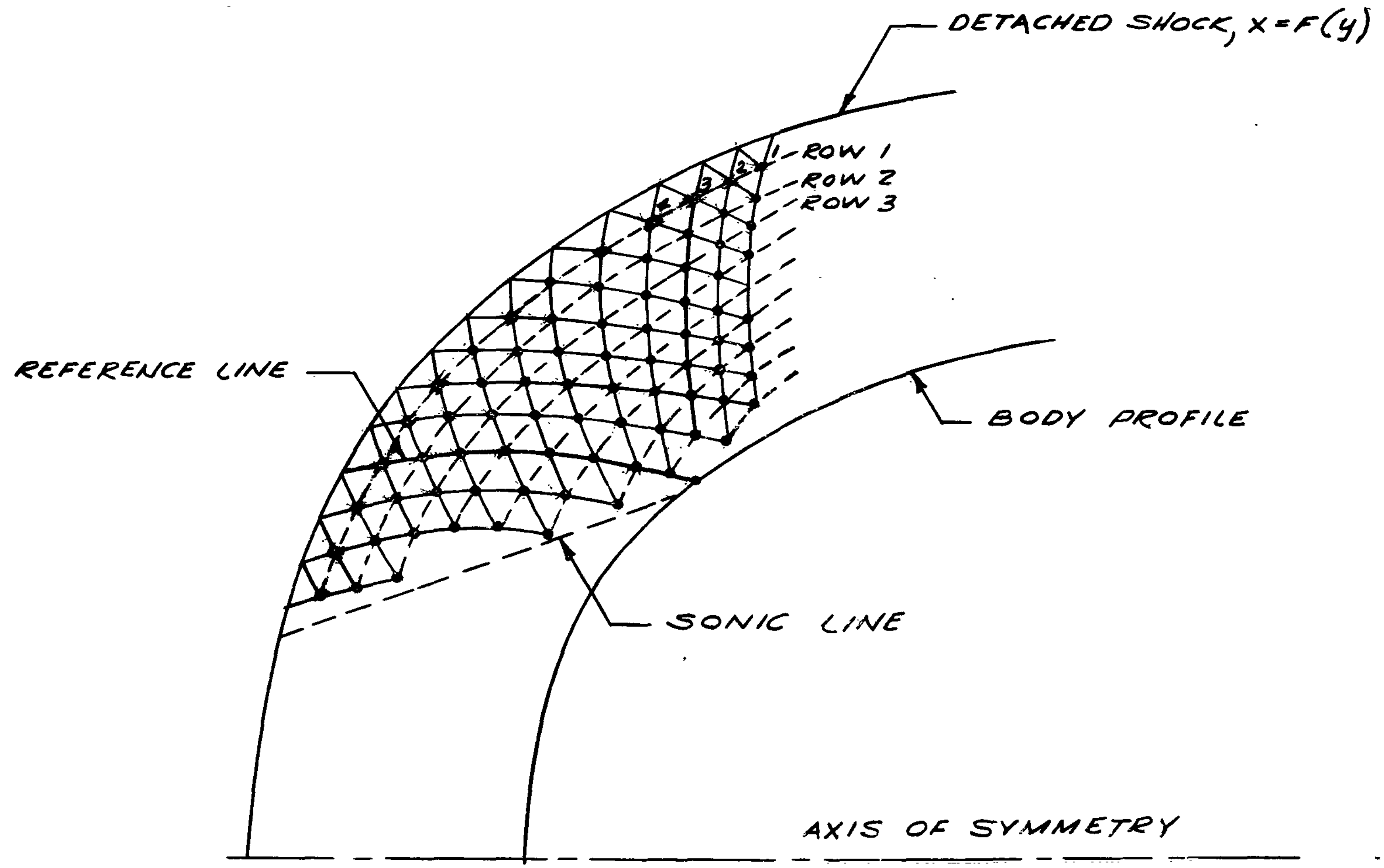

FIG. IV MESH OF CHARACTERISTICS IN TRANSONIC REGION

NOMENCLATURE

This section will define all symbols and their units which have not been adequately defined within the context of the description of the analysis. Since some symbols have been utilized in both the Transonic-Subsonic analysis as well as the Supersonic analysis, and may have different connotations, this table of nomenclature is subdivided as indicated to avoid confusion.

Transonic-Subsonic Analysis

ρ	Density, slugs/cu. ft.
γ	Adiabatic exponent
δ_o	Detachment distance at axis
u	Velocity component in x direction, ft./sec.
$\bar{\bar{\Pi}}$	Dimensionless pressure
R_{b_o}	Radius of curvature of body, at axis
R_{sh_o}	Radius of curvature of detached shock, at axis
v	Velocity component in y direction, ft./sec.
τ	(Basic Shock Polynominal Analysis)
Φ	$\bar{\bar{\Pi}} \bar{\bar{P}}^{-\gamma}$
c	Dimensionless stagnation enthalpy
U	Dimensionless velocity component in x direction
V	Dimensionless velcoity component in y direction

θ	Velocity direction measured from x axis, radians
μ	Mach angle, radians
$f(\tau, y) = F$ (output listing)	Dimensionless function describing entropy distribution
$\tilde{P}$	Dimensionless pressure
$R = P = \delta \frac{\rho}{\rho_\infty}$	Dimensionless density, $\delta = \frac{\gamma - 1}{\gamma + 1}$

Subscripts:

w	Property behind detached shock
o	Property at axis of symmetry
b	Property at body

Superscript:

*	Property at assumed sonic point

Supersonic Analysis

W	Resultant Velocity, ft./sec.
M	Mach Number
γ	Adiabatic exponent
a	Speed of sound, ft./sec.
$K_1/2$	Stagnation enthalpy, ft./sec.

C_{p_∞}	Specific heat at constant pressure
θ'	Reference temperature for vibrational excitation of air, ^oR
T_t	Stagnation temperature including effects of vibrational excitation, ^oR
T	Absolute temperature, ^oR
ρ	Density, slugs/cu. ft.
ρ'	Dimensionless density
p	Pressure, lbs/sq. ft.
P'	Dimensionless pressure
h	Enthalpy, ft /sec
h'	Dimensionless enthalpy
u	Velocity component in x direction, ft. /sec.
v	Velocity component in y direction, ft. /sec.
ϵ	Angle of inclination of shock with respect to x axis, radians
m	Mass flow slugs/sec.
$S/_R$	Entropy
A_{ij}, B_{mn}	Coefficients of numerical fit of the Mollier diagram for air
θ	Velocity direction measured from x axis, radians
μ	Mach angle, radians

<u>Subscript:</u>

∞	Free stream condition

REFERENCES

1. Lieberman, E.,"General Description of IBM 704 Computer Programs for Flow Field About Blunt-Nosed Bodies of Revolution in Hypersonic Flight," GASL Technical Report No. 134, August 1960.

2. Vaglio-Laurin, Roberto and Ferri, Antonio, "Theoretical Investigation of the Flow Field About Blunt-Nosed Bodies in Supersonic Flight", Journal of the Aero/Space Sciences, December 1958.

3. Vaglio-Laurin, Roberto, "On the Determination of Real Gas Flows About Blunt-Nosed Bodies", GASL Technical Report No. 104, Part 10, July 1959.

APPENDIX I

CHECK OF MASS FLOW ALONG REFERENCE LINE

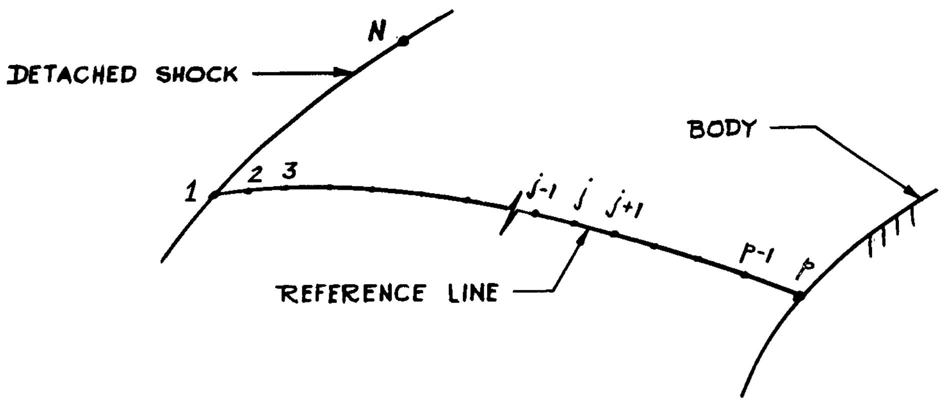

For the purpose of establishing an accurate relationship between mass flow and entropy, it is necessary to integrate mass flow through the shock layer along the reference line, from body (point p) to detached shock (point 1). This integrated value, m_1^*, is compared with the mass flow crossing the detached shock between the axis and point 1: $m_1 = {}^1/_2 \; \rho_\infty W_\infty y_1^2$. The error has been found to be very small, but for purposes of consistency it is "carried along" in all subsequent calculations of mass flow across the detached shock. Thus we define this error, $\epsilon = \frac{m_1^*}{m_1} - 1$: then the mass flow crossing the detached shock at any point, N, is calculated as $m_N = {}^1/_2 \; \rho_\infty \; W_\infty \; (y_N^2 + \epsilon \, y_1^2)$

The numerical integration of mass flow along the reference line is calculated as follows:

$$m^* = \sum_{j=p-1}^{1} {}^1/_2 \left[\rho_j \, W_j \sin\left(\theta_j - \varphi_j^{j+1}\right) y_j + \rho_{j+1} W_{j+1} \sin\left(\theta_{j+1} - \varphi_j^{j+1}\right) y_{j+1} \right]$$

$$\cdot \left[(x_j - x_{j+1})^2 + (y_j - y_{j+1})^2 \right]^{1/2}$$

where $\varphi_j^{j+1} = \tan^{-1} \left[\dfrac{y_j - y_{j+1}}{x_j - x_{j+1}} \right]$

APPENDIX II

FLOW DIAGRAMS

Most copies of this report contain only 4 pages of flow diagrams which describe, in general, the logical flow of these programs. These are contained on pages F1, F21, F28 and F49.

A few copies include very comprehensive and detailed flow diagrams of these programs. These are included for reference by those expert programmers who have the coding listings available, and who wish to study them in some detail.

Those who wish to modify the coding should note that the TRANSONIC-SUBSONIC program (LINK 1) consumes virtually all of core storage.

TRANSONIC-SUBSONIC FLOW CHART

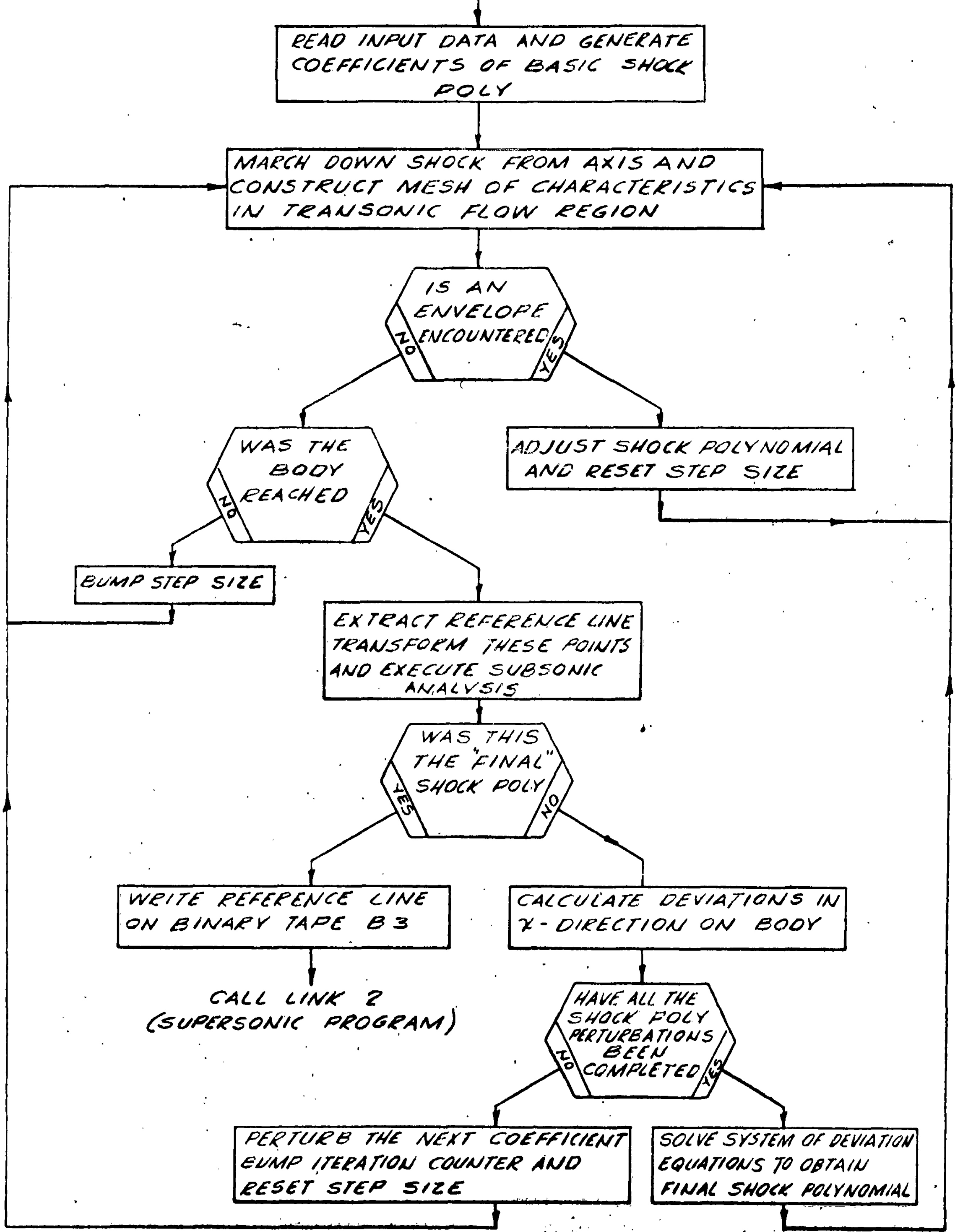

SUPERSONIC FLOW FIELD

READ IN POINTS ALONG REFERENCE LINE, THE FREE STREAM CONDITIONS AND THE BODY EQUATIONS.

↓

AFTER CALCULATING CERTAIN INVARIANT PROPERTIES, CONSTRUCT THE MESH OF CHARACTERISTIC FAMILY LINES IN REGION A BY MARCHING UP FIRST FAMILY LINES FROM REFERENCE LINE TO DETACHED SHOCK

↓

CONSTRUCT THE MESH IN REGION B BY MARCHING DOWN SECOND FAMILY LINES, FROM THE FINAL FIRST FAMILY LINE IN REGION A, TO THE BODY. AT EACH BODY POINT TEST FOR THE TERMINATION OF A BODY EQUATION TO DETECT EITHER A CONTINUOUS OR A DISCONTINUOUS BODY PROFILE. FOR THE LATTER CASE, PROVISION IS MADE TO EITHER CONSTRUCT A SECONDARY SHOCK OR AN EXPANSION FAN. SENSE LIGHT 3 IS ON DURING REGION B; SENSE LIGHT 4 GOES ON IF A SECONDARY SHOCK IS ENCOUNTERED

↓

THE REMAINDER OF THE FLOW FIELD (REGION C) IS CONSTRUCTED BY MARCHING DOWN SECOND FAMILY LINES FROM THE DETACHED SHOCK TO THE BODY. DISCONTINUITIES OF BODY PROFILE ARE TREATED AS INDICATED ABOVE FOR REGION B. SENSE LIGHT 3 IS TURNED OFF AND SENSE LIGHT 1 WILL BLINK UNLESS SENSE LIGHT 4 IS TURNED ON.

SUPERSONIC PROGRAM FLOW FIELD

MAIN PROGRAM

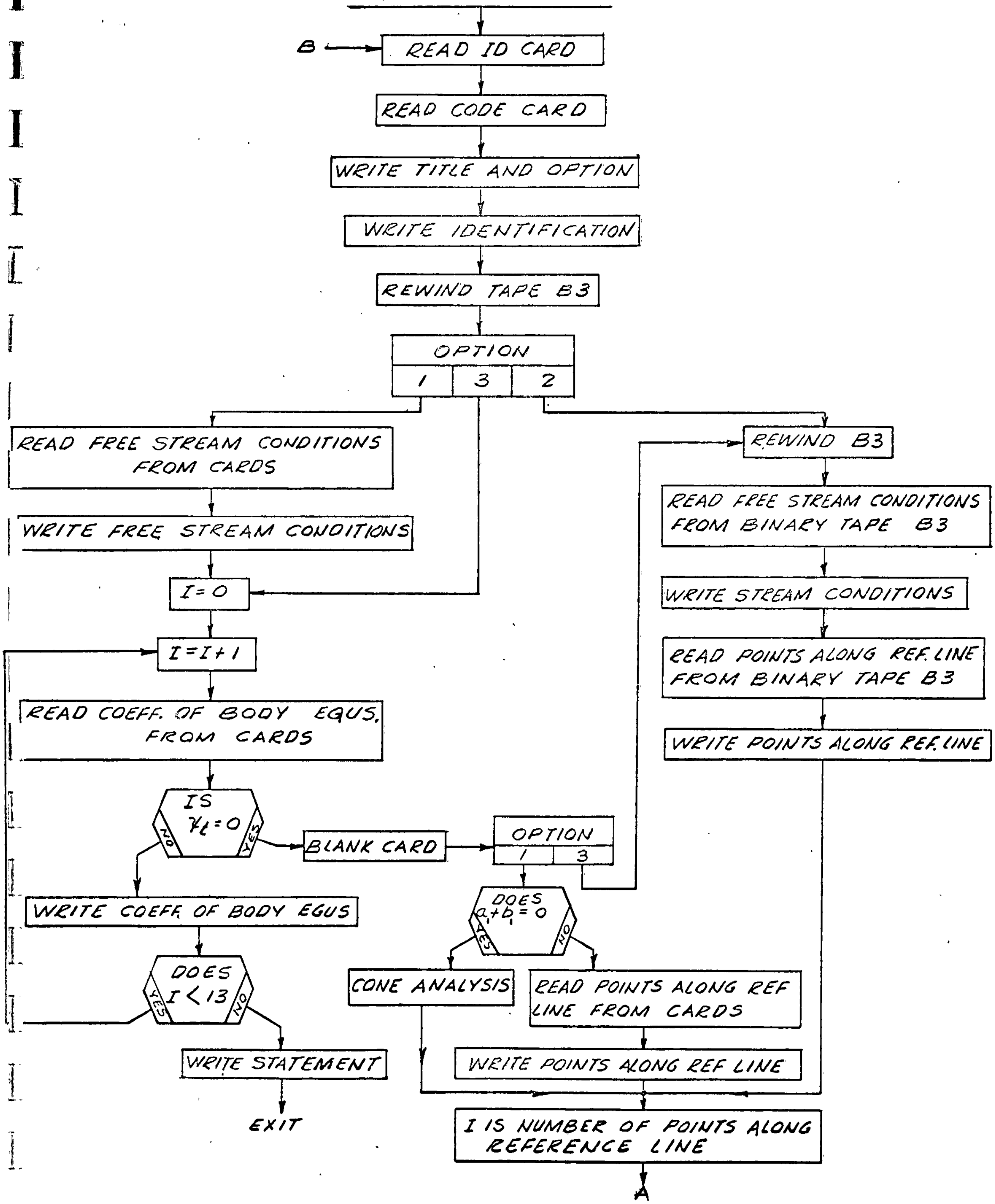

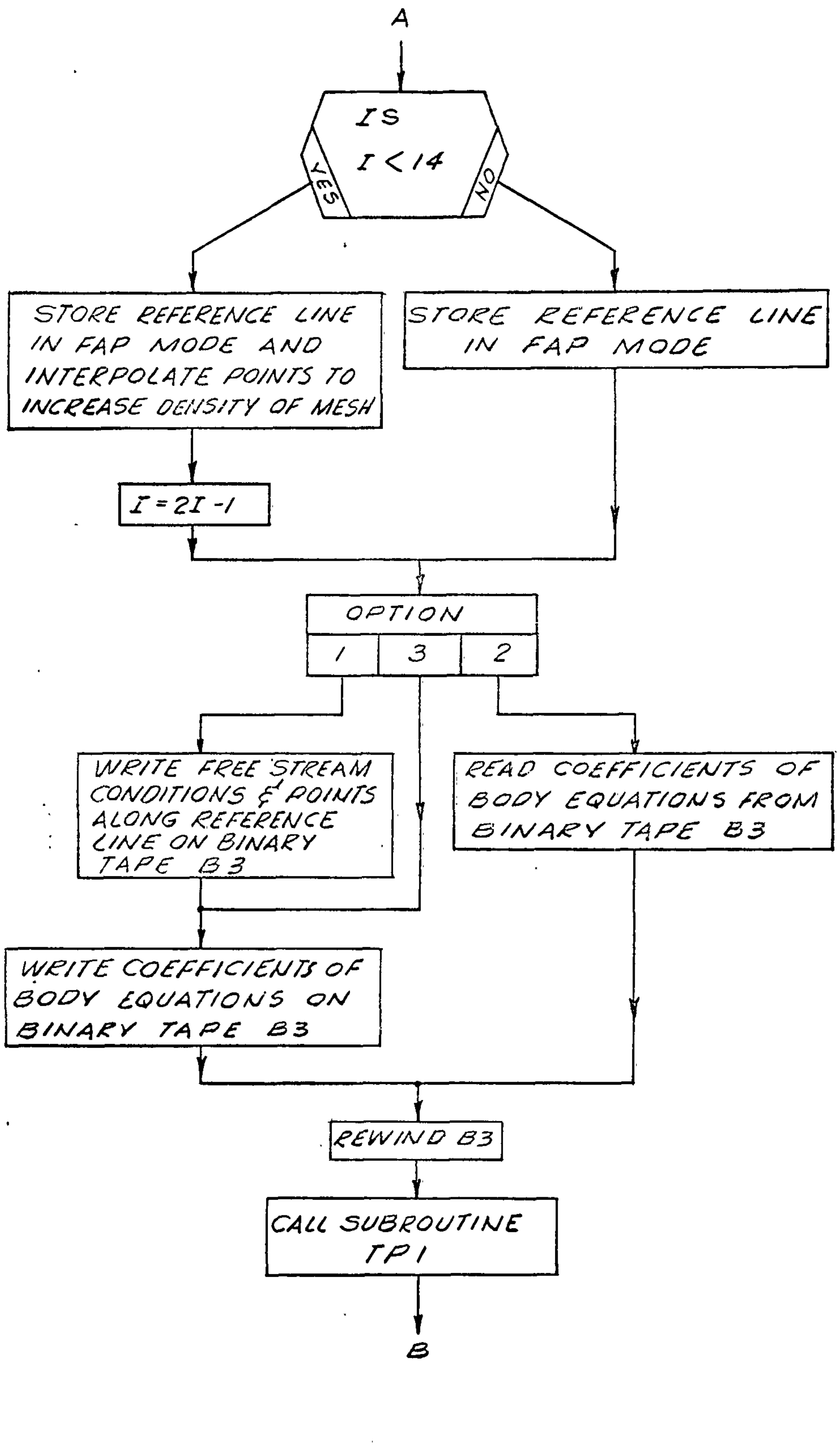
A
IS
I < 14
YES
NO
STORE REFERENCE LINE IN FAP MODE AND INTERPOLATE POINTS TO INCREASE DENSITY OF MESH
STORE REFERENCE LINE IN FAP MODE
I = 2I - 1
OPTION
1
3
2
WRITE FREE STREAM CONDITIONS & POINTS ALONG REFERENCE LINE ON BINARY TAPE B3
READ COEFFICIENTS OF BODY EQUATIONS FROM BINARY TAPE B3
WRITE COEFFICIENTS OF BODY EQUATIONS ON BINARY TAPE B3
REWIND B3
CALL SUBROUTINE TP1
B

APPENDIX III

SAMPLE INPUT AND OUTPUT LISTINGS

Some typical sample listings of input data cards and of program output are included and described below:

Page S 1 contains a listing of input data cards to the SUBSONIC (and FLOW FIELD) Program at the top of the page. The listing at the bottom of the page is of the input cards to the SUPERSONIC program, option number 1.

Pages S 2 through S 5 contain the entire output of the SUBSONIC Program, when sense switches 1 and 2 are both UP. Page S 2 consists of the input data, which is written for purposes of identification and checking. Page S 3 consists of the final reference line which is scaled so as to be compatible with the prescribed body profile. This scaling precludes the possibility of mesh crossings in region A of the SUPERSONIC Program, due to any small inconsistancy, between the body point on the reference line generated by the Transonic analysis, and the prescribed body profile. Pages S 4 and S 5 exhibit the properties within the Subsonic region of the flow field.

Pages S 6 through S 20 contain a few sheets of the output listing of the SUPERSONIC program. Page S 6, which is the first page of output, lists the input data cards for identification and checking. Pages S 7, S 8, and S 9 follow, and are the first points generated by the program in region A. The final first family characteristic line originates at the body, which is the last input point on the reference line (x = .33118, y = .6804 on page S 6), continues with the first IN (interior) point on page S 10, and terminates at the DS (detached shock) point on page S 11. Region B follows with the BD (body) point on page S 11, and

S12.

Further on in region B an expansion corner is detected as illustrated on page S13. Still further on in region B, a reentrant corner is detected and the beginning of the resulting secondary shock and surrounding flow field is shown on pages S 14 through S 17. A typical second family characteristic line in region C, originating at the detached shock, crossing a secondary shock, and terminating at the body, is shown on pages S 18, S 19, and S 20.

S1

```
1     RE-ENTRY BODY 20  ALT = 180K   (10 - 15)  NOSE RADIUS = 1/4                1
   22.224    497.49     28.937 0.12028-5 0.10272+1                               2
  0.29289   0.70711   0.61732   0.92388   0.39270       1.0
      1.0       1.0      -2.0       0.0       0.0   0.82635       0.0          3
      0.0       0.0  0.210138  -1.19175       1.0    176.72 0.0872665          4
      0.0       0.0 -.0174532 0.0651361       1.0     326.0       0.0          5
1     0.01.01837545.07282647.16135195  0.233961  0.292891   0.35721
      0.0 .19082252 .37463215 .54467371  0.64279   0.70711   0.76604
 5    0.2                            4    0.25                                 8
```

```
0  EQUILIBRIUM FLOW FIELD-NOL SPHERE-P(INF)=50MMHG, V(INF)=16000 FPS     ENOL-001
1
     14.32     139.25     520.0   26.5098    1.1086 0.1561-03
       1.0        1.0    -2.128              0.1321       0.5   -0.5994
                                      1.0  -0.82577       0.7       0.3
                         0.3093      -1.0   0.60926       5.0      -0.3
                                      1.0  -2.15576      10.0

.13202  .53000    2.6171  .90534  35.843  23.303 -.20696  1.3234  .75691 ENOL-003
.14108  .53760    2.6051  .90381  35.865  23.333 -.21248  1.3236  .75982 ENOL-004
.15014  .54519    2.5930  .90228  35.886  23.363 -.21804  1.3238  .76264 ENOL-005
.15969  .55268    2.5796  .90030  35.910  23.393 -.22421  1.3241  .76565 ENOL-006
.16924  .56017    2.5661  .89831  35.934  23.423 -.23034  1.3243  .76858 ENOL-007
.17891  .56769    2.5515  .89542  35.959  23.453 -.23699  1.3245  .77161 ENOL-008
.18858  .57521    2.5369  .89252  35.983  23.483 -.24364  1.3247  .77459 ENOL-009
.19837  .58274    2.5215  .88888  36.009  23.513 -.25067  1.3249  .77767 ENOL-010
.20816  .59026    2.5060  .88524  36.036  23.543 -.25768  1.3251  .78079 ENOL-011
.21807  .59780    2.4900  .88100  36.061  23.573 -.26497  1.3254  .78383 ENOL-012
.22797  .60533    2.4739  .87675  36.088  23.603 -.27222  1.3256  .78701 ENOL-013
.23443  .61286    2.4574  .87198  36.115  23.632 -.27974  1.3258  .79014 ENOL-014
.24799  .62038    2.4408  .86721  36.142  23.663 -.28721  1.3260  .79343 ENOL-015
.25827  .62791    2.4238  .86209  36.169  23.692 -.29494  1.3262  .79661 ENOL-016
.26853  .63543    2.4067  .85696  36.197  23.723 -.30264  1.3265  .80005 ENOL-017
.27879  .64295    2.3896  .85145  36.225  23.753 -.31042  1.3267  .80333 ENOL-018
.28906  .65045    2.3724  .84594  36.252  23.783 -.31816  1.3269  .80677 ENOL-019
.29952  .65795    2.3550  .84019  36.280  23.812 -.32605  1.3271  .81008 ENOL-020
.30998  .66545    2.3375  .83443  36.308  23.842 -.33391  1.3273  .81358 ENOL-021
.32058  .67294    2.3199  .82844  36.335  23.872 -.34186  1.3276  .81702 ENOL-022
.33118  .6804226  2.3023  .82245  36.364  23.903 -.34982  1.3278  .82068 ENOL-023
```

RE-ENTRY BODY 20 ALT = 180K (10 - 15) NOSE RADIUS = 1/4

FREE STREAM PROPERTIES - MACH NO.=22.224 TEMPERATURE=497.49 ENTROPY (S/R)=28.937 DENSITY=.12028E-05 PRESSURE=.1027E 01

NOSE POINTS USED TO CONSTRUCT BASIC SHOCK POLYNOMIAL

SONIC POINT X= 0.29289 Y= 0.70711 X= 0.61732 Y= 0.92388 THETA= 0.39270 RB=1.0000

COORDINATES OF BODY PROFILE IN NOSE REGION

ITERATION POINT	X	Y
YES	0.	0.
YES	0.0184	0.1908
YES	0.0728	0.3746
YES	0.1614	0.5447
YES	0.2340	0.6428
YES	0.2929	0.7071
YES	0.3572	0.7660

SUBSONIC MESH STATISTICS

NUMBER OF DELTA TAU INTERVALS	DELTA TAU	NUMBER OF DELTA Y INTERVALS	DELTA Y
5	0.200	4	0.250
-0	-0.	-0	-0.
-0	-0.	-0	-0.

S3

POINTS ALONG REFERENCE LINE

	X	Y	P PRIME	THETA	S/R	H PRIME	RHO PRIME	GAMMA	MU	RHO	P	H
BS	0.2581	0.8039	-1.6203	0.8211	46.7816	42.2532	-2.2166	1.1696	0.3974	0.1517E-04	0.4187E 03	0.1904E 09
IN	0.2664	0.8076	-1.6535	0.8142	47.1450	43.4262	-2.2379	1.1673	0.4112	0.1444E-04	0.4050E 03	0.1957E 09
IN	0.2749	0.8112	-1.6872	0.8070	47.5024	44.5751	-2.2584	1.1649	0.4252	0.1378E-04	0.3916E 03	0.2009E 09
IN	0.2834	0.8147	-1.7211	0.7994	47.8537	45.6978	-2.2787	1.1625	0.4400	0.1315E-04	0.3786E 03	0.2059E 09
IN	0.2920	0.8179	-1.7553	0.7915	48.1961	46.7846	-2.2986	1.1603	0.4555	0.1256E-04	0.3658E 03	0.2108E 09
IN	0.3006	0.8209	-1.7896	0.7833	48.5286	47.8325	-2.3182	1.1582	0.4716	0.1201E-04	0.3535E 03	0.2155E 09
IN	0.3093	0.8237	-1.8240	0.7748	48.8495	48.8354	-2.3374	1.1562	0.4884	0.1149E-04	0.3415E 03	0.2201E 09
IN	0.3179	0.8262	-1.8584	0.7661	49.1576	49.7897	-2.3563	1.1544	0.5058	0.1100E-04	0.3300E 03	0.2244E 09
IN	0.3266	0.8285	-1.8928	0.7571	49.4519	50.6919	-2.3749	1.1527	0.5237	0.1054E-04	0.3188E 03	0.2284E 09
IN	0.3352	0.8306	-1.9271	0.7479	49.7313	51.5392	-2.3931	1.1511	0.5422	0.1010E-04	0.3081E 03	0.2322E 09
IN	0.3437	0.8324	-1.9614	0.7384	49.9955	52.3299	-2.4109	1.1497	0.5610	0.9699E-05	0.2977E 03	0.2358E 09
IN	0.3523	0.8339	-1.9955	0.7288	50.2440	53.0631	-2.4233	1.1483	0.5800	0.9316E-05	0.2877E 03	0.2391E 09
IN	0.3607	0.8352	-2.0294	0.7190	50.4765	53.7378	-2.4454	1.1471	0.5992	0.8957E-05	0.2781E 03	0.2421E 09
IN	0.3690	0.8362	-2.0632	0.7090	50.6933	54.3549	-2.4622	1.1460	0.6182	0.8619E-05	0.2689E 03	0.2449E 09
IN	0.3772	0.8369	-2.0969	0.6988	50.8942	54.9139	-2.4785	1.1449	0.6369	0.8300E-05	0.2600E 03	0.2474E 09
IN	0.3853	0.8374	-2.1304	0.6885	51.0798	55.4171	-2.4945	1.1440	0.6551	0.8000E-05	0.2514E 03	0.2497E 09
IN	0.3931	0.8377	-2.1638	0.6780	51.2503	55.8650	-2.5101	1.1431	0.6724	0.7717E-05	0.2431E 03	0.2517E 09
IN	0.4008	0.8377	-2.1971	0.6674	51.4061	56.2590	-2.5254	1.1422	0.6887	0.7450E-05	0.2352E 03	0.2535E 09
IN	0.4082	0.8375	-2.2302	0.6567	51.5481	56.6027	-2.5404	1.1415	0.7037	0.7198E-05	0.2275E 03	0.2551E 09
IN	0.4154	0.8372	-2.2632	0.6458	51.6764	56.8963	-2.5550	1.1407	0.7172	0.6959E-05	0.2201E 03	0.2564E 09
IN	0.4222	0.8367	-2.2961	0.6347	51.7920	57.1435	-2.5693	1.1401	0.7289	0.6734E-05	0.2130E 03	0.2575E 09
IN	0.4287	0.8361	-2.3289	0.6235	51.8954	57.3458	-2.5834	1.1394	0.7386	0.6520E-05	0.2061E 03	0.2584E 09
IN	0.4348	0.8354	-2.3616	0.6121	51.9872	57.5060	-2.5971	1.1388	0.7463	0.6317E-05	0.1995E 03	0.2591E 09
IN	0.4405	0.8346	-2.3942	0.6006	52.0681	57.6266	-2.6106	1.1382	0.7519	0.6124E-05	0.1931E 03	0.2597E 09
BD	0.4475	0.8335	-2.4364	0.5853	52.1617	57.7418	-2.6278	1.1375	0.7568	0.5886E-05	0.1851E 03	0.2602E 09

PROPERTIES BEHIND BOW SHOCK

X	Y	U	V	P	R	F
-0.058061	0.	0.066709	0.	0.934737	0.990904	0.944539
-0.045738	0.172000	0.085870	0.132303	0.915577	0.990716	0.925378
-0.007283	0.344000	0.147021	0.261640	0.854425	0.990058	0.864228
0.061756	0.516000	0.255422	0.374696	0.746025	0.988630	0.755827
0.168807	0.688000	0.403881	0.448096	0.597566	0.985845	0.607370

PROPERTIES AT MESH LINE, TAU= 0.800

X	Y	U	V	P	R	F
-0.049082	0.	0.052746	0.	0.947312	1.002571	0.944539
-0.036420	0.174138	0.071434	0.123460	0.925088	0.996424	0.928879
0.003274	0.348277	0.130275	0.242315	0.856838	0.977571	0.879316
0.074901	0.522415	0.234144	0.343606	0.744346	0.947821	0.791303
0.187243	0.696553	0.391454	0.404028	0.547012	0.840730	0.666817

PROPERTIES AT MESH LINE, TAU= 0.600

X	Y	U	V	P	R	F
-0.039355	0.	0.039216	0.	0.956789	1.011352	0.944539
-0.026286	0.176261	0.057100	0.113094	0.931639	0.999145	0.932550
0.014955	0.352521	0.112248	0.219427	0.859555	0.965238	0.894982
0.089721	0.528782	0.208619	0.306255	0.752611	0.919285	0.828504
0.209853	0.705042	0.367273	0.359349	0.508585	0.726715	0.732192

PROPERTIES AT MESH LINE, TAU= 0.400

X	Y	U	V	P	R	F
-0.028538	0.	0.025987	0.	0.963408	1.017478	0.944539
-0.015014	0.178136	0.042577	0.100454	0.935757	0.999392	0.936407
0.028077	0.356272	0.092148	0.191416	0.863388	0.953852	0.911233
0.106464	0.534408	0.177470	0.260816	0.767659	0.898749	0.867148
0.237496	0.712544	0.339170	0.308049	0.467682	0.623096	0.802563

PROPERTIES AT MESH LINE, TAU= 0.200

X	Y	U	V	P	R	F
-0.015980	0.	0.012947	0.	0.967322	1.021098	0.944539
-0.002023	0.179208	0.027498	0.084151	0.938019	0.997743	0.940441
0.043172	0.358415	0.068547	0.155151	0.869664	0.944768	0.927939
0.125437	0.537623	0.137167	0.203820	0.788133	0.884671	0.906466
0.271509	0.716831	0.310648	0.252688	0.411527	0.516293	0.875277

PROPERTIES AT MESH LINE, TAU= 0.

X	Y	U	V	P	R	F

-0.000011	0.	0.	0.	0.968617	1.022296	0.944539	
0.014183	0.178350	0.011275	0.060852	0.939395	0.995228	0.944539	S5
0.062100	0.356699	0.037784	0.101258	0.881898	0.941660	0.944539	
0.148406	0.535049	0.076319	0.123700	0.816825	0.880508	0.944539	
0.313336	0.713399	0.298904	0.198114	0.323049	0.390687	0.944539	

SUPERSONIC FLOW FIELD CALCULATION

OPTION NUMBER 1

EQUILIBRIUM FLOW FIELD-NOL SPHERE-P(INF)=50MMHG, V(INF)=16000 FPS

FREE STREAM CONDITIONS - MACH NO.=14.320 DENSITY=0.156100E-03 PRESSURE=139.2500 TEMP.= 520.00 ENTROPY=26.50980
EPSILON= 1.1086000

BODY EQUATION NUMBER 1, A= 1.0000 B= 1.0000 C= -2.1280 D= -0. E= 0.1321 X TERM.= 0.5000 ALPHA=-0.5994

BODY EQUATION NUMBER 2, A= -0. B= -0. C= -0. D= 1.0000 E= -0.8258 X TERM.= 0.7000 ALPHA= 0.3000

BODY EQUATION NUMBER 3, A= -0. B= -0. C= 0.3093 D= -1.0000 E= 0.6093 X TERM.= 2.0000 ALPHA=-0.3000

BODY EQUATION NUMBER 4, A= -0. B= -0. C= -0. D= 1.0000 E= -1.2279 X TERM.= 4.0000 ALPHA=-0.

X	Y	P PRIME	THETA	S/R	H PRIME	RO PRIME	GAMMA	MU
0.132020	0.530000	2.617100	0.905340	35.843000	23.303000	-0.206960	1.323400	0.756910
0.141080	0.537600	2.605100	0.903810	35.865000	23.333000	-0.212480	1.323600	0.759820
0.150140	0.545190	2.593000	0.902280	35.886000	23.363000	-0.218040	1.323800	0.762640
0.159690	0.552680	2.579600	0.900300	35.910000	23.393000	-0.224210	1.324100	0.765650
0.169240	0.560170	2.566100	0.898310	35.934000	23.423000	-0.230340	1.324300	0.768580
0.178910	0.567690	2.551500	0.895420	35.959000	23.453000	-0.236990	1.324500	0.771610
0.188580	0.575210	2.536900	0.892520	35.983000	23.483000	-0.243640	1.324700	0.774590
0.198370	0.582740	2.521500	0.888880	36.009000	23.513000	-0.250670	1.324900	0.777670
0.208160	0.590260	2.506000	0.885240	36.036000	23.543000	-0.257680	1.325100	0.780790
0.218070	0.597800	2.490000	0.881000	36.061000	23.573000	-0.264970	1.325400	0.783830
0.227970	0.605330	2.473900	0.876750	36.088000	23.603000	-0.272220	1.325600	0.787010
0.234430	0.612860	2.457400	0.871980	36.115000	23.632000	-0.279740	1.325800	0.790140
0.247990	0.620380	2.440800	0.867210	36.142000	23.663000	-0.287210	1.326000	0.793430
0.258270	0.627910	2.423800	0.862090	36.169000	23.692000	-0.294940	1.326200	0.796610
0.268530	0.635430	2.406700	0.856960	36.197000	23.723000	-0.302640	1.326500	0.800050
0.278790	0.642950	2.389600	0.851450	36.225000	23.753000	-0.310420	1.326700	0.803330
0.289060	0.650450	2.372400	0.845940	36.252000	23.783000	-0.318160	1.326900	0.806770
0.299520	0.657950	2.355000	0.840190	36.280000	23.812000	-0.326050	1.327100	0.810080
0.309980	0.665450	2.337500	0.834430	36.308000	23.842000	-0.333910	1.327300	0.813580
0.320580	0.672940	2.319900	0.828440	36.335000	23.872000	-0.341860	1.327600	0.817020
0.331180	0.680423	2.302300	0.822450	36.364000	23.903000	-0.349820	1.327800	0.820680

S7

	X	Y	P PRIME	THETA	S/R	H PRIME	RO PRIME	GAMMA	MU	RHO	P	H (EPSILON)
DS	0.1361	0.5383	2.6047	0.8880	36.3004	23.2154	-0.2538	1.2446	0.7664	0.1392E-02	0.2863E 05	0.1110E 01
IN	0.1410	0.5389	2.6173	0.8979	35.8556	21.6786	-0.2322	1.2544	0.6545	0.1464E-02	0.2899E 05	0.9768E 08

S8

	X	Y	P PRIME	THETA	S/R	H PRIME	RO PRIME	GAMMA	MU	RHO	P	H (EPSILON)
DS	0.1411	0.5484	2.6116	0.8917	36.3342	23.3648	-0.2525	1.2438	0.7805	0.1397E-02	0.2883E 05	0.1117E 01
IN	0.1449	0.5489	2.6056	0.8931	36.2455	23.0226	-0.2514	1.2457	0.7494	0.1400E-02	0.2866E 05	0.1037E 09

S9

	X	Y	P PRIME	THETA	S/R	H PRIME	RO PRIME	GAMMA	MU	RHO	P	H (EPSILON)
DS	0.1445	0.5552	2.6039	0.8875	36.2962	23.1970	-0.2540	1.2447	0.7647	0.1392E-02	0.2860E 05	0.1109E 01
IN	0.1497	0.5496	2.5997	0.8954	35.8585	21.6206	-0.2388	1.2545	0.6507	0.1441E-02	0.2849E 05	0.9742E 08
IN	0.1499	0.5558	2.5982	0.8905	36.3067	23.2022	-0.2566	1.2448	0.7653	0.1384E-02	0.2844E 05	0.1045E 09

S10

	X	Y	P PRIME	THETA	S/R	H PRIME	RO PRIME	GAMMA	MU	RHO	P	H (EPSILON)
DS	0.3724	0.8952	2.2805	0.7239	34.7859	17.1678	-0.3084	1.2786	0.4638	0.1228E-02	0.2070E 05	0.8750E 00
IN	0.3311	0.6816	2.2699	0.8337	36.3591	22.0625	-0.3816	1.2478	0.6717	0.1038E-02	0.2048E 05	0.9941E 08
IN	0.3316	0.6899	2.2710	0.8277	36.3064	21.8983	-0.3791	1.2487	0.6612	0.1043E-02	0.2051E 05	0.9867E 08
IN	0.3323	0.6981	2.2722	0.8218	36.2538	21.7247	-0.3766	1.2497	0.6506	0.1050E-02	0.2053E 05	0.9789E 08
IN	0.3331	0.7057	2.2732	0.8165	36.2057	21.5665	-0.3743	1.2507	0.6413	0.1055E-02	0.2055E 05	0.9718E 08
IN	0.3341	0.7153	2.2741	0.8103	36.1467	21.3719	-0.3716	1.2519	0.6303	0.1062E-02	0.2057E 05	0.9630E 08
IN	0.3352	0.7232	2.2749	0.8051	36.1192	21.2833	-0.3702	1.2524	0.6255	0.1065E-02	0.2059E 05	0.9590E 08
IN	0.3363	0.7314	2.2755	0.8001	36.0474	21.0475	-0.3671	1.2539	0.6130	0.1073E-02	0.2060E 05	0.9484E 08
IN	0.3372	0.7370	2.2761	0.7967	36.0141	20.9398	-0.3655	1.2545	0.6075	0.1077E-02	0.2061E 05	0.9435E 08
IN	0.3384	0.7438	2.2766	0.7927	35.9734	20.8074	-0.3637	1.2553	0.6009	0.1081E-02	0.2062E 05	0.9376E 08
IN	0.3401	0.7533	2.2773	0.7872	35.9178	20.6281	-0.3611	1.2565	0.5922	0.1088E-02	0.2064E 05	0.9295E 08
IN	0.3424	0.7651	2.2773	0.7809	35.8444	20.3756	-0.3583	1.2583	0.5808	0.1095E-02	0.2064E 05	0.9181E 08
IN	0.3446	0.7754	2.2767	0.7757	36.2792	21.8177	-0.3761	1.2494	0.6567	0.1051E-02	0.2062E 05	0.9831E 08
IN	0.3456	0.7830	2.2768	0.7716	36.1879	21.5202	-0.3723	1.2510	0.6387	0.1060E-02	0.2062E 05	0.9697E 08
IN	0.3472	0.7927	2.2762	0.7666	36.0663	21.1122	-0.3676	1.2535	0.6164	0.1071E-02	0.2061E 05	0.9513E 08
IN	0.3491	0.8027	2.2754	0.7617	35.9425	20.7019	-0.3628	1.2560	0.5957	0.1083E-02	0.2060E 05	0.9328E 08
IN	0.3507	0.8102	2.2753	0.7580	35.8579	20.4261	-0.3593	1.2577	0.5827	0.1092E-02	0.2060E 05	0.9204E 08
IN	0.3530	0.8198	2.2747	0.7536	35.7423	20.0513	-0.3547	1.2600	0.5659	0.1104E-02	0.2058E 05	0.9035E 08
IN	0.3552	0.8286	2.2742	0.7498	35.6402	19.7246	-0.3505	1.2621	0.5522	0.1115E-02	0.2057E 05	0.8888E 08
IN	0.3573	0.8363	2.2741	0.7464	35.5459	19.4272	-0.3464	1.2640	0.5403	0.1125E-02	0.2057E 05	0.8754E 08
IN	0.3600	0.8453	2.2736	0.7426	35.4411	19.0990	-0.3420	1.2661	0.5277	0.1137E-02	0.2056E 05	0.8606E 08
IN	0.3628	0.8545	2.2730	0.7389	35.3343	18.7687	-0.3373	1.2682	0.5157	0.1149E-02	0.2055E 05	0.8457E 08
IN	0.3652	0.8617	2.2730	0.7360	35.2577	18.5356	-0.3338	1.2697	0.5075	0.1158E-02	0.2055E 05	0.8352E 08
IN	0.3684	0.8713	2.2724	0.7323	35.1459	18.1968	-0.3288	1.2719	0.4960	0.1172E-02	0.2053E 05	0.8199E 08
IN	0.3714	0.8797	2.2721	0.7292	35.0459	17.8986	-0.3242	1.2738	0.4863	0.1184E-02	0.2053E 05	0.8065E 08
IN	0.3747	0.8885	2.2718	0.7260	34.9424	17.5935	-0.3193	1.2758	0.4766	0.1198E-02	0.2052E 05	0.7928E 08
IN	0.3778	0.8966	2.2717	0.7230	34.8503	17.3254	-0.3148	1.2775	0.4684	0.1210E-02	0.2052E 05	0.7807E 08

S11

	X	Y	P PRIME	THETA	S/R	H PRIME	RO PRIME	GAMMA	MU	RHO	P	H (EPSILON)
DS	0.3816	0.9062	2.2711	0.7197	34.7436	17.0174	-0.3097	1.2795	0.4592	0.1224E-02	0.2051E 05	0.8696E 00
BD	0.3325	0.6818	2.2336	0.8205	36.3640	21.9330	-0.3952	1.2481	0.6628	0.1065E-02	0.1975E 05	0.9883E 08
IN	0.3332	0.6901	2.2346	0.8146	36.3129	21.7788	-0.3929	1.2490	0.6532	0.1011E-02	0.1977E 05	0.9814E 08
BD	0.3416	0.6915	2.2015	0.8072	36.3640	21.8229	-0.4073	1.2483	0.6553	0.9779E-03	0.1913E 05	0.9833E 08
IN	0.3341	0.6984	2.2357	0.8089	36.2622	21.6119	-0.3905	1.2500	0.6433	0.1016E-02	0.1980E 05	0.9738E 08
IN	0.3425	0.6998	2.2026	0.8015	36.3138	21.6582	-0.4049	1.2493	0.6454	0.9833E-03	0.1915E 05	0.9759E 08
BD	0.3510	0.7011	2.1689	0.7938	36.3640	21.6971	-0.4194	1.2487	0.6471	0.9510E-03	0.1852E 05	0.9777E 08
IN	0.3350	0.7061	2.2367	0.8037	36.2157	21.4596	-0.3883	1.2509	0.6346	0.1022E-02	0.1981E 05	0.9670E 08
IN	0.3435	0.7075	2.2036	0.7963	36.2674	21.5062	-0.4027	1.2502	0.6366	0.9884E-03	0.1917E 05	0.9691E 08
IN	0.3520	0.7089	2.1699	0.7886	36.3180	21.5469	-0.4172	1.2496	0.6384	0.9558E-03	0.1854E 05	0.9709E 08
BD	0.3599	0.7101	2.1381	0.7812	36.3640	21.5786	-0.4309	1.2490	0.6396	0.9262E-03	0.1795E 05	0.9723E 08
IN	0.3363	0.7156	2.2374	0.7976	36.1574	21.2678	-0.3857	1.2521	0.6240	0.1028E-02	0.1983E 05	0.9583E 08
IN	0.3448	0.7171	2.2043	0.7902	36.2090	21.3141	-0.4001	1.2514	0.6259	0.9943E-03	0.1918E 05	0.9604E 08
IN	0.3534	0.7186	2.1708	0.7825	36.2601	21.3564	-0.4146	1.2507	0.6277	0.9616E-03	0.1855E 05	0.9623E 08
IN	0.3614	0.7198	2.1390	0.7750	36.3066	21.3902	-0.4283	1.2501	0.6290	0.9318E-03	0.1797E 05	0.9638E 08
BD	0.3714	0.7213	2.0978	0.7652	36.3640	21.4246	-0.4459	1.2494	0.6302	0.8943E-03	0.1725E 05	0.9654E 08
IN	0.3375	0.7237	2.2381	0.7926	36.1256	21.1650	-0.3841	1.2527	0.6185	0.1031E-02	0.1984E 05	0.9537E 08
IN	0.3461	0.7252	2.2052	0.7851	36.1609	21.1577	-0.3978	1.2523	0.6175	0.9995E-03	0.1920E 05	0.9534E 08
IN	0.3547	0.7266	2.1716	0.7774	36.2121	21.2004	-0.4123	1.2517	0.6192	0.9666E-03	0.1857E 05	0.9553E 08
IN	0.3627	0.7279	2.1399	0.7700	36.2587	21.2348	-0.4260	1.2511	0.6205	0.9367E-03	0.1799E 05	0.9568E 08
IN	0.3728	0.7294	2.0988	0.7601	36.3173	21.2731	-0.4436	1.2503	0.6219	0.8994E-03	0.1726E 05	0.9586E 08
BD	0.3812	0.7306	2.0640	0.7516	36.3640	21.2960	-0.4584	1.2498	0.6225	0.8693E-03	0.1667E 05	0.9596E 08
IN	0.3388	0.7319	2.2386	0.7876	36.0601	20.9504	-0.3813	1.2540	0.6074	0.1038E-02	0.1985E 05	0.9440E 08
IN	0.3475	0.7335	2.2056	0.7802	36.1269	21.0471	-0.3962	1.2530	0.6118	0.1003E-02	0.1921E 05	0.9484E 08
IN	0.3562	0.7350	2.1722	0.7725	36.1627	21.0393	-0.4101	1.2526	0.6108	0.9716E-03	0.1858E 05	0.9480E 08
IN	0.3642	0.7363	2.1404	0.7650	36.2095	21.0745	-0.4238	1.2520	0.6121	0.9415E-03	0.1800E 05	0.9496E 08
IN	0.3744	0.7378	2.0994	0.7552	36.2686	21.1148	-0.4414	1.2513	0.6135	0.9040E-03	0.1727E 05	0.9514E 08
IN	0.3829	0.7391	2.0646	0.7467	36.3159	21.1397	-0.4562	1.2507	0.6142	0.8737E-03	0.1668E 05	0.9526E 08

S12

	X	Y	P PRIME	THETA	S/R	H PRIME	RO PRIME	GAMMA	MU	RHO	P	H (EPSILON)
BD	0.3916	0.7402	2.0275	0.7374	36.3640	21.1586	-0.4719	1.2501	0.6145	0.8427E-03	0.1607E 05	0.9534E 08
IN	0.3398	0.7375	2.2391	0.7843	36.0290	20.8501	-0.3798	1.2546	0.6023	0.1042E-02	0.1986E 05	0.9395E 08
IN	0.3485	0.7391	2.2062	0.7769	36.0794	20.8929	-0.3941	1.2539	0.6039	0.1008E-02	0.1922E 05	0.9414E 08
IN	0.3572	0.7406	2.1727	0.7691	36.1365	20.9552	-0.4088	1.2531	0.6065	0.9744E-03	0.1859E 05	0.9442E 06
IN	0.3654	0.7419	2.1410	0.7617	36.1768	20.9691	-0.4222	1.2527	0.6067	0.9448E-03	0.1801E 05	0.9449E 08
IN	0.3756	0.7435	2.1000	0.7518	36.2367	21.0121	-0.4399	1.2519	0.6081	0.9072E-03	0.1728E 05	0.9468E 08
IN	0.3841	0.7448	2.0652	0.7433	36.2844	21.0384	-0.4547	1.2513	0.6089	0.8767E-03	0.1669E 05	0.9480E 08
IN	0.3929	0.7460	2.0282	0.7341	36.3325	21.0574	-0.4704	1.2507	0.6092	0.8457E-03	0.1608E 05	0.9488E 08
BD	0.3989	0.7467	2.0029	0.7277	36.3640	21.0662	-0.4810	1.2504	0.6092	0.8252E-03	0.1568E 05	0.9492E 08
IN	0.3411	0.7444	2.2395	0.7804	35.9881	20.7176	-0.3780	1.2554	0.5958	0.1046E-02	0.1987E 05	0.9335E 08
IN	0.3498	0.7460	2.2066	0.7729	36.0401	20.7654	-0.3924	1.2547	0.5976	0.1012E-02	0.1923E 05	0.9357E 08
IN	0.3586	0.7475	2.1731	0.7652	36.1156	20.8881	-0.4079	1.2536	0.6031	0.9767E-03	0.1859E 05	0.9412E 08
IN	0.3668	0.7489	2.1415	0.7578	36.1399	20.8497	-0.4206	1.2534	0.6007	0.9485E-03	0.1801E 05	0.9395E 08
IN	0.3771	0.7505	2.1004	0.7479	36.1963	20.8814	-0.4381	1.2527	0.6015	0.9110E-03	0.1729E 05	0.9409E 08
IN	0.3857	0.7518	2.0657	0.7394	36.2450	20.9109	-0.4529	1.2521	0.6024	0.8804E-03	0.1670E 05	0.9422E 08
IN	0.3945	0.7530	2.0287	0.7302	36.2943	20.9342	-0.4687	1.2515	0.6029	0.8491E-03	0.1609E 05	0.9433E 08
IN	0.4005	0.7538	2.0034	0.7238	36.3249	20.9400	-0.4792	1.2511	0.6028	0.8286E-03	0.1569E 05	0.9436E 08
BD	0.4079	0.7547	1.9718	0.7157	36.3640	20.9498	-0.4926	1.2506	0.6027	0.8036E-03	0.1520E 05	0.9440E 08
IN	0.3430	0.7538	2.2401	0.7750	35.9341	20.5435	-0.3756	1.2565	0.5875	0.1052E-02	0.1988E 05	0.9257E 06
IN	0.3518	0.7555	2.2072	0.7676	35.9836	20.5835	-0.3898	1.2558	0.5889	0.1018E-02	0.1924E 05	0.9275E 08
IN	0.3606	0.7571	2.1738	0.7598	36.0353	20.6282	-0.4043	1.2551	0.5904	0.9847E-03	0.1861E 05	0.9295E 08
IN	0.3689	0.7585	2.1421	0.7524	36.0811	20.6603	-0.4179	1.2545	0.5914	0.9543E-03	0.1803E 05	0.9310E 08
IN	0.3792	0.7602	2.1011	0.7426	36.1416	20.7054	-0.4356	1.2537	0.5929	0.9163E-03	0.1730E 05	0.9330E 08
IN	0.3879	0.7615	2.0663	0.7341	36.1884	20.7291	-0.4503	1.2532	0.5935	0.8856E-03	0.1671E 05	0.9341E 08
IN	0.3969	0.7628	2.0293	0.7249	36.2386	20.7553	-0.4661	1.2525	0.5941	0.8541E-03	0.1610E 05	0.9352E 06
IN	0.4030	0.7636	2.0041	0.7185	36.2701	20.7642	-0.4767	1.2521	0.5941	0.8334E-03	0.1570E 05	0.9356E 08
IN	0.4104	0.7645	1.9724	0.7104	36.3096	20.7751	-0.4901	1.2517	0.5941	0.8082E-03	0.1521E 05	0.9361E 08
BD	0.4208	0.7657	1.9271	0.6986	36.3640	20.7840	-0.5091	1.2510	0.5937	0.7736E-03	0.1454E 05	0.9365E 08

S13

	X	Y	P PRIME	THETA	S/R	H PRIME	RO PRIME	GAMMA	MU	RHO	P	H (EPSILON)
IN	0.3938	0.8138	2.1034	0.7160	36.0704	20.4832	-0.4317	1.2551	0.5824	0.9244E-03	0.1734E 05	0.9230E 08
IN	0.4029	0.8150	2.0692	0.7075	35.8855	19.7679	-0.4365	1.2591	0.5507	0.9144E-03	0.1676E 05	0.8907E 08
IN	0.4125	0.8165	2.0321	0.6984	35.9359	19.7976	-0.4522	1.2583	0.5513	0.8818E-03	0.1615E 05	0.8921E 08
IN	0.4189	0.8175	2.0068	0.6921	35.9694	19.8133	-0.4630	1.2579	0.5515	0.8603E-03	0.1575E 05	0.8928E 08
IN	0.4269	0.8186	1.9751	0.6842	36.0107	19.8303	-0.4764	1.2573	0.5517	0.8341E-03	0.1525E 05	0.8936E 08
IN	0.4381	0.8201	1.9296	0.6726	36.0685	19.8508	-0.4956	1.2566	0.5518	0.7981E-03	0.1458E 05	0.8945E 08
IN	0.4523	0.8218	1.8700	0.6571	36.1420	19.8696	-0.5206	1.2556	0.5515	0.7533E-03	0.1373E 05	0.8953E 08
IN	0.4632	0.8230	1.8244	0.6452	36.1944	19.8724	-0.5396	1.2550	0.5509	0.7212E-03	0.1312E 05	0.8955E 08
IN	0.4714	0.8238	1.7889	0.6357	36.2338	19.8703	-0.5543	1.2545	0.5502	0.6971E-03	0.1266E 05	0.8954E 08
IN	0.4826	0.8247	1.7384	0.6220	36.2865	19.8562	-0.5751	1.2539	0.5488	0.6646E-03	0.1204E 05	0.8947E 08
IN	0.4942	0.8256	1.6844	0.6071	36.3384	19.8271	-0.5970	1.2533	0.5466	0.6318E-03	0.1141E 05	0.8934E 08
BD	0.5003	0.8260	1.6550	0.5989	36.3640	19.8032	-0.6089	1.2530	0.5452	0.6147E-03	0.1108E 05	0.8923E 08
BD	0.5003	0.8260	1.5408	0.5589	36.3640	19.4031	-0.6505	1.2536	0.5273	0.5586E-03	0.9880E 04	0.8743E 08
BD	0.5003	0.8260	1.4243	0.5190	36.3640	19.0059	-0.6927	1.2540	0.5105	0.5069E-03	0.8793E 04	0.8564E 08
BD	0.5003	0.8260	1.3053	0.4790	36.3640	18.6090	-0.7356	1.2544	0.4944	0.4591E-03	0.7807E 04	0.8385E 08
BD	0.5003	0.8260	1.1839	0.4391	36.3640	18.2125	-0.7793	1.2545	0.4791	0.4153E-03	0.6914E 04	0.8207E 08
BD	0.5003	0.8260	1.0599	0.3991	36.3640	17.8163	-0.8237	1.2546	0.4645	0.3749E-03	0.6108E 04	0.8028E 08
BD	0.5003	0.8260	0.9332	0.3591	36.3640	17.4206	-0.8688	1.2545	0.4504	0.3379E-03	0.5381E 04	0.7850E 08
BD	0.5003	0.8260	0.8037	0.3192	36.3640	17.0252	-0.9148	1.2543	0.4368	0.3039E-03	0.4727E 04	0.7672E 08
BD	0.5003	0.8260	0.6713	0.2792	36.3640	16.6302	-0.9617	1.2540	0.4238	0.2729E-03	0.4141E 04	0.7494E 08
BD	0.5003	0.8260	0.5359	0.2393	36.3640	16.2355	-1.0094	1.2536	0.4112	0.2444E-03	0.3617E 04	0.7316E 08
BD	0.5003	0.8260	0.3975	0.1993	36.3640	15.8412	-1.0582	1.2530	0.3990	0.2185E-03	0.3149E 04	0.7138E 08
BD	0.5003	0.8260	0.2558	0.1593	36.3640	15.4472	-1.1080	1.2525	0.3873	0.1948E-03	0.2733E 04	0.6961E 08
BD	0.5003	0.8260	0.1109	0.1194	36.3640	15.0535	-1.1588	1.2518	0.3759	0.1733E-03	0.2365E 04	0.6783E 08
BD	0.5003	0.8260	-0.0375	0.0794	36.3640	14.6600	-1.2109	1.2512	0.3649	0.1537E-03	0.2038E 04	0.6606E 08
BD	0.5003	0.8260	-0.1894	0.0395	36.3640	14.2667	-1.2642	1.2506	0.3543	0.1360E-03	0.1751E 04	0.6429E 08
BD	0.5003	0.8260	-0.3450	-0.0005	36.3640	13.8736	-1.3188	1.2500	0.3440	0.1199E-03	0.1499E 04	0.6251E 08
IN	0.3555	0.8203	2.2497	0.7458	35.7717	20.0544	-0.3652	1.2597	0.5657	0.1077E-02	0.2007E 05	0.9037E 08

S14

	X	Y	P PRIME	THETA	S/R	H PRIME	RO PRIME	GAMMA	MU	RHO	P	H (EPSILON)
IN	0.5846	0.8657	-0.0420	0.0775	36.2691	14.4237	-1.2074	1.2524	0.3597	0.1549E-03	0.2029E 04	0.6499E 08
IN	0.5918	0.8636	-0.1915	0.0384	36.2761	14.0578	-1.2603	1.2517	0.3498	0.1372E-03	0.1748E 04	0.6334E 08
IN	0.5995	0.8612	-0.3440	-0.0007	36.2828	13.6918	-1.3142	1.2511	0.3404	0.1212E-03	0.1500E 04	0.6170E 08
IN	0.6252	0.8521	-0.3311	0.0026	36.3037	13.7728	-1.3109	1.2509	0.3422	0.1221E-03	0.1520E 04	0.6206E 08
IN	0.6455	0.8449	-0.3346	0.0017	36.3199	13.8012	-1.3130	1.2507	0.3427	0.1215E-03	0.1515E 04	0.6219E 08
IN	0.6630	0.8387	-0.3370	0.0011	36.3335	13.8268	-1.3146	1.2505	0.3432	0.1211E-03	0.1511E 04	0.6230E 08
IN	0.6836	0.8313	-0.3400	0.0003	36.3508	13.8590	-1.3166	1.2503	0.3439	0.1205E-03	0.1506E 04	0.6245E 08
BD	0.6991	0.8258	-0.3414	0.	36.3640	13.8860	-1.3178	1.2501	0.3444	0.1202E-03	0.1504E 04	0.6257E 08

S15

	X	Y	P PRIME	THETA	S/R	H PRIME	RO PRIME	GAMMA	MU	RHO	P	H (EPSILON)
SS	0.7000	0.8258	0.7114	0.3000	36.6836	17.6240	-0.9637	1.2498	0.4529	0.2716E-03	0.4311E 04	0.5852E 00
IN	0.3681	0.8624	2.2472	0.7285	35.2882	18.5407	-0.3446	1.2693	0.5073	0.1130E-02	0.2002E 05	0.8354E 08
IN	0.3792	0.8649	2.2014	0.7174	35.4100	18.7566	-0.3669	1.2672	0.5142	0.1073E-02	0.1913E 05	0.8452E 08
IN	0.3891	0.8669	2.1681	0.7099	35.5112	18.9523	-0.3836	1.2655	0.5207	0.1033E-02	0.1850E 05	0.8540E 08
IN	0.3985	0.8687	2.1367	0.7028	35.6165	19.1682	-0.3999	1.2637	0.5282	0.9948E-03	0.1793E 05	0.8637E 08
IN	0.4105	0.8709	2.0960	0.6934	35.7445	19.4236	-0.4204	1.2615	0.5373	0.9488E-03	0.1721E 05	0.8752E 08
IN	0.4203	0.8724	2.0617	0.6851	35.8480	19.6264	-0.4376	1.2598	0.5448	0.9121E-03	0.1663E 05	0.8844E 08
IN	0.4308	0.8739	2.0252	0.6763	35.9531	19.8270	-0.4555	1.2580	0.5524	0.8752E-03	0.1604E 05	0.8934E 08
IN	0.4381	0.8748	2.0004	0.6702	36.0305	19.9830	-0.4680	1.2568	0.5585	0.8504E-03	0.1564E 05	0.9004E 08
IN	0.4471	0.8758	1.9693	0.6625	36.1246	20.1696	-0.4834	1.2552	0.5660	0.8207E-03	0.1517E 05	0.9088E 08
IN	0.4595	0.8770	1.9249	0.6512	36.2532	20.4194	-0.5052	1.2531	0.5765	0.7805E-03	0.1451E 05	0.9201E 08
IN	0.4752	0.8782	1.8669	0.6360	35.8454	18.9322	-0.5087	1.2614	0.5154	0.7743E-03	0.1369E 05	0.8531E 08
IN	0.4871	0.8796	1.8210	0.6244	35.9008	18.9561	-0.5277	1.2603	0.5152	0.7411E-03	0.1308E 05	0.8542E 08
IN	0.4960	0.8806	1.7853	0.6152	35.9410	18.9564	-0.5426	1.2598	0.5147	0.7162E-03	0.1262E 05	0.8542E 08
IN	0.5084	0.8818	1.7343	0.6018	35.9957	18.9488	-0.5636	1.2591	0.5136	0.6824E-03	0.1199E 05	0.8538E 08
IN	0.5212	0.8830	1.6798	0.5873	36.0529	18.9370	-0.5859	1.2583	0.5122	0.6481E-03	0.1135E 05	0.8533E 08
IN	0.5280	0.8835	1.6501	0.5794	36.0826	18.9260	-0.5981	1.2579	0.5113	0.6303E-03	0.1102E 05	0.8528E 08
IN	0.5322	0.8838	1.5339	0.5412	36.1208	18.6503	-0.6419	1.2577	0.4997	0.5698E-03	0.9812E 04	0.8404E 08
IN	0.5366	0.8839	1.4157	0.5029	36.1292	18.2854	-0.6849	1.2579	0.4854	0.5161E-03	0.8718E 04	0.8239E 08
IN	0.5412	0.8840	1.2952	0.4646	36.1370	17.9194	-0.7285	1.2579	0.4715	0.4668E-03	0.7729E 04	0.8074E 08
IN	0.5460	0.8840	1.1724	0.4262	36.1463	17.5578	-0.7728	1.2579	0.4584	0.4215E-03	0.6836E 04	0.7912E 08
IN	0.5511	0.8838	1.0472	0.3877	36.1592	17.2062	-0.8181	1.2576	0.4459	0.3798E-03	0.6031E 04	0.7753E 08
IN	0.5564	0.8835	0.9195	0.3492	36.1717	16.8534	-0.8640	1.2572	0.4339	0.3417E-03	0.5308E 04	0.7594E 08
IN	0.5621	0.8830	0.7894	0.3107	36.1840	16.5002	-0.9107	1.2567	0.4221	0.3068E-03	0.4660E 04	0.7435E 08
IN	0.5681	0.8824	0.6567	0.2720	36.1959	16.1458	-0.9582	1.2562	0.4107	0.2751E-03	0.4081E 04	0.7275E 08
IN	0.5745	0.8815	0.5213	0.2334	36.2073	15.7903	-1.0064	1.2555	0.3996	0.2461E-03	0.3564E 04	0.7115E 08
IN	0.5813	0.8803	0.3832	0.1947	36.2183	15.4338	-1.0555	1.2549	0.3888	0.2198E-03	0.3105E 04	0.6954E 08
IN	0.5885	0.8789	0.2424	0.1559	36.2286	15.0760	-1.1055	1.2541	0.3783	0.1959E-03	0.2697E 04	0.6793E 08

S16

	X	Y	P PRIME	THETA	S/R	H PRIME	RO PRIME	GAMMA	MU	RHO	P	H (EPSILON)
IN	0.5962	0.8772	0.0988	0.1171	36.2381	14.7167	-1.1564	1.2534	0.3681	0.1743E-03	0.2336E 04	0.6631E 08
IN	0.6045	0.8750	-0.0476	0.0783	36.2472	14.3569	-1.2082	1.2527	0.3581	0.1547E-03	0.2018E 04	0.6469E 08
IN	0.6134	0.8725	-0.1970	0.0395	36.2558	13.9965	-1.2611	1.2520	0.3485	0.1369E-03	0.1738E 04	0.6307E 08
IN	0.6229	0.8695	-0.3492	0.0006	36.2638	13.6358	-1.3150	1.2514	0.3392	0.1209E-03	0.1493E 04	0.6144E 08
IN	0.6485	0.8604	-0.3363	0.0039	36.2843	13.7154	-1.3117	1.2512	0.3410	0.1219E-03	0.1512E 04	0.6180E 08
IN	0.6689	0.8533	-0.3398	0.0030	36.3012	13.7453	-1.3138	1.2509	0.3415	0.1213E-03	0.1507E 04	0.6194E 08
IN	0.6865	0.8471	-0.3422	0.0024	36.3152	13.7715	-1.3154	1.2507	0.3420	0.1208E-03	0.1503E 04	0.6205E 08
IN	0.7072	0.8398	-0.3453	0.0017	36.3312	13.8007	-1.3174	1.2505	0.3426	0.1203E-03	0.1499E 04	0.6219E 08
IN	0.7228	0.8343	-0.3466	0.0013	36.3439	13.8266	-1.3185	1.2503	0.3431	0.1200E-03	0.1496E 04	0.6230E 08
BD	0.7071	0.8280	0.7114	0.3000	36.6836	17.6240	-0.9637	1.2498	0.4529	0.2716E-03	0.4311E 04	0.7941E 08

S17

	X	Y	P PRIME	THETA	S/R	H PRIME	RO PRIME	GAMMA	MU	RHO	P	H (EPSILON)
SS	0.7162	0.8365	0.7055	0.2998	36.6577	17.5342	-0.9645	1.2501	0.4501	0.2711E-03	0.4286E 04	0.5836E 00
BD	0.7286	0.8346	0.6998	0.3000	36.6836	17.5880	-0.9678	1.2498	0.4517	0.2690E-03	0.4261E 04	0.7925E 08
IN	0.3715	0.8721	2.2464	0.7249	35.1801	18.2128	-0.3399	1.2714	0.4961	0.1142E-02	0.2001E 05	0.8207E 08
IN	0.3827	0.8747	2.2004	0.7139	35.2992	18.4173	-0.3622	1.2694	0.5023	0.1085E-02	0.1911E 05	0.8299E 08
IN	0.3926	0.8768	2.1669	0.7064	35.4058	18.6269	-0.3793	1.2676	0.5090	0.1043E-02	0.1848E 05	0.8393E 08
IN	0.4020	0.8787	2.1353	0.6993	35.5005	18.8076	-0.3951	1.2659	0.5149	0.1006E-02	0.1790E 05	0.8475E 08
IN	0.4141	0.8809	2.0945	0.6899	35.6331	19.0737	-0.4160	1.2637	0.5240	0.9584E-03	0.1719E 05	0.8595E 08
IN	0.4239	0.8826	2.0600	0.6817	35.7327	19.2616	-0.4331	1.2620	0.5305	0.9215E-03	0.1660E 05	0.8679E 08
IN	0.4344	0.8842	2.0233	0.6728	35.8450	19.4818	-0.4515	1.2601	0.5384	0.8833E-03	0.1601E 05	0.8779E 08
IN	0.4418	0.8852	1.9983	0.6668	35.9168	19.6182	-0.4638	1.2589	0.5434	0.8587E-03	0.1561E 05	0.8840E 08
IN	0.4508	0.8863	1.9671	0.6591	36.0103	19.8006	-0.4793	1.2574	0.5503	0.8285E-03	0.1513E 05	0.8922E 08
IN	0.4633	0.8877	1.9224	0.6478	36.1373	20.0418	-0.5012	1.2553	0.5597	0.7878E-03	0.1447E 05	0.9031E 08
IN	0.4801	0.8891	1.8640	0.6330	36.3008	20.3373	-0.5300	1.2532	0.5722	0.7372E-03	0.1365E 05	0.9164E 08
IN	0.4918	0.8899	1.8197	0.6211	35.8484	18.7805	-0.5260	1.2617	0.5092	0.7440E-03	0.1306E 05	0.8463E 08
IN	0.5009	0.8909	1.7839	0.6119	35.8911	18.8013	-0.5408	1.2607	0.5091	0.7192E-03	0.1260E 05	0.8472E 08
IN	0.5134	0.8922	1.7328	0.5987	35.9459	18.7942	-0.5618	1.2600	0.5080	0.6852E-03	0.1197E 05	0.8469E 08
IN	0.5265	0.8934	1.6783	0.5843	36.0017	18.7781	-0.5841	1.2592	0.5065	0.6508E-03	0.1134E 05	0.8461E 08
IN	0.5335	0.8939	1.6485	0.5764	36.0326	18.7709	-0.5963	1.2588	0.5058	0.6328E-03	0.1100E 05	0.8458E 08
IN	0.5384	0.8942	1.5318	0.5385	36.0526	18.4412	-0.6394	1.2589	0.4925	0.5730E-03	0.9792E 04	0.8310E 08
IN	0.5435	0.8945	1.4130	0.5006	36.0716	18.1091	-0.6831	1.2588	0.4795	0.5182E-03	0.8695E 04	0.8160E 08
IN	0.5490	0.8946	1.2920	0.4626	36.1154	17.8479	-0.7286	1.2583	0.4692	0.4667E-03	0.7704E 04	0.8042E 08
IN	0.5547	0.8946	1.1690	0.4244	36.1242	17.4852	-0.7730	1.2582	0.4561	0.4213E-03	0.6812E 04	0.7879E 08
IN	0.5606	0.8944	1.0435	0.3862	36.1325	17.1215	-0.8180	1.2580	0.4434	0.3798E-03	0.6009E 04	0.7715E 08
IN	0.5670	0.8940	0.9156	0.3480	36.1403	16.7570	-0.8638	1.2576	0.4311	0.3418E-03	0.5288E 04	0.7551E 08
IN	0.5737	0.8935	0.7852	0.3097	36.1527	16.4049	-0.9105	1.2571	0.4195	0.3069E-03	0.4641E 04	0.7392E 08
IN	0.5808	0.8927	0.6523	0.2713	36.1659	16.0550	-0.9581	1.2566	0.4083	0.2751E-03	0.4063E 04	0.7234E 08
IN	0.5883	0.8916	0.5167	0.2329	36.1790	15.7049	-1.0065	1.2559	0.3974	0.2461E-03	0.3548E 04	0.7077E 08
IN	0.5963	0.8903	0.3785	0.1945	36.1916	15.3539	-1.0557	1.2552	0.3868	0.2197E-03	0.3090E 04	0.6918E 08

S18

	X	Y	P PRIME	THETA	S/R	H PRIME	RO PRIME	GAMMA	MU	RHO	P	H (EPSILON)
OS	0.4078	0.9359	2.2032	0.6904	34.4426	15.9723	-0.3181	1.2849	0.4290	0.1201E-02	0.1916E 05	0.8322E 00
IN	0.4181	0.9386	2.1696	0.6835	34.6891	16.5509	-0.3432	1.2807	0.4444	0.1134E-02	0.1853E 05	0.7458E 08
IN	0.4279	0.9410	2.1370	0.6766	34.8252	16.8323	-0.3619	1.2784	0.4519	0.1086E-02	0.1793E 05	0.7585E 08
IN	0.4403	0.9438	2.0949	0.6673	34.9469	17.0459	-0.3832	1.2764	0.4575	0.1034E-02	0.1719E 05	0.7681E 08
IN	0.4505	0.9460	2.0592	0.6593	35.0504	17.2294	-0.4012	1.2747	0.4624	0.9918E-03	0.1659E 05	0.7764E 08
IN	0.4615	0.9482	2.0214	0.6507	35.1605	17.4257	-0.4202	1.2728	0.4677	0.9492E-03	0.1598E 05	0.7852E 08
IN	0.4691	0.9496	1.9957	0.6448	35.2349	17.5584	-0.4331	1.2716	0.4714	0.9214E-03	0.1557E 05	0.7912E 08
IN	0.4785	0.9513	1.9634	0.6372	35.3207	17.7038	-0.4490	1.2702	0.4754	0.8885E-03	0.1508E 05	0.7977E 08
IN	0.4916	0.9534	1.9172	0.6263	35.4435	17.9129	-0.4715	1.2681	0.4813	0.8435E-03	0.1440E 05	0.8072E 08
IN	0.5092	0.9560	1.8568	0.6118	35.6102	18.2059	-0.5013	1.2654	0.4899	0.7876E-03	0.1355E 05	0.8204E 08
IN	0.5224	0.9576	1.8109	0.6005	35.7269	18.3998	-0.5233	1.2635	0.4956	0.7486E-03	0.1294E 05	0.8291E 08
IN	0.5327	0.9587	1.7753	0.5916	35.8219	18.5642	-0.5407	1.2620	0.5007	0.7193E-03	0.1249E 05	0.8365E 08
IN	0.5467	0.9599	1.7246	0.5786	35.9419	18.7534	-0.5646	1.2601	0.5064	0.6808E-03	0.1187E 05	0.8450E 08
IN	0.5615	0.9610	1.6707	0.5645	36.0713	18.9609	-0.5901	1.2581	0.5130	0.6420E-03	0.1125E 05	0.8544E 08
IN	0.5697	0.9614	1.6415	0.5569	36.1392	19.0670	-0.6038	1.2570	0.5164	0.6220E-03	0.1093E 05	0.8592E 08
IN	0.5807	0.9619	1.5256	0.5203	36.2211	18.9180	-0.6497	1.2563	0.5092	0.5596E-03	0.9731E 04	0.8524E 08
IN	0.5905	0.9620	1.4083	0.4830	36.2947	18.7438	-0.6955	1.2555	0.5011	0.5036E-03	0.8654E 04	0.8446E 08
IN	0.6007	0.9618	1.2895	0.4455	36.2880	18.3355	-0.7379	1.2557	0.4851	0.4567E-03	0.7684E 04	0.8262E 08
IN	0.6115	0.9614	1.1683	0.4079	35.8622	16.7446	-0.7601	1.2625	0.4350	0.4340E-03	0.6808E 04	0.7545E 08
IN	0.6232	0.9611	1.0410	0.3714	35.8946	16.4678	-0.8067	1.2614	0.4251	0.3898E-03	0.5994E 04	0.7420E 08
IN	0.6356	0.9604	0.9116	0.3348	35.9240	16.1676	-0.8540	1.2606	0.4152	0.3496E-03	0.5266E 04	0.7285E 08
IN	0.6487	0.9593	0.7799	0.2981	35.9520	15.8631	-0.9018	1.2598	0.4053	0.3131E-03	0.4617E 04	0.7148E 08
IN	0.6627	0.9578	0.6460	0.2613	35.9779	15.5529	-0.9503	1.2590	0.3956	0.2801E-03	0.4038E 04	0.7008E 08
IN	0.6775	0.9558	0.5099	0.2244	36.0032	15.2411	-0.9995	1.2581	0.3860	0.2501E-03	0.3524E 04	0.6868E 08
IN	0.6933	0.9533	0.3714	0.1874	36.0282	14.9285	-1.0494	1.2572	0.3767	0.2230E-03	0.3068E 04	0.6727E 08
IN	0.7101	0.9500	0.2307	0.1504	36.0506	14.6097	-1.0999	1.2563	0.3674	0.1985E-03	0.2666E 04	0.6583E 08
IN	0.7282	0.9461	0.0878	0.1133	36.0721	14.2895	-1.1512	1.2554	0.3584	0.1764E-03	0.2311E 04	0.6439E 08
IN	0.7475	0.9412	-0.0574	0.0761	36.1171	14.0256	-1.2046	1.2543	0.3509	0.1560E-03	0.1998E 04	0.6320E 08

S19

	X	Y	P PRIME	THETA	S/R	H PRIME	RO PRIME	GAMMA	MU	RHO	P	H (EPSILON)
IN	0.7681	0.9354	-0.2045	0.0388	36.1273	13.6806	-1.2567	1.2536	0.3418	0.1383E-03	0.1725E 04	0.6164E 08
IN	0.7903	0.9285	-0.3537	0.0016	36.1369	13.3369	-1.3097	1.2530	0.3331	0.1224E-03	0.1486E 04	0.6010E 08
IN	0.8148	0.9200	-0.3411	0.0047	36.1506	13.3992	-1.3061	1.2529	0.3345	0.1235E-03	0.1505E 04	0.6038E 08
IN	0.8356	0.9129	-0.3446	0.0039	36.1666	13.4268	-1.3082	1.2527	0.3350	0.1229E-03	0.1499E 04	0.6050E 08
IN	0.8534	0.9068	-0.3469	0.0033	36.1807	13.4532	-1.3098	1.2525	0.3355	0.1224E-03	0.1496E 04	0.6062E 08

S20

	X	Y	P PRIME	THETA	S/R	H PRIME	RO PRIME	GAMMA	MU	RHO	P	H (EPSILON)
SS	0.8336	0.9126	0.6816	0.2877	36.4709	16.9508	-0.9636	1.2526	0.4328	0.2716E-03	0.4184E 04	0.5640E 00
IN	0.8472	0.9106	0.6780	0.2884	36.5001	17.0192	-0.9663	1.2522	0.4347	0.2699E-03	0.4169E 04	0.7669E 08
IN	0.8620	0.9084	0.6743	0.2893	36.5315	17.0931	-0.9692	1.2518	0.4368	0.2681E-03	0.4154E 04	0.7702E 08
IN	0.8757	0.9064	0.6711	0.2901	36.5606	17.1624	-0.9719	1.2514	0.4387	0.2665E-03	0.4140E 04	0.7733E 08
IN	0.8932	0.9038	0.6652	0.2907	36.5980	17.2465	-0.9758	1.2509	0.4410	0.2641E-03	0.4116E 04	0.7771E 08
IN	0.9021	0.9024	0.6705	0.2935	36.6174	17.3157	-0.9749	1.2506	0.4431	0.2646E-03	0.4138E 04	0.7802E 08
BD	0.9329	0.8978	0.6775	0.3000	36.6836	17.5189	-0.9757	1.2498	0.4492	0.2641E-03	0.4167E 04	0.7894E 08